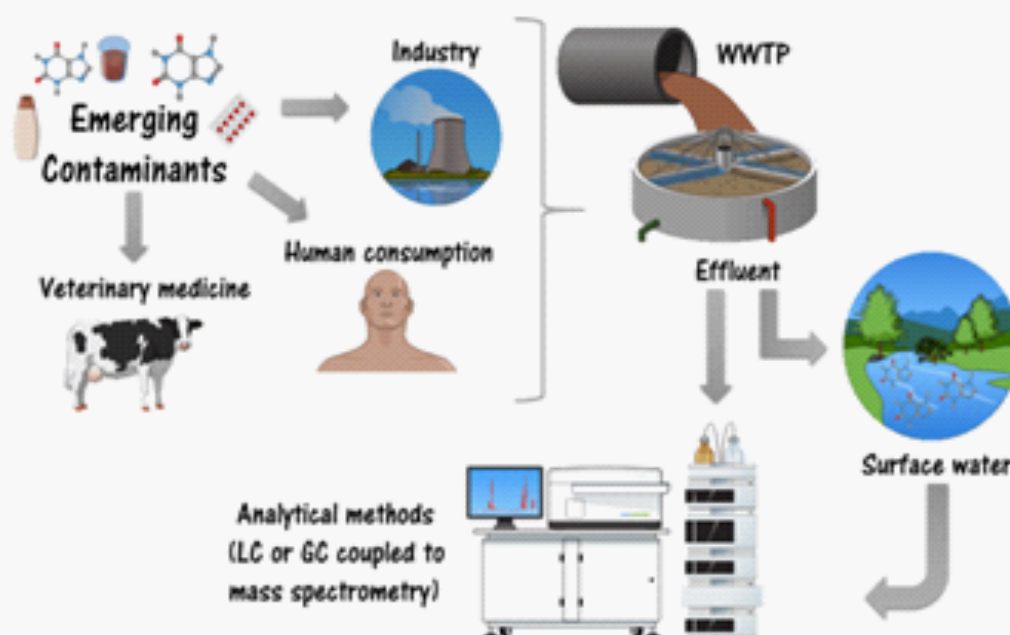


Eclética Química Journal

Volume 44 • number 4 • year 2019

Occurrence of caffeine in wastewater and sewage and applied techniques for analysis: a review



Emerging contaminants in wastewater represent a potential risk to the environment. This review shows what are the emerging contaminants, mainly caffeine, and the other aspects that surround the theme.

Influence of Ce(IV) ions amount on the electrochemical behavior of organic-inorganic hybrid coatings in 0.1 mol L⁻¹ NaCl solution

Determination of trace amounts of selenium in natural spring waters and tea samples by catalytic kinetic spectrophotometry

Rapid and selective extraction of trace amount of Pb(II) in aqueous samples using a magnetic ion-imprinted polymer and detection by flame atomic absorption spectrometry

Larvicidal activity, molluscicide and toxicity of the essential oil of *Citrus limon* peels against, respectively, *Aedes aegypti*, *Biomphalaria glabrata* and *Artemia salina*

unesp

UNIVERSIDADE ESTADUAL PAULISTA
"JÚLIO DE MESQUITA FILHO"



Instituto de Química
UNESP
Araraquara

ISSN 1678-4618



UNIVERSIDADE ESTADUAL PAULISTA

Reitor

Sandro Roberto Valentini

Vice-reitor

Sergio Roberto Nobre

Pró-reitor de Planejamento Estratégico e Gestão

Leonardo Theodoro Büll

Pró-reitora de Graduação

Gladis Massini-Cagliari

Pró-reitora de Pós-Graduação

Telma Teresinha Berchielli

Pró-reitora de Extensão Universitária

Cleopatra da Silva Planeta

Pró-reitor de Pesquisa

Carlos Frederico de Oliveira Graeff



INSTITUTO DE QUÍMICA

Diretor

Eduardo Maffud Cilli

Vice-Diretora

Dulce Helena Siqueira Silva

Editorial Team

Editors

Prof. Assis Vicente Benedetti, Institute of Chemistry Unesp Araraquara, Brazil (Editor-in-Chief)

Prof. Arnaldo Alves Cardoso, Institute of Chemistry Unesp Araraquara, Brazil

Prof. Antonio Eduardo Mauro, Institute of Chemistry Unesp Araraquara, Brazil

Prof. Horacio Heinzen, Faculty of Chemistry UdelaR, Montevideo, Uruguay

Prof. Maysa Furlan, Institute of Chemistry Unesp Araraquara, Brazil

Prof. Maria Célia Bertolini, Institute of Chemistry Unesp Araraquara, Brazil

Prof. Paulo Clairmont Feitosa de Lima Gomes, Institute of Chemistry, Unesp Araraquara, Brazil

Editorial Board

Prof. Jairton Dupont, Instituto de Química, Universidade Federal do Rio Grande do Sul, UFRGS, RS, Brazil

Prof. Enric Brillas, Facultat de Química, Universitat de Barcelona, Spain

Prof. Verónica Cortés de Zea Bermudez, Escola de Ciências da Vida e do Ambiente, Universidade de Trás-os-Montes e Alto Douro, Vila Real, Portugal

Prof. Lauro Kubota, Instituto de Química, Universidade Estadual de Campinas, Unicamp, SP, Brazil

Prof. Ivano Gerardt Rolf Gutz, Instituto de Química, Universidade de São Paulo, USP, SP, Brazil

Prof. Massuo Jorge Kato, Instituto de Química, Universidade de São Paulo, USP, SP, Brazil

Prof. Francisco de Assis Leone, Faculdade de Filosofia, Ciências e Letras, Universidade de São Paulo, Ribeirão Preto, USP-RP, SP, Brazil

Prof. Roberto Santana da Silva, Faculdade de Ciências Farmacêuticas, Universidade de São Paulo, Ribeirão Preto, USP-RP, SP, Brazil

Prof. José Antônio Maia Rodrigues, Faculdade de Ciências, Universidade do Porto, Portugal

Prof. Bayardo Baptista Torres, Instituto de Química, Universidade de São Paulo, USP, SP, Brazil

Technical Staff

Gustavo Marcelino de Souza

Letícia Amanda Miguel

Editorial

Aiming to offer the best for our readers, the Editor is convinced of the high quality of this volume of **Eclética Química Journal**, which contains a review and four original articles. The review focus on caffeine, an emergent contaminant of water that can cause harmful effects to nontarget organisms and affect the ecosystem balance. Caffeine is present in medicines, beverages, foodstuff, several other products, and is worldwide used and recognized as an anthropogenic activity marker. The review discusses the samples preparation, analysis and removal technologies.

In the first full paper, the influence of ceric ions to the hydrolysis solution on the corrosion protection afforded by organic-inorganic hybrid coating to a carbon steel substrate in 0.1 mol L^{-1} NaCl solution is described and the possible mechanism discussed together with the strategies used to detect cerium (IV) and (III) ions in the coating. The second article describes a new method for the determination of trace Se(IV) in natural spring waters and commercial tea samples. The method is based on catalytic kinetic spectrophotometry, which is a low cost, robust and easy-to-operate analytical technique, comparable to most of the similar spectrophotometric and kinetic spectrophotometric methods reported in the literature in terms of linear working range, sensitivity, selectivity and reproducibility. The third full paper describes the synthesis of magnetic Pb(II) ion-imprinted polymer using magnetic $\text{Fe}_3\text{O}_4@ \text{SiO}_2$ nanospheres as support, organic compounds as ligand, monomer and crosslinker. The properties of the sorbent were extensively analyzed by different techniques and its high selectivity and successful application to removal lead in real samples were demonstrated. This year's volume closes with an article that describes the extraction and characterization of essential oil obtained from *Citrus limon* peels and tested the larvicidal activity, molluscicide and toxicity of the oil, respectively against third stage larvae of *Aedes aegypti*, snail *Biomphalaria glabrata*, and *Artemia salina* applying the method adopted by the Brazilian Ministry of Health and the World Health Organization.

A novelty that will be implemented in our next number is the insertion of Supplementary Material in a proper file with its exclusive DOI number. When appropriate, important data to complement and a better comprehension of the article can be submitted as Supplementary File, which will be published online and will be made available as links in the original article. This might include additional figures, tables, text, equations, videos or other materials that are necessary to fully document the research contained in the paper or to facilitate the readers' ability to understand the work. Supplementary Materials should be presented in appropriate .docx file for text, tables, figures and graphics. The full title of the paper, authors' names and affiliations, and corresponding author should be included in the header. All supplementary figures, tables and videos should be referred in the manuscript body as "Table S1, S2...", "Fig. S1, S2..." and "Video S1, S2 ...".

The Editor and his team wish to express their sincere thanks to the authors and reviewers for their outstanding collaboration.

Instructions for Authors

Preparation of manuscripts

• **Only manuscripts in English will be accepted.** British or American usage is acceptable, but they should not be mixed.

• **The corresponding author should submit the manuscript online at**
<http://revista.iq.unesp.br/ojs/index.php/eclética/author>

• **Manuscripts must be sent in editable files as *.doc, *.docx or *.odt.** The text must be typed using font style Times New Roman and size 11. Space between lines should be 1.5 mm and paper size A4.

• **The manuscript should be organized in sections as follows:** Introduction, Experimental, Results and Discussion, Conclusions, and References. Sections titles must be written in bold and sequentially numbered; only the first letter should be in uppercase letter. Subsections should be written in normal and italic lowercase letters. For example: **1. Introduction;** *1.1 History;* **2. Experimental;** *2.1 Surface characterization;* *2.1.1 Morphological analysis.*

• **The cover letter should include:** the authors' full names, e-mail addresses, ORCID code and affiliations, and remarks about the novelty and relevance of the work. The cover letter should also contain a declaration of the corresponding author, on behalf of the other authors, that the article being submitted is original and its content has not been published previously and is not under consideration for publication elsewhere, that no conflict of interest exists and if accepted, the article will not be published elsewhere in the same form, in any language, without the written consent of the publisher. Finally, the cover letter should also contain the suggestion of 3 (three) suitable reviewers (please, provide full name, affiliation, and e-mail).

• **The first page of the manuscript** should contain the title, abstract and keywords. **Please, do not give authors names and affiliation, and acknowledgements since a double-blind review system is used. Acknowledgements should be added to the proof only.**

• **All contributions should include** an Abstract (200 words maximum), three to five Keywords and a Graphical Abstract (8 cm wide × 4 cm high) with an explicative text (2 lines maximum).

• **Citations should be sequentially numbered** and presented in square brackets throughout the text, and references should be compiled in square brackets at the end of the manuscript as follows:

Journal:

[1] Adorno, A. T. V., Benedetti, A. V., Silva, R. A. G. da, Blanco, M., Influence of the Al content on the phase transformations in Cu-Al-Ag Alloys, *Eclét. Quim.* 28 (1) (2003) 33-38. <https://doi.org/10.1590/S0100-46702003000100004>.

Book:

[2] Wendlant, W. W., *Thermal Analysis*, Wiley-Interscience, New York, 3rd ed., 1986, ch1.

Chapter in a book:

[3] Ferreira, A. A. P., Uliana, C. V., Souza Castilho, M. de, Canaverolo Pesquero, N., Foguel, N. V., Pilon dos Santos, G., Fugivara, C. S., Benedetti, A. V., Yamanaka, H., Amperometric Biosensor for Diagnosis of Disease, In: State of the Art in Biosensors - Environmental and Medical Applications, Rincken, T., ed., InTech: Rijeka, Croatia, 2013, Ch. 12.

Material in process of publication:

[4] Valente Jr., M. A. G., Teixeira, D. A., Lima Azevedo, D., Feliciano, G. T., Benedetti, A. V., Fugivara, C. S., Caprylate Salts Based on Amines as Volatile Corrosion Inhibitors for Metallic Zinc: Theoretical and Experimental Studies, *Frontiers in Chemistry*. <https://doi.org/10.3389/fchem.2017.00032>.

- Figures, Schemes, and Tables should be numbered sequentially and presented at the end of the manuscript.
- Nomenclature, abbreviations, and symbols should follow IUPAC recommendations.
- Figures, schemes, and photographs already published by the same or different authors in other publications may be reproduced in manuscripts of **Eclet. Quím. J.** only with permission from the editor house that holds the copyright.
- Graphical Abstract (GA) should be a high-resolution figure (900 dpi) summarizing the manuscript in an interesting way to catch the attention of the readers and accompanied by a short explicative text (two lines maximum). GA must be submitted as *.jpg, *.jpeg or *.tif.
- **Communications** should cover relevant scientific results and are limited to 1,500 words or three pages of the Journal, not including the title, authors' names, figures, tables and references. However, Communications suggesting fragmentation of complete contributions are strongly discouraged by Editors.
- **Review articles** should be original and present state-of-the-art overviews in a coherent and concise form covering the most relevant aspects of the topic that is being revised and indicate the likely future directions of the field. Therefore, before beginning the preparation of a Review manuscript, send a letter (one page maximum) to the Editor with the subject of interest and the main topics that would be covered in the Review manuscript. The Editor will communicate his decision in two weeks. Receiving this type of manuscript does not imply acceptance to be published in **Eclet. Quím. J.** It will be peer-reviewed.
- **Short reviews** should present an overview of the state-of-the-art in a specific topic within the scope of the Journal and limited to 5,000 words. Consider a table or image as corresponding to 100 words. Before beginning the preparation of a Short Review manuscript, send a letter (one page maximum) to the Editor with the subject of interest and the main topics that would be covered in the Short Review manuscript.
- **Technical Notes:** descriptions of methods, techniques, equipment or accessories developed in the authors' laboratory, as long as they present chemical content of interest. They should follow the usual form of presentation, according to the peculiarities of each work. They should have a maximum of 15 pages, including figures, tables, diagrams, etc.
- **Articles in Education in Chemistry and chemistry-correlated areas:** research manuscript related to undergraduate teaching in Chemistry and innovative experiences in undergraduate and graduate education. They should have a maximum of 15 pages, including figures, tables, diagrams, and other elements.

Special issues with complete articles dedicated to Symposia and Congresses can be published by **Eclet. Quim. J.** under the condition that a previous agreement with Editors is established. All the guides of the journal must be followed by the authors.

Eclet. Quim. J. Ethical Guides and Publication Copyright:

Before beginning the submission process, please be sure that all ethical aspects mentioned below were followed. Violation of these ethical aspects may prevent authors from submitting and/or publishing articles in **Eclet. Quim. J.**

- The corresponding author is responsible for listing as coauthors only researchers who have really taken part in the work, for informing them about the entire manuscript content and for obtaining their permission to submit and publish it.
- Authors are responsible for carefully searching for all the scientific work relevant to their reasoning irrespective of whether they agree or not with the presented information.
- Authors are responsible for correctly citing and crediting all data used from works of researchers other than the ones who are authors of the manuscript that is being submitted to **Eclet. Quim. J.**
- Citations of Master's Degree Dissertations and PhD Theses are not accepted; instead, the publications resulting from them must be cited.
- Explicit permission of a nonauthor who has collaborated with personal communication or discussion to the manuscript being submitted to **Eclet. Quim. J.** must be obtained before being cited.
- Simultaneous submission of the same manuscript to more than one journal is considered an ethical deviation and is conflicted to the declaration has been done below by the authors.
- Plagiarism, self-plagiarism, and the suggestion of novelty when the material was already published are unaccepted by **Eclet. Quim. J.**
- The word-for-word reproduction of data or sentences as long as placed between quotation marks and correctly cited is not considered ethical deviation when indispensable for the discussion of a specific set of data or a hypothesis.
- Before reviewing a manuscript, the *Turnitin* antiplagiarism software will be used to detect any ethical deviation.
- The corresponding author transfers the copyright of the submitted manuscript and all its versions to **Eclet. Quim. J.**, after having the consent of all authors, which ceases if the manuscript is rejected or withdrawn during the review process.
- Before submitting manuscripts involving human beings, materials from human or animals, the authors need to confirm that the procedures established, respectively, by the institutional committee on human experimentation and Helsinki's declaration, and the recommendations of the animal care institutional committee were followed. Editors may request complementary information on ethical aspects.
- When a published manuscript in EQJ is also published in other Journal, it will be immediately withdrawn from EQJ and the authors informed of the Editor decision.

• Manuscript Submissions

For the first evaluation: the manuscripts should be submitted in three files: the cover letter as mentioned above, the graphical abstract and the entire manuscript.

The entire manuscript should be submitted as *.doc, *.docx or *.odt files.

The Graphical Abstract (GA) 900 dpi resolution is mandatory for this Journal and should be submitted as *.jpg, *.jpeg or *.tif files as supplementary file.

The cover letter should contain the title of the manuscript, the authors' names and affiliations, and the relevant aspects of the manuscript (no more than 5 lines), and the suggestion of 3 (three) names of experts in the subject: complete name, affiliation, and e-mail).

When appropriate, important data to complement and a better comprehension of the article can be submitted as Supplementary File, which will be published online and will be made available as links in the original article. This might include additional figures, tables, text, equations, videos or other materials that are necessary to fully document the research contained in the paper or to facilitate the readers' ability to understand the work. Supplementary Materials should be presented in appropriate .docx file for text, tables, figures and graphics. The full title of the paper, authors' names and affiliations, and corresponding author should be included in the header. All supplementary figures, tables and videos should be referred in the manuscript body as "Table S1, S2...", "Fig. S1, S2..." and "Video S1, S2 ...".

• Reviewing

The time elapsed between the submission and the first response of the reviewers is around 3 months. The average time elapsed between submission and publication is seven months.

• **Resubmission** (manuscripts "rejected in the present form" or subjected to "revision"): **A LETTER WITH THE RESPONSES TO THE COMMENTS/CRITICISM AND SUGGESTIONS OF REVIEWERS/EDITORS SHOULD ACCOMPANY THE REVISED MANUSCRIPT. ALL MODIFICATIONS MADE TO THE ORIGINAL MANUSCRIPT MUST BE HIGHLIGHTED.**

• Editor's requirements

Authors who have a manuscript accepted in **Eclética Química Journal** may be invited to act as reviewers.

Only the authors are responsible for the correctness of all information, data and content of the manuscript submitted to **Eclética Química Journal**. Thus, the Editors and the Editorial Board cannot accept responsibility for the correctness of the material published in **Eclética Química Journal**.

• Proofs

After accepting the manuscript, **Eclét. Quim. J.** technical assistants will contact you regarding your manuscript page proofs to correct printing errors only, i.e., other corrections or content improvement are not permitted. The proofs shall be returned in 3 working days (72 h) via e-mail.

• Authors Declaration

The corresponding author declares, on behalf of the other authors, that the article being submitted is original and has been written by the stated authors who are all aware of its content and approve its submission. Declaration should also state that the article has not been published previously and is not under consideration for publication elsewhere, that no conflict of interest exists and if accepted, the article will not be published elsewhere in the same form, in any language, without the written consent of the publisher.

• Appeal

Authors may only appeal once about the decision regarding a manuscript. To appeal against the Editorial decision on your manuscript, the corresponding author can send a rebuttal letter to the editor, including a detailed response to any comments made by the reviewers/editor. The editor will consider the rebuttal letter, and if deemed appropriate, the manuscript will be sent to a new reviewer. The Editor decision is final.

• Contact

Gustavo Marcelino de Souza (ecletica@journal.iq.unesp.br)

Submission Preparation Checklist

As part of the submission process, authors are required to check off their submission's compliance with all of the following items, and submissions may be returned to authors that do not adhere to these guidelines.

In **Step 1**, select the appropriate section for this submission.

Be sure that Authors' names, affiliations and acknowledgements were removed from the manuscript. The manuscript must be in *.doc, *.docx or *.odt format before uploading in **Step 2**.

In **Step 3**, add the full name of each author including the ORCID IDs in its full URL ONLY WITH HTTP, NOT HTTPS (eg. <http://orcid.org/0000-0002-1825-0097>).

Add the authors in the same order as they appear in the manuscript in **step 3**.

Be sure to have the COVER LETTER and GRAPHICAL ABSTRACT (according to the Author Guidelines) to upload them in **Step 4**.

Check if you've followed all the previous steps before continuing the submission of your manuscript.

Copyright Notice

The corresponding author transfers the copyright of the submitted manuscript and all its versions to **Eclét. Quím. J.**, after having the consent of all authors, which ceases if the manuscript is rejected or withdrawn during the review process.

Self-archive to institutional, thematic repositories or personal web page is permitted just after publication.

The articles published by **Eclética Química Journal** are licensed under the Creative Commons Attribution 4.0 International License.

SUMMARY

EDITORIAL BOARD.....	3
EDITORIAL.....	4
INSTRUCTIONS FOR AUTHORS.....	5

ORIGINAL REVIEW

Occurrence of caffeine in wastewater and sewage and applied techniques for analysis: a review.....	11
<i>César Augusto Marasco Júnior, Natália da Costa Luchiari, Paulo Clairmont Feitosa Lima Gomes</i>	

ORIGINAL ARTICLES

Influence of Ce(IV) ions amount on the electrochemical behavior of organic-inorganic hybrid coatings in 0.1 mol L ⁻¹ NaCl solution.....	27
<i>Fernando Santos da Silva, Hercílio Gomes de Melo, Assis Vicente Benedetti, Patrícia Hatsue Suegama</i>	

Determination of trace amounts of selenium in natural spring waters and tea samples by catalytic kinetic spectrophotometry.....	57
<i>Ramazan Gürkan, Nevalnur Zeynep Gürkan</i>	

Rapid and selective extraction of trace amount of Pb(II) in aqueous samples using a magnetic ion-imprinted polymer and detection by flame atomic absorption spectrometry.....	73
<i>Saeed Babaee, Seyed Ghorban Hosseini, Mohammad Mirzaei</i>	

Larvicidal activity, molluscicide and toxicity of the essential oil of <i>Citrus limon</i> peels against, respectively, <i>Aedes aegypti</i> , <i>Biomphalaria glabrata</i> and <i>Artemia salina</i>	85
<i>Paulo Roberto Barros Gomes, Marlucy Bezerra Oliveira, Dionney Andrade de Sousa, Jeremias Caetano da Silva, Romer Pêsoa Fernandes, Hilton Costa Louzeiro, Rayone Wesly Santos de Oliveira, Maria do Livramento de Paula, Victor Elias Mouchrek Filho, Maria Alves Fontenele</i>	

Occurrence of caffeine in wastewater and sewage and applied techniques for analysis: a review

César Augusto Marasco Júnior¹, Natália da Costa Luchiarini¹, Paulo Clairmont Feitosa Lima Gomes^{1*}

1 São Paulo State University (Unesp), Institute of Chemistry, 55 Prof. Francisco Degni St, Araraquara, São Paulo, Brazil

*Corresponding author: Paulo Clairmont Feitosa Lima Gomes, Phone: +55 16 3301-9613 email address: paulo.clairmont@unesp.br

ARTICLE INFO

Article history:

Received: December 21, 2018

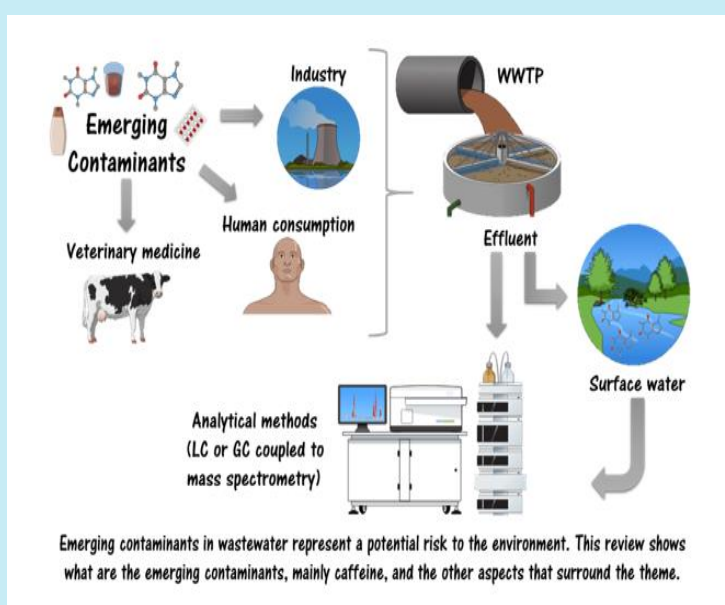
Accepted: September 16, 2019

Published: October 1, 2019

Keywords:

1. emerging contaminants
2. caffeine
3. wastewaters

ABSTRACT: Emerging contaminants are substances found in the environment whose concentrations vary from μg to ng L^{-1} and whose presence in wastewater has gained popularity in the scientific community due to the potential impacts these compounds can cause to the environment. This designation concerns the lack of legislation to regulate their discharge or even to monitor these compounds. Moreover, emerging contaminants are capable of causing harmful effects to nontarget organisms and therefore affect the ecosystem balance. There are several compounds classified as emerging contaminants such as pharmaceuticals, illicit drugs, hormones, pesticides, among others. And among them, caffeine is considered an emerging contaminant and can be highlighted due its presence in medicines, beverages, foodstuff and several other products. In addition, it is a compound used worldwide recognized as a marker of anthropogenic activity. In this review, we present a discussion about emerging contaminants, focusing on caffeine, regulatory aspects that involve the theme, as well as effects on organisms, removal technologies and techniques for analyzing these compounds in environmental matrices.



CONTENTS

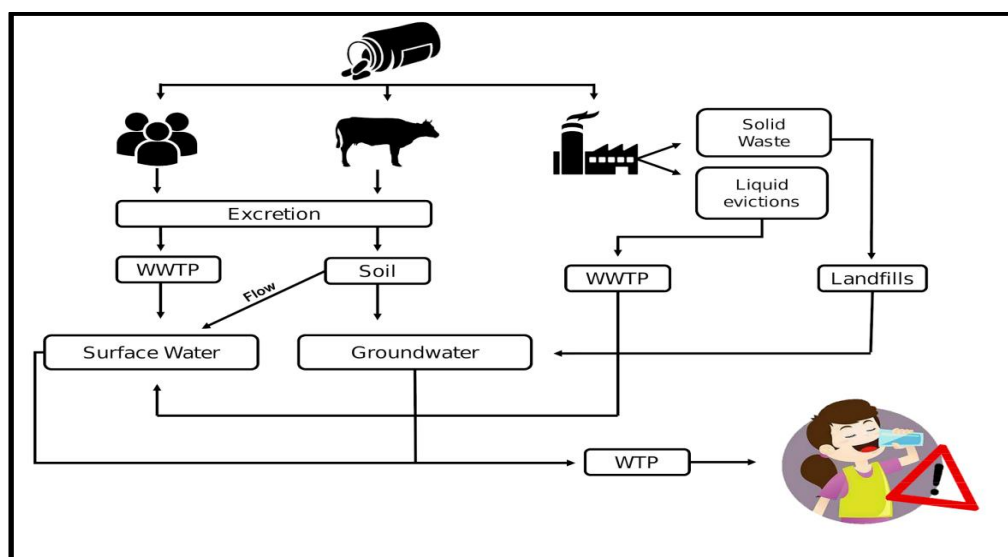
1. Emerging Contaminants
2. Legislation of the emerging contaminants
3. Caffeine as an emerging contaminant: concentrations and ecotoxicological effects
4. Emerging contaminants: removal technologies
5. Emerging contaminants: sample preparation and applied techniques for analysis
6. Conclusion
7. Acknowledgements
8. References

1. Emerging Contaminants

Emerging contaminants are chemicals that present a potential risk to human health or to the environment without any standard or legislation established related to the control of these compounds. These compounds are found in the environment at concentrations ranging from $\mu\text{g L}^{-1}$ to ng L^{-1} in effluents from wastewater treatment plants (WWTPs), untreated sewage, often directly discharged into water bodies, and even in surface and groundwater, respectively¹. Pharmaceuticals and personal care products (PPCPs), plasticizers,

illicit drugs, pesticides, hormones and other compounds can be classified as emerging contaminants and the entry routes of these

contaminants into the environment are diverse, coming from numerous sources, as it can be seen in Figure 1.



Legend: WWTP = wastewater treatment plant; WTP = water treatment plant.

Fig 1. Adapted flowchart of entry routes of PPCPs into the environment¹.

Currently, these compounds are daily present in modern society, and their potential harmful effects to humans and to the environment have generated attention and alertness, in a way, NORMAN network has already been identified at least 700 substances in the European aquatic environment². Even at these concentration levels, these compounds could cause undesirable effects and risks to human health, fauna and environmental flora³⁻⁶.

After consumption, pharmaceutical compounds are metabolized, and a significant part is excreted by humans in domestic sewage or even disposed directly into the sewage network after reaching expiration date. We would like to highlight that the pharmaceuticals, when excreted by humans, reach the sewage network in unchanged form or by metabolites, since the pharmaceuticals are not fully metabolized. For example, caffeine (CAF), after consumption, it is rapidly absorbed into the gastrointestinal system, but approximately 5% is not metabolized, being excreted in the urine, thus reaching the sewage system along with discarded products from food and beverages which contain CAF in their composition⁷.

The same process occurs to pharmaceutical compounds used in veterinary treatment, either for prophylactic purposes or as growth promoters. Furthermore, during the production process by the

pharmaceutical industry, residues of pharmaceutical compounds may be discharged directly in water resources after being used to wash industrial parts and having contaminated this resource. This impact could be harmful if there is no adequate treatment prior to disposal into the sewage system⁸.

The US Environmental Protection Agency (US EPA) defines risk as the possibility of a physical, chemical or biological agent in inducing adverse effects on human health or biological systems⁹. Linked to this information, the presence of contaminants in the environment can be considered a risk to fauna and flora, being able to cause irreversible damages to the organisms exposed to these substances.

However, the concern about these contaminants is limited to the impact these can have on water quality and ecosystem balance, but not only affected humans also the fauna and flora exposed to water containing these substances should gain relevance in the proposed discussion. Moreover, aquatic fauna and flora are non-targeted organisms and spend all or most of the lifecycle in this environment.

Inserted in the problematic of the emerging contaminants in the water bodies and the human exposure to these substances, in 2017, the United Nations (UN) and the United Nations Children's

Fund (UNICEF) presented a report related to the progress in drinking water, sanitation and hygiene stating that about 2.1 billion people do not have access to drinking water and 2.3 billion do not have basic sanitation¹⁰.

In Brazil, according to the National Water Agency (ANA), 9.1 thousand tons of sewage are generated per day, resulting in a current scenario in which 43% of the country's population has sewage collected and treated, 12% use a septic tank, 18% have their sewage collected and untreated and 27% have neither collection or treatment¹¹.

Still, according to the 23rd *Diagnosis of Water and Sewage Services* (2017) published by the National Sanitation Information System (SNIS), about 60% of the urban population has a sewage network, and only 46% of the total sewage generated is treated¹². Table 1 shows the sewage collection and treatment data of each Brazilian macro region according to the SNIS.

Table 1. Sewage collection and treatment data in Brazil.

Region	Sewage collection (%)	Sewage treatment (%)
North	13.0	22.6
Northeast	34.8	34.7
South	50.6	44.9
Southeast	83.2	50.4
Midwest	59.5	52.0

Source: Adapted from National Sanitation Information System¹².

These figures reveal the lack of effective public policies for the collection and treatment of sewage, demonstrating the precarious service of the population in the service of basic sanitation. In this way, much of the untreated sewage is dumped directly into the environment, causing environmental and sanitary problems.

2. Legislation of the emerging contaminants

The authors Sauv e and Desrosiers mentioned Rachel Carson's *Silent Spring* book as a mark in the history of environmental management and sustainability, and also as the first alert to the emerging contaminants issue¹³.

As previously mentioned, these contaminants do not have specific control legislation and the risk assessment of these pollutants should not be

restricted only to their impact on ecosystems, but also to the health of the population, either directly or indirectly, that is constantly in contact with the water containing these pollutants^{2,14}.

The discussion becomes even more relevant, supported by the United Nations World Report on Water Resources Development, which calls for research to understand the emerging contaminants dynamics and to improve technologies to remove these compounds from sewage and wastewater¹⁵.

To accomplish this goal, based on research to study these pollutants, several countries have implemented legal regulations for some substances, which have been prioritized according to the adverse effects they cause in organisms such as fish from *Danio rerio* species and mollusk *Mytilus galloprovincialis* among others¹⁶.

The United States and the European Union have demonstrated some concern about this issue by creating directives to regulate or control the disposal of these substances.

The Environmental Protection Agency (EPA) is the US agency responsible for the legal regulation of the substance's disposal into the environment, through two federal laws: the Clean Water Act (CWA) and the Safe Drinking Water Act (SDWA)¹⁷.

One of the first steps by US agencies to attempt to establish limits and regulations on PPCPs came under the Food Quality Protection Act (FQPA) and amendments to the SDWA. These amendments authorized the US EPA to track chemicals and formulations that could show some type of endocrine activity if they reached any water supply line¹⁴.

EPA uses two main regulations to monitor emerging contaminants in water: The Contaminant Candidate List (CCL) and the Unregulated Pollutant Monitoring Rule (UCMR).

The CCL lists water contaminants that are not subject to any regulations, setting priorities to assess the occurrence and toxicity of these contaminants. The SDWA regulates that the EPA must publish the CCL every five years and regulate at least five contaminants, demonstrating the potential adverse effects a contaminant can exert on human health and the environment¹⁷.

EPA made available in 2016 the Contaminant Candidate List-4 (CCL-4), the fourth update presents contaminants candidates for future regulations. It includes, among the hundred chemical compounds such as estrogens, pharmaceutical compounds, personal care and

hygiene products, industrial products and pesticides^{16,18}. Moreover, the fifth update of this list (CCL-5) is already under development.

The second mechanism is the UCMR, developed in coordination with the CCL. EPA collects data about contaminants suspected of being present in drinking water and that do not have limits defined by SDWA. The results are compared with ecotoxicological research and risk assessment to determine if a contaminant should have an established threshold and thus be inserted into the CCL¹⁷.

In the same way, the European Environment Agency (EEA) assists member countries of the European Union (EU) in making relevant decisions for environmental improvement and the impact of the adopted policies¹⁹. The EEA works under the European Water Framework Directive (EU WFD) with the aim of ensuring quality for all EU waters. Given the large number of chemicals released into the environment, Von der Ohe *et al.* have presented a new approach for assessing the ecotoxicological risk used to prioritize 500 organic contaminants²⁰.

In the European Union, actions to raise the priority compounds to be legislated began in 1999¹⁶. By taking the European Union's regulations as an example, the REACH (registration, evaluation, authorization and restriction of chemicals) regulates the use of almost all chemicals into the European Union (EC Regulation No. 1907/2006)². To facilitate this study, in 2005, the European Commission funded the NORMAN project to promote a permanent network of reference laboratories and research centers to support EU member countries concerning the environmental impacts caused by the adoption of their economic policies²¹.

The creation of laws and regulations presents itself as a viable way to aid in the control of these contaminants. Currently, most of these compounds are not regulated in many parts of the world, including in Brazil, but as discussed earlier there are some attempts in the European Union and the US to try to reduce environmental contamination by these substances. It is therefore believed that effective regulations are the basis for efficient water resource management.

3. Caffeine as an emerging contaminant: concentrations and ecotoxicological effects

Caffeine or 1,3,7-trimethylxanthine, with molecular formula corresponding to $C_8H_{10}N_4O_2$, as

it can be seen in Figure 2, is an alkaloid from the xanthine group naturally found in the environment.

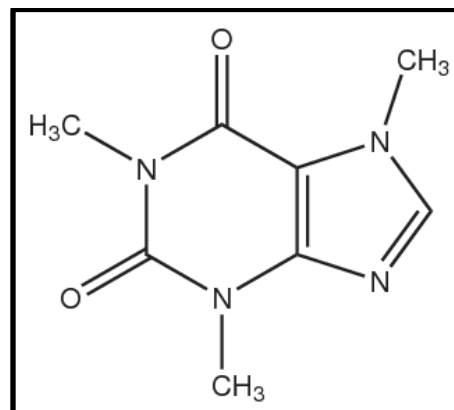


Fig 2. Planar structure of caffeine.

Caffeine is present in tea, chocolate, sodas and in a wide variety of food consumed worldwide, culminating in its occurrence in wastewater and eventually causing aquatic ecosystems impairment^{22,23}. Moreover, it can be considered as a marker of anthropogenic activity, since its consumption is thoroughly related to human habits^{16,23,24}, and it is also persistent in environmental matrices, standing out as one of the most ubiquitous wastewater microcontaminants²⁵.

In order to evaluate the water quality and to observe possible contamination by effluents produced by the anthropogenic action, it is important to determine the presence of such contamination markers.

The ideal marker should assertively indicate the contamination source, and moreover, establish a quantitative relationship with the contamination by other chemical compounds. According to Gonçalves, Rodrigues and Silva-Filho (2016), the average global consumption per day of caffeine is approximately 70.0 mg per person²⁴. However, countries like Switzerland, United Kingdom and the United States of America have this average consumption per person estimated at 300 mg, 440 mg and 210 mg, respectively²⁵.

Caffeine presents stability, high solubility and low partition coefficient octanol-water (K_{ow}). These characteristics permits caffeine detection in the environment which are essential to correlate the risk it may offer to humans and ecosystems^{16,22,26,27}. Recent studies confirm the presence of this substance in environmental matrices.

Edwards, Kulikov and Garner-O'Neale (2015) analyzed wastewater from two WWTPs in Barbados, a city with about 300 thousand people,

and the concentrations of caffeine determined ranged from 0.100 – 6.90 $\mu\text{g L}^{-1}$ ²⁵. Senta *et al.* (2015) determined caffeine at concentrations of 17.6-67.6 $\mu\text{g L}^{-1}$ in 13 WWTPs located in northern, central and southern Italy²⁸. These WWTPs are responsible for the collection and treatment of sewage of about 50 to 500 thousand inhabitants, according to the region in which each one is located.

Even in one of the most remote regions of the planet, Antarctic Peninsula, González-Alonso *et al.* (2017) determined caffeine in the concentration of 71.3 ng L^{-1} during the period from December 2012 to February 2013 in ten sites that were thought to have anthropogenic impact, whether due to tourism or proximity to human settlements²⁹.

Williams *et al.* (2019) determined caffeine at concentrations up to 37.5 $\mu\text{g L}^{-1}$ when analyzing surface water of the Ahar River, which flows through the city of Udaipur, India, a city with about 450 thousand people, which has no wastewater treatment³⁰.

In Brazil, Ferreira (2005) detected caffeine in the concentration of 134 to 147 ng L^{-1} in the Guanabara Bay, Rio de Janeiro (RJ), Brazil, while in the Leopoldina Basin the concentration of caffeine in the water samples collected from the rivers reached concentrations of 160 to 357 $\mu\text{g L}^{-1}$ ²⁷. The sample area of the study is highly populated, with an estimated population of 1,135,000 inhabitants, distributed among 30 housing projects and 8 slums, accounting for the largest portion of untreated domestic and industrial sewage discharged in the Guanabara Bay.

Sposito *et al.* (2018) detected caffeine in all analyzed samples of the Dourados and Brilhante rivers³¹. The highest concentration of caffeine determined was 1040 ng L^{-1} , measured at a point near the city of Dourados, a city with 218,000 inhabitants.

Gonçalves, Rodrigues and Silva-Filho (2016) analyzing water from the Paquequer River determined caffeine from 0.150 - 47.5 $\mu\text{g L}^{-1}$ ²⁴. The Paquequer River flows through the urban area of the city of Teresópolis, with a population of approximately 125,000 inhabitants. The city of Teresópolis has no wastewater treatment plant and therefore Paquequer is the main body of water that receives most of the urban drainage and sanitary effluents drained without any treatment.

In the study of Campanha *et al.* (2018), to investigate the occurrence and spatiotemporal distribution of some important pharmaceuticals,

hormones, and triclosan in surface water of the Monjolinho River determined caffeine at concentration of 129,585 ng L^{-1} ³². The Monjolinho River is located in São Carlos city, central region of São Paulo state. This city houses about 220,000 inhabitants and has an extensive industrial park, especially in the sectors of automotive, refrigeration, paper and cardboard, school supplies, cosmetics, and textiles.

Montagner and Jardim (2011) determined caffeine in the Atibaia River and the levels varied between 174 and 127 ng L^{-1} ³³. The Atibaia River basin, located in São Paulo state (Brazil), covers an area of approximately 2,800 km^2 and is the main source of public supply in the city of Campinas, in São Paulo state, Brazil.

All these studies show that caffeine besides to be an anthropogenic marker, is an emerging contaminant and thus assessing exposure to a given risk is important to ensure the integrity of human health and the diversity of aquatic ecosystems³⁴⁻³⁶.

Aguirre-Martínez, Delvalls and Martín-Díaz (2015) have studied the markers effects such as caffeine at concentrations of 0.1, 5.0, 15, 50 $\mu\text{g L}^{-1}$ and carbamazepine at concentration levels of 0.1, 1.0, 10, 50 $\mu\text{g L}^{-1}$ in mussels of the species *Corbicula fluminea*³⁷. After 21 days of experiment, it was observed breaks in the DNA chain in the digestive gland tissues.

Cruz *et al.* (2016) demonstrated that long-term exposure to caffeine concentrations at $\mu\text{g L}^{-1}$ level induced oxidative stress in mollusks of *Ruditapes philippinarum*³⁸.

Pires *et al.* (2016) studied the caffeine effects on annelids from species *Arenicola marina* and *Diopatra neapolitana*³⁹. After 28 days of exposure, oxidative stress was induced in both species. *D. neapolitana* presented a 12.5 % mortality rate at concentrations of 3.00 and 18.0 $\mu\text{g L}^{-1}$. *A. marina* mortality rate was recorded only at the highest concentration (18.0 $\mu\text{g L}^{-1}$), where 22.2 % of the individuals did not survive.

According to the mentioned characteristics and the intense consumption of pharmaceutical drugs and food containing caffeine, these habits affect several water compartments, such as surface or groundwater, or even sediments and soils.

Based on these previous published studies is clear the concern to monitor caffeine in wastewater, although, other emerging contaminants could be found increasing the risks of harmful effects. Also associated with this concern the current wastewater treatment plants are

designed only to reduce the load of organic compounds such as, nitrogen, phosphorus and sulfur compounds, odor control, wastewater turbidity and reduce microbial pathogens.

In order to achieve WWTP aims different treatment technologies using bioreactors such as up-flow anaerobic sludge blanket (UASB) reactors, aeration ponds, aerated lagoons, activated sludge and membrane bioreactors. All these technologies were not designed for the removal of emerging contaminants^{16,40}. Due to the growing need to reuse water improvements in sewage collection and treatment systems are essential.

4. Emerging contaminants: removal technologies

The conventional sewage treatments were designed to remove or to decrease the pathogens and the charge of organic/inorganic pollutants to avoid the eutrophication of lakes and rivers which the wastewater is dispensed. In general, WWTPs have been not designed to remove residues of organic compounds such as pharmaceuticals compounds which are frequently detected in effluents and influents from wastewater treatment plants⁴¹.

According to the pharmacodynamics and pharmacokinetics, pharmaceutical compounds could be discharged in the environment as a metabolite, unchanged or conjugated form. In the WWTP these compounds are either partially retained in the sludge or metabolized. Their removal in WWTPs is variable and depends the substance properties and process conditions (e.g. sludge retention time, hydraulic retention time, temperature and organic loading).

Activated sludge is the most used process present in sewage treatment plants, according to Buttiglieri and Knepper (2008, p. 3)⁴¹ "is the biomass produced in wastewater by the growth of organisms in aeration tanks in the presence of dissolved oxygen responsible for removal of organic and inorganic compounds". In Brazil, associated to activated sludge there may be other sewage treatment technologies such as: stabilization ponds or anaerobic sludge blanket bioreactors.

Many technologies have been studied and developed involving the emerging contaminants removal such as membrane bioreactor, ozonation, photocatalytic processes and anaerobic bioreactors.

In the paragraphs below, we present a brief discussion about each one of these technologies.

The membrane bioreactor technology (MBR) combines biological-activated sludge process and membrane filtration. This technology has emerged due to the increasing need for water reuse and together with a better understanding of the emerging contaminants dynamics in the wastewater. The MBR demonstrate suitable to become a technology capable to remove these contaminants. The most widely applied membrane separation processes are microfiltration (MF), ultrafiltration (UF), nanofiltration (NF), reverse osmosis (RO), electrodialysis (ED) and electro deionization (EDI)⁴².

The two main processes that use MBR technology are reverse osmosis and nanofiltration. Both mechanisms remove efficiently various substances, being a technology of choice for emerging contaminants removal in developed countries⁴³.

Anaerobic bioreactors are units containing a diverse microbiota which promotes different types of chemical and biochemical reactions applied in the wastewater treatment. These units are used in the Southeast of Brazil since it requires climate with average of temperature of 20 °C to avoid low microbial activity. The anaerobic reactors present advantages: demand low land area, present low energy consumption compared to aerobic processes, microbiota requires low nutrition substrate, low production of solids compared to aerobic processes, produces methane and hydrogen which could be used as power source and present tolerance to wastewater containing high organic load. Although, the anaerobic bioreactors present as disadvantages: possible generation of bad odors such as H₂S, not suitable to remove nitrogen, phosphorus and pathogen, requires post-treatment, the anaerobic microbiota present a complex biochemistry and it is susceptible to inhibition, bioreactor to reach steady-state regimen can be slow. The removal process involving anaerobic bioreactors are mainly adsorption in the biomass and chemical and biochemical reactions with the microbial community present in the biomass⁴⁴.

The UASB bioreactor expanded the application of anaerobic bioreactors in the sewage treatment system present in many different Brazilian cities. There are many other anaerobic bioreactors configurations applied to remove emerging contaminants. For example, horizontal fixed-bed anaerobic bioreactor (HAIB) is a versatile and

simple to be maintained. HAIB is a fixed-bed bioreactor containing biomass immobilized in polyurethane foams. The polyurethane foams permit the biomass growth and attachment. The wastewater flow through as tubular ideal reactor. In the different sections along the bioreactor length, the anaerobic microbial community is diverse favoring different types of metabolism, therefore, the removal of organic compounds and wastewater with high organic load^{45,46}.

The HAIB bioreactor was successfully applied for removal of benzene, toluene, ethyl benzene and ethanol⁴⁷, pentachlorophenol⁴⁸, bioremediation of gasoline-contaminated groundwater⁴⁶, linear alkylbenzene sulfonate⁴⁹, sulfamethoxazole and ciprofloxacin⁵⁰, sulfamethazine^{51,52}, sulfamethoxazole and trimethoprim⁵³.

Ozone has a strong oxidative action allowing to be used in the treatment of surface water, groundwater or wastewater. Ozone-based technologies have the common objective to improve the disinfection and removal of organic compounds in the water. The search for this optimization is not only due to the fact that it is an expensive oxidant, but also because ozone induces the formation of toxic intermediate radicals. In addition, coupling ozonation with other processes, such as coagulation and filtration or even with the aid of UV, improves the biodegradability and organic compounds removal⁵⁴.

The advanced oxidative processes (AOPs) have high mineralization capacity of organic matter. However, the large-scale applications for these oxidative processes are still scarce and future applications are aimed with the use of solar energy and photocatalysis. Therefore, two AOPs have concentrated most of the studies which are the homogeneous catalysis by the photo-Fenton reaction and the heterogeneous catalysis assisted by UV/TiO₂⁵⁵.

Although there are many technologies for wastewater treatment, some mentioned in this article, adsorption has still been widely used and studied, albeit limited by the appearance of new materials.

The most common sorbent materials used are activated carbon, zeolites, silica gel and activated alumina. However, advances in nanoscale technology have led to the development of new nanomaterials, mainly the carbon-based materials which are already applied in water treatment processes and carbon-based material obtained from

solids residues (biochar) are environmentally friendly⁵⁶.

The development of new technologies and materials for wastewater treatment and water supply have grown significantly. However, there is a need for advancement in wastewater treatment technologies designed for emerging contaminants removal. As there is no single treatment capable to remove all compounds, moreover, there are different types of emerging contaminants, with distinct physicochemical properties which would require different treatments technologies.

Therefore, treatment technology suitable to be applied should be chosen according to the characteristics of the effluent (organic load, turbidity, conductivity, chemical and biochemical oxygen demand, emerging contaminants present). To evaluate the removal efficiency from a treatment technology is fundamental to apply analytical tests whether a target compounds or target class of compounds are evaluated in order to estimate the treatment efficiency.

The development of new treatment technologies is mainly focus in the removal efficiency besides the transformation products formed during the treatment applied. There is a lack of studies in this area requiring toxicity research involving the compounds formed during the wastewater treatment.

5. Emerging contaminants: sample preparation and applied techniques for analysis

According to the arguments presented above, and, because there is no specific legislation that regulates the disposal of these contaminants in the environment, the scientific community raised the concern about the development of analytical methods able to determine emerging contaminants present in several environmental matrices.

Moreover, during 2000-2010 occurred a huge development in analytical instrumentation, specially, in equipment using mass spectrometry. The development of new configuration improving the sample ionization, new mass analyzer such as Orbitrap or combining mass analyzers such as quadrupole (Q) with linear ion-trap (QTRAP) and Q with time-of-flight (QToF) permitted to detect compounds in pg L^{-1} to $\mu\text{g L}^{-1}$ concentration. This analytical advancement was essential to found emerging contaminants in wastewater and sewage.

Currently, most of the literature published on the issue of emerging contaminants is focused on

the monitoring of target compounds. This traditional approach may prove to be insufficient since it excludes the metabolites or possible transformation products generated which could presents the environmental relevance. And many of these transformation products or metabolites may be “ecotoxicologically” more harmful than the target compound itself. Despite the efforts, it is still difficult to screen untargeted compounds due to a lack of analytical standards and databases that allow the search of a possible structure for a given elemental composition within the instrument software⁵⁷.

Although the occurrence of pharmaceutical compounds in the environment has been reported for more than 20 years, in 2007 official methods have emerged using liquid and gas chromatography coupled to mass spectrometry for the determination of these compounds, respectively^{58,59}. Thus, the use of LC-MS/MS for the determination of these substances were systematized, mainly in Europe and the United States of America⁶⁰.

The determination of pharmaceutical compounds in environmental samples can also be performed by gas chromatography coupled to mass spectrometry (GC-MS). However, many compounds are not thermally stable, making GC-MS determinations difficult, and derivatization reactions would be essential. Since most pharmaceuticals are soluble in the mobile phase, high performance liquid chromatography coupled to sequential mass spectrometry (LC-MS/MS) has been widely used as a method of analysis.

According to Silva and Collins (2011), this fact can be explained by the versatility of the LC-MS/MS technique, which can be used for analytes with different polarities⁶¹. This method is able to reach limits of detection and quantification at ng L^{-1} concentration level.

Silva *et al.* (2011) determined simultaneously 43 drugs in surface waters of the Ebro river basin, Spain, of different therapeutic classes, such as anticonvulsants, anti-inflammatories, antidepressants, hormones and others in a concentration range of the order of ng L^{-1} by liquid chromatography coupled to a tandem mass spectrometry (LC-MS/MS)⁶². Stewart *et al.* (2014) carried out a multi-residue analysis of 46 pharmaceutical drugs in estuaries also using LC-MS/MS, and it was possible to quantify 21 of the substances classified as emerging contaminants present located in Auckland, New Zealand⁶³.

Despite the several advances in analytical instrumentation, the sample preparation step is still necessary and extremely important. Environmental samples are complex, and it is essential to pre-concentrate the analytes, eliminate or remove with high efficiency interferences and sample components. This process is essential to decrease the matrix effect and to avoid possible damages to the equipment.

Previous published papers as Silva *et al.* (2011)⁶² and Williams *et al.* (2019)³⁰ presented solid phase extraction (SPE) as the technique of choice for conducting their experiments and this technique of sample preparation proved to be satisfactory for the determination of emerging contaminants.

Introduced in the early 1970s, the SPE is an extraction technique by sorption. This technique appeared to replace the traditional liquid-liquid extraction (LLE), since the LLE requires large volumes of samples and solvents, there is the formation of emulsion and still the solvents used in this kind of extraction are toxic like chloroform, toluene, hexane and others, and end up generating toxic and non-environmentally friendly waste^{64,65}.

SPE is currently the most popular technique of sample preparation and the most common form uses solid phases called sorbents immobilized in a cartridge. The commercially available solid phases are based on organic groups such as C18, C8, cyclohexyl, phenyl and others chemically bonded to silica. These phases are the same used in the columns of liquid chromatography. Besides these, other phases are characterized as polystyrene divinylbenzene, with high surface area, great stability in different pH ranges and high retention capacity, and the graphitized carbon, responsible for low resistance mechanical materials, homogeneous, crystalline structure and great retention power⁶⁴.

Although there is an extensive variety of commercially available sorbents, the most commonly known and used commercial hydrophilic sorbent is Oasis HLB from Waters. This material is a macroporous poly(N-vinylpyrrolidone-divinylbenzene) (PVP-DVB) copolymer with a high surface area. This stationary phase proved to be versatile, becoming popular for the sample preparation due to being suitable to extract compounds with different polarities, cleaning of complex matrices with effectiveness in terms of interference removal⁶⁶. This stationary phase was chosen in many studies of emerging

contaminants in environmental samples for the extraction and determination of pharmaceuticals compounds^{29,62}, illicit drugs^{67,68} among other compounds.

The analytical method development using SPE in environmental analysis allowed the use of large sample volumes, around 50 to 1000 mL⁶⁶, and this way as indicated by Jardim (2010, p. 15)⁶⁴ “the concentration can be increased by a factor of 100 to 5000, making possible the qualitative and quantitative analysis at the trace levels.”

Other hydrophilic polymeric sorbents have been also developed, such as Bond Elut Plexa (Agilent Technologies)⁶⁶ or Strata-X (Phenomenex)^{66,69}, which are the most commonly used chemically modified sorbents with polar functionalities. In the Table 2, we show some studies and the results obtained, mainly for the extraction of pharmaceutical compounds in environmental samples, using the stationary phases for SPE discussed in this article.

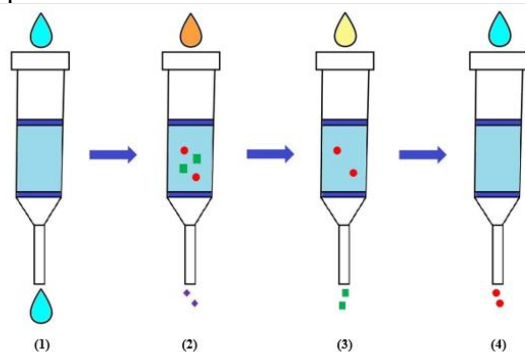
Table 2. Application of some commercial polymeric sorbents for SPE.

Sorbent	Target analytes	Matrix	Sample volume (mL)	Recovery (%)	Matrix effect (%)	LD (ng L ⁻¹)	Reference
Oasis HLB (Waters)	Pharmaceuticals	Surface and wastewater	50.0	21.0-116	6.00-123	1.00-500*	[70]
	Pharmaceuticals	Surface and wastewater	100-500	35.0-116	< 25.0	0.500-60.0	[71]
	Illicit drugs	Surface water	250	71.0-104	80.0-100	0.0100-1.54	[68]
Strata-X (Phenomenex)	Pharmaceuticals	Wastewater	100	26.0-117	70.0-130	0.100-5.00	[72]
Bond Elut Plexa (Agilent Technologies)	PCPs	Surface water	500	46.0-101	45.0-108	1.00-4.00	[73]

Legend: LD = limit of detection; *method quantification limits.

Source: Withdrawn and adapted from Gilart *et al.*⁶⁶.

The SPE is a technique that requires at least four steps for the sample preparation: sorbent conditioning, sample loading, clean-up (remove the interferers and matrix concomitants) and elution of the analytes^{64,69,74}. Figure 3 shows these steps:



Legend:

● Analytes

■ ◆ Interferers

Fig 3. Adapted SPE analytical steps: 1) conditioning; 2) loading sample; 3) wash; 4) elution⁷⁴.

This technique has extensive applications being a consolidated technique in sample preparation, mainly in environmental field. Moreover, EPA method establishes SPE as sample preparation technique of choice for organic contaminants^{58,74}.

It is also worth mention the development of new SPE sorbent materials produced several modifications in recent years, with most based on miniaturization and automation resulting in novel extraction techniques, such as solid phase dynamic extraction (SPDE), microextraction by packed sorbent (MEPS), matrix solid phase dispersion (MSPD) stir-bar sorptive extraction (SBSE), solid phase microextraction (SPME) and other technologies also applied in the sample preparation of wastewaters^{66,74}. However, in this review, we focus only on traditional SPE (off-line) and on-line.

Although a conventional setup of SPE (SPE off-line) is the most common choice and the most used method for the sample preparation it is a tedious and time-consuming procedure. In this mode the chromatography analysis is separated from sample preparation procedure and in order to avoid sample

cross-contamination, sample loss, decrease in the volume of solvents usage and increase the analytical frequency, it is fundamental to integrate sample preparation and chromatographic separation.

On-line SPE incorporates all the steps involved in conventional SPE into an integrated system for chromatography. In order to effectively occur this integration between sample preparation and chromatography, a strategy called column switching mode enables integrated analysis in an efficient and productive way^{69,74}.

The coupling of this technique has become accessible, based on an instrumental arrangement that includes the coupling of a six-port valve with two positions to the system^{74,75}. In this way, the system works using two pumps, in which a pump loads the sample into the sample preconcentration column, where the analytes are retained. The other pump then elutes the analytes using the gradient elution for the analytical column^{74,75}. The used system can be seen in the Figure 4.

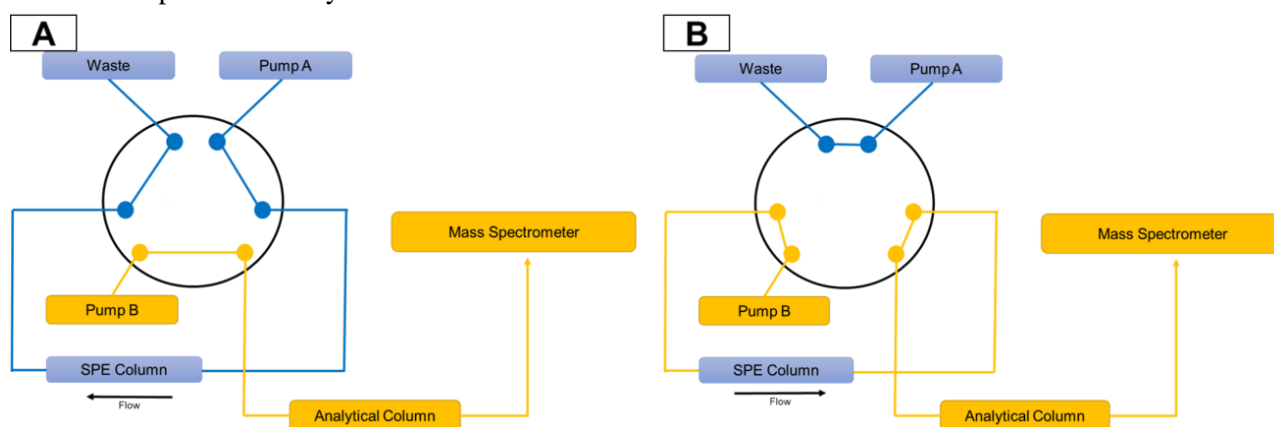


Fig 4. Column switching configuration in backflush mode: a) loading; b) elution.

According to mentioned above and demonstrated by the Figure 4, the on-line mode overcomes some limitations of off-line mode, in addition to avoid problems such as sample cross-contamination, minimizes the volume of waste generated and reduces the amount of solvent used,

although it might require available dedicated devices or instrumental arrangement with valves and pumps⁷⁵. Table 3 shows some advantages and disadvantages among SPE on-line and off-line.

Table 3. Comparison between SPE configurations.

SPE on-line	SPE off-line
Requires small sample volumes	High sample volumes are necessary
Reusable cartridges	Disposable cartridges
Less flexibility, most systems do not allow coupling	Sequential extraction and possibility of using different combinations of cartridges connected in series
Direct and fast elution of the sample after preconcentration	Risk of degradation of compounds (longer overall analysis time)
Minimal consumption of organic solvents	Consumption of organic solvents for elution
Reduced analysis time and high throughput	Longer analysis time
Expensive equipment (requires auxiliary instruments such as pumps and valves assemblies)	Economical equipment

Source: Withdrawn and adapted from Rodriguez-Mozaz *et al.*⁷⁶.

The development of new stationary phases permitted to develop suitable methods in complex environmental matrices and provide an efficient and well-succeed analysis. In addition, the sample preparation procedure automation through column switching and coupling to the detection system (LC-MS/MS) permitted a great progress in analyzing environmental samples, especially emerging contaminants, proving to be fast, accurate and with reduced solvent consume.

6. Conclusion

Emerging contaminants have attracted the scientific community attention due to the wide variety of compounds that fit into this class. Those compounds can cause harmful effects to ecosystems balance and even to human health, besides the lack of research related to this topic.

In this review, the focus was given to caffeine, a natural substance present in several consumed products such as medicines, personal care products and food in general. Considered as a marker of anthropogenic activity, caffeine has been the subject of ecotoxicity studies at similar concentrations to those found in the environment and adverse effects on organisms of several species have been reported.

The risks caused by caffeine and emerging contaminants to the biota and the lack of legislation capable of regulating or controlling the disposal of these contaminants into the environment are the main issue.

Moreover, we can notice the efforts on the development of new sorbent materials, as well as on the advancement of analytical instrumentation in order to reach ever lower concentrations. Among the existing sample preparation techniques, SPE is considered the most extensively used technique due to its advantages that include simplicity, flexibility, automation possibilities and many other factors. SPE is a technique that allows enhancement to further increase the quality of analysis with better precision and accuracy.

Allied to this, seeking alternative solutions or technologies for emerging contaminants removal in association to the mass spectrometry and sample preparation advancement are an important role to evaluate the proposed removal technology. The development of these analytical techniques and methods advancement provide essential pieces of information to understand the emerging contaminants dynamics in the environment as well

as permit monitoring them in the most diverse environmental matrices supporting ecotoxicological researches related to human, fauna and flora effects.

Therefore, government and environmental authorities' decisions should be based on scientific data which permits to elaborate normative controlling the sewage and wastewater discharge, which would reduce the emerging contaminants present in the wastewater and others environmental matrices.

7. Acknowledgements

The authors are grateful to Fundação de Amparo à Pesquisa do Estado de São Paulo (FAPESP No. 2016/03369-3, 2018/11700-7, 2018/22393-8 and INCT-DATREM No. 14/50945-4), Conselho Nacional de Desenvolvimento Científico e Tecnológico (CNPq), Coordenação de Aperfeiçoamento de Pessoal de Nível Superior (CAPES) and the Institute of Chemistry – São Paulo State University (IQ/UNESP).

8. References

- [1] Quesada, H. B., Baptista, A. T. A., Cusioli, L. F., Seibert, D., Bezerra, C. O., Bergamasco, R., Surface water pollution by pharmaceuticals and an alternative of removal by low-cost adsorbents: A review, *Chemosphere* 222 (2019) 766-780. <https://doi.org/10.1016/j.chemosphere.2019.02.009>.
- [2] Geissen, V., Mol, H., Klumpp, E., Umlauf, G., Nadal, M., Van Der Ploeg, M., Van De Zee, S. E. A. T. M., Ritsema, C. J., Emerging pollutants in the environment: A challenge for water resource management, *International Soil and Water Conservation Research* 3 (1) (2015) 57-65. <https://doi.org/10.1016/j.iswcr.2015.03.002>.
- [3] Aubakirova, B., Beisenova, R., Boxall, A., Prioritization of pharmaceuticals based on risks to aquatic environments in Kazakhstan, *Integrated Environmental Assessment and Management* 13 (5) (2017) 832-839. <https://doi.org/10.1002/ieam.1895>.
- [4] Bai, X., Lutz, A., Carroll, R., Keteles, K., Kenneth, D., Murphy, M., Nguyen, D., Occurrence, distribution, and seasonality of emerging contaminants in urban watersheds. *Chemosphere* 200 (2018) 133-142. <https://doi.org/10.1016/j.chemosphere.2018.02.106>.
- [5] Biel-Maeso, M., Corada-Fernández, C., Lara-Martín, P. A., Monitoring the occurrence of

- pharmaceuticals in soils irrigated with reclaimed wastewater, *Environmental Pollution* 235 (2018) 312-321. <https://doi.org/10.1016/j.envpol.2017.12.085>.
- [6] Chen, W., Cheng, J., Lin, X. Systematic screening and identification of the chlorinated transformation products of aromatic pharmaceuticals and personal care products using high-resolution mass spectrometry, *Science of the Total Environment* 637-638 (2018) 253-263. <https://doi.org/10.1016/j.scitotenv.2018.05.011>.
- [7] James, J. E., Critical review of dietary caffeine and blood pressure: a relationship that should be taken more seriously, *Psychosomatic Medicine* 66 (1) (2004) 63-71. <https://doi.org/10.1097/10.PSY.0000107884.78247.F9>.
- [8] Gros, M., Rodríguez-Mozaz, S., Barceló, D., Rapid analysis of multiclass antibiotic residues and some of their metabolites in hospital, urban wastewater and river water by ultra-high-performance liquid chromatography coupled to quadrupole-linear ion trap tandem mass spectrometry, *Journal of Chromatography A* 1292 (2013) 173-188. <https://doi.org/10.1016/j.chroma.2012.12.072>.
- [9] United States Environmental Protection Agency. About risk assessment: learn about risk assessment. <https://www.epa.gov/risk/about-risk-assessment#whatisrisk>.
- [10] World Health Organization (WHO); United Nations Children's Fund (UNICEF), Progress on Drinking Water, Sanitation and Hygiene: 2017 Update and SDG Baselines. https://www.unicef.org/publications/index_96611.html.
- [11] Agência Nacional das Águas (ANA). Atlas Esgotos: Despoluição das bacias hidrográficas. <http://atlasesgotos.ana.gov.br>.
- [12] BRAZIL., 23rd Diagnosis of Water and Sewage Services – 2017, Ministry of Regional Development, National Sanitation Information System. <http://www.snis.gov.br/component/content/article?id=175>.
- [13] Sauv e, S., Desrosiers, M., A review of what is an emerging contaminant, *Chemistry Central Journal* 8 (15) (2014) 1-7. <https://doi.org/10.1186/1752-153X-8-15>.
- [14] Bolong, N., Ismail, A.F., Salim, M.R., Matsuura, T., A review of the effects of emerging contaminants in wastewater and options for their removal, *Desalination* 239 (2009) 229-246. <https://doi.org/10.1016/j.desal.2008.03.020>.
- [15] United Nations World Water Assessment Programme (WWAP). 2017. The United Nations World Water Development Report 2017. Wastewater: The Untapped Resource. Paris, UNESCO.
- [16] Montagner, C. C., Vidal, C., Acayaba, R. D., Contaminantes emergentes em matrizes aquáticas do Brasil: cenário atual e aspectos analíticos, ecotoxicológicos e regulatórios, *Química Nova* 40 (9) (2017) 1094-1110. <https://doi.org/10.21577/0100-4042.20170091>.
- [17] Guasch, H., Serra, A., Corcoll, N., Bonet, B., Leira, M., Metal ecotoxicology in fluvial biofilms: potential influence of water scarcity. In: Sabater, S., Barceló, D., (Eds) *Water Scarcity in the Mediterranean. The Handbook of Environmental Chemistry*, Springer Berlin Heidelberg, 2010. <https://doi.org/10.1007/978-3-642-03971-3>.
- [18] EPA. Contaminant Candidate List (CCL) and Regulatory Determination. <https://www.epa.gov/ccl/contaminant-candidate-list-4-ccl-4-0>.
- [19] Islas-Flores, H., Gómez-Oliván, L. M., Legislation Controlling the Discharge of Pharmaceuticals into the Environment. In: *The Handbook of Environmental Chemistry, Ecopharmacovigilance*, Springer 66 (2017) 95-117. https://doi.org/10.1007/698_2017_170.
- [20] Von Der Ohe, P. C., Dulio, V., Slobodnik, J., Deckere, E., Kühne, R., Ebert, R-U., Ginebreda, A., Cooman, W., Sch urman, G., Brack, W., A new risk assessment approach for the prioritization of 500 classical and emerging organic microcontaminants as potential river basin specific pollutants under the European Water Framework Directive, *Science of the Total Environment* 409 (11) (2011) 2064-2077. <https://doi.org/10.1016/j.scitotenv.2011.01.054>.
- [21] Dulio, V., Van Bavel, B., Brorstr m-Lund n, E., Harmsen, J., Hollender, J., Schlabach, M., Slobodnik, J., Thomas, K., Koschorreck, J., Emerging pollutants in the EU: 10 years of NORMAN in support of environmental policies and regulations, *Environmental Sciences Europe* 30 (5) (2018) 1-13. <https://doi.org/10.1186/s12302-018-0135-3>.
- [22] Wu, J., Yue, J., Hu, R., Yang, Z., Zhang, L., Use of caffeine and human pharmaceutical compounds to identify sewage contamination, *International Journal of Biomedical and Biological Engineering* 2 (8) (2008) 289-293. <https://publications.waset.org/8464/pdf>.
- [23] Montagner, C. C., Umbuzeiro, G. A., Pasquini, C., Jardim, W. F., Caffeine as an indicator of estrogenic activity in source water. *Environmental Science:*

- Processes Impacts 16 (8) (2014) 10-13. <https://doi.org/10.1039/C4EM00058G>.
- [24] Gonçalves, E. S., Rodrigues, S. V., Silva-Filho, E. V., The use of caffeine as a chemical marker of domestic wastewater contamination in surface waters: seasonal and spatial variations in Teresópolis, Brazil, *Revista Ambiente & Água* 12 (2) (2016) 192-202. <https://doi.org/10.4136/ambi-agua.1974>.
- [25] Edwards, Q. A., Kulikov, S. M., Garner-O'neale, L. D., Caffeine in surface and wastewaters in Barbados, West Indies, *Springer Plus* 4 (57) (2015) 1-12. <https://doi.org/10.1186/s40064-015-0809-x>.
- [26] Gracia-Lor, E., Castiglioni, S., Bade, R., Been, F., Castrignanò, E., Covaci, A., González-Mariño, I., Hapeshi, E., Kasprzyk-Hordern, B., Kinyua, J., Lai, F. Y., Letzel, T., Lopardo, L., Meyer, M. R., O'Brien, J., Ramin, P., Rousis, N. I., Rydevik, A., Ryu, Y., Santos, M. M., Senta, I., Thomaidis, N. S., Veloutsou, S., Yang, Z., Zuccato, E., Bijlsma, L., Measuring biomarkers in wastewater as a new source of epidemiological information: Current state and future perspectives, *Environment International* 99 (2017) 131-150. <https://doi.org/10.1016/j.envint.2016.12.016>.
- [27] Ferreira, A. P., Caffeine as an environmental indicator for assessing urban aquatic ecosystems, *Cadernos de Saúde Pública* 21 (6) (2005) 1884-1892. <https://doi.org/10.1590/S0102-311X2005000600038>.
- [28] Senta, I., Gracia-Lor, E., Borsotti, A., Zuccato, E., Castiglioni, S., Wastewater analysis to monitor use of caffeine and nicotine and evaluation of their metabolites as biomarkers for population size assessment, *Water Research* 74 (2015) 23-33. <https://doi.org/10.1016/j.watres.2015.02.002>.
- [29] González-Alonso, S., Merino, L. M., Esteban, S., Alda, M. L., Barceló, D., Durán, J. J., López-Martínez, J., Aceña, J., Pérez, S., Mastroianni, N., Silva, A., Catalá, M., Valcárcel, Y., Occurrence of pharmaceutical, recreational and psychotropic drug residues in surface water on the northern Antarctic Peninsula region, *Environmental Pollution* 229 (2017) 241-254. <https://doi.org/10.1016/j.envpol.2017.05.060>.
- [30] Williams, M., Kookana, R. S., Mehta, A., Yadav, S. K., Tailor, B. L., Maheshwari, B., Emerging contaminants in a river receiving untreated wastewater from an Indian urban centre, *Science of the Total Environment* 647 (2019) 1256-1265. <https://doi.org/10.1016/j.scitotenv.2018.08.084>.
- [31] Sposito, J. C. V., Montagner, C. C., Casado, M., Navarro-Martín, L., Solórzano, J. C. J., Piña, B., Grisolia, A. B., Emerging contaminants in Brazilian rivers: Occurrence and effects on gene expression in zebrafish (*Danio rerio*) embryos, *Chemosphere* 209 (2018) 696-704. <https://doi.org/10.1016/j.chemosphere.2018.06.046>.
- [32] Campanha, M. B., Awan, A. T., Sousa, D. N. R., Grosseli, G. M., Mozeto, A. A., Fadini, P. S., A 3-year study on occurrence of emerging contaminants in an urban stream of São Paulo State of Southeast Brazil, *Environmental Science and Pollution Research* 22 (10) (2015) 7936-7947. <https://doi.org/10.1007/s11356-014-3929-x>.
- [33] Montagner, C. C., Jardim, W. F. Spatial and seasonal variations of pharmaceuticals and endocrine disruptors in the Atibaia River, São Paulo State (Brazil), *Journal of the Brazilian Chemical Society* 22 (8) (2011) 1452-1462. <https://doi.org/10.1590/S0103-50532011000800008>
- [34] Cunha, V., Burkhardt-Medicke, K., Wellner, P., Santos, M. M., Moradas-Ferreira, P., Luckenbach, T., Ferreira, M., Effects of pharmaceuticals and personal care products (PPCPs) on multixenobiotic resistance (MXR) related efflux transporter activity in zebrafish (*Danio rerio*) embryos, *Ecotoxicology and Environmental Safety* 136 (2017) 14-23. <https://doi.org/10.1016/j.ecoenv.2016.10.022>.
- [35] Fraz, S., Lee, A. H., Wilson, J. Y., Gemfibrozil and carbamazepine decrease steroid production in zebra fish testes (*Danio rerio*), *Aquatic Toxicology* 198 (2018) 1-9. <https://doi.org/10.1016/j.aquatox.2018.02.006>.
- [36] Sehonova, P., Svobodova, Z., Dolezelova, P., Vosmerova, P., Faggio, C., Effects of waterborne antidepressants on non-target animals living in the aquatic environment: A review, *Science of the Total Environment* 631-632 (2018) 789-794. <https://doi.org/10.1016/j.scitotenv.2018.03.076>.
- [37] Aguirre-Martínez, G. V., Delvals, A. T., Laura Martín-Díaz, M. Yes, caffeine, ibuprofen, carbamazepine, novobiocin and tamoxifen have an effect on *Corbicula fluminea* (Müller, 1774). *Ecotoxicology and Environmental Safety* 120 (2015) 142-154. <https://doi.org/10.1016/j.ecoenv.2015.05.036>.
- [38] Cruz, D., Almeida, Â., Calisto, V., Esteves, V. I., Schneider, R. J., Wrona, F. J., Soares, A. M. V. M., Figueira, E., Freitas, R., Caffeine impacts in the clam *Ruditapes philippinarum*: Alterations on energy reserves, metabolic activity and oxidative stress biomarkers, *Chemosphere* 160 (2016) 95-103. <https://doi.org/10.1016/j.chemosphere.2016.06.068>.
- [39] Pires, A., Almeida, Â., Calisto, V., Schneider, R. J., Esteves, V. I., Wrona, F. J., Soares, A. M. V. M.,

- Figueira, E., Freitas, R., Long-term exposure of polychaetes to caffeine: Biochemical alterations induced in *Diopatra neapolitana* and *Arenicola marina*, *Environmental Pollution* 214 (2016) 456-463. <https://doi.org/10.1016/j.envpol.2016.04.031>.
- [40] Brandt, E. M. F., Queiroz, F. B., Afonso, R. J. C. F., Aquino, S. F., Chernicharo, C. A. L., Behaviour of pharmaceuticals and endocrine disrupting chemicals in simplified sewage treatment systems, *Journal of Environmental Management* 128 (2013) 718-726. <https://doi.org/10.1016/j.jenvman.2013.06.003>.
- [41] Buttiglieri, G., Knepper, T. P. Removal of emerging contaminants in wastewater treatment: conventional activated sludge treatment. In: Barceló, D., Petrovic, M. (Eds) *Emerging contaminants from industrial and municipal waste: removal technologies*, The Handbook of Environmental Chemistry, Springer Berlin Heidelberg, 2008. https://doi.org/10.1007/978-3-540-79210-9_1.
- [42] Radjenovic, J., Matosic, M., Mijatovic, I., Petrovic, M., Barceló, D., Membrane bioreactor (MBR) as an advanced wastewater treatment technology. In: Barceló, D., Petrovic, M. (Eds) *Emerging contaminants from industrial and municipal waste: removal technologies*, The Handbook of Environmental Chemistry, Springer Berlin Heidelberg, 2008. https://doi.org/10.1007/698_5_093.
- [43] Kunst, B., Kosutic, K., Removal of emerging contaminants in water treatment by nanofiltration and reverse osmosis. In: Barceló, D., Petrovic, M. (Eds) *Emerging contaminants from industrial and municipal waste: removal technologies*, The Handbook of Environmental Chemistry, Springer Berlin Heidelberg, 2008. https://doi.org/10.1007/978-3-540-79210-9_3.
- [44] Chernicharo, C. A. L. *Anaerobic reactors*, London: IWA, 2007.
- [45] Zaiat, M., Passig, F. H., Foresti, E., Treatment of domestic sewage in horizontal-flow anaerobic immobilized biomass (HAIB) reactor, *Environmental Technology* 21 (10) (2000) 1139-1145. <https://doi.org/10.1080/09593330.2000.9619000>.
- [46] Ribeiro, R., Nardi, I. R., Fernandes, B. S., Foresti, E., Zaiat, M., BTEX removal in a horizontal-flow anaerobic immobilized biomass reactor under denitrifying conditions, *Biodegradation* 24 (2) (2013) 269-278. <https://doi.org/10.1007/s10532-012-9585-2>.
- [47] Gusmão, V. R., Martins, T. H., Chinalia, F. A., Sakamoto, I. K., Thiemann, O. H., Varesche, M. B. A., BTEX and ethanol removal in horizontal-flow anaerobic immobilized biomass reactor, under denitrifying condition, *Process Biochemistry* 41 (6) (2006) 1391-1400. <https://doi.org/10.1016/j.procbio.2006.02.001>.
- [48] Damianovic, M. H. R. Z., Moraes, E. M., Zaiat, M., Foresti, E., Pentachlorophenol (PCP) dechlorination in horizontal-flow anaerobic immobilized biomass (HAIB) reactors, *Bioresource Technology* 100 (9) (2009) 4361-4367. <https://doi.org/10.1016/j.biortech.2009.01.076>.
- [49] Oliveira, L. L., Silveira Duarte, I. C., Sakamoto, I. K., Varesche, M. B. A., Influence of support material on the immobilization of biomass for the degradation of linear alkylbenzene sulfonate in anaerobic reactors, *Journal of Environmental Management* 90 (2) (2009) 1261-1268. <https://doi.org/10.1016/j.jenvman.2008.07.013>.
- [50] Chatila, S., Amparo, M. R., Carvalho, L. S., Penteadó, E. D., Tomita, I. N., Santos-Neto, Á. J., Gomes, P. C. F. L., Zaiat, M., Sulfamethoxazole and ciprofloxacin removal using a horizontal-flow anaerobic immobilized biomass reactor, *Environmental Technology* 37 (7) (2016) 847-853. <https://doi.org/10.1080/09593330.2015.1088072>.
- [51] Oliveira, G. H. D., Santos-Neto, Á. J., Zaiat, M., Removal of the veterinary antimicrobial sulfamethazine in a horizontal-flow anaerobic immobilized biomass (HAIB) reactor subjected to step changes in the applied organic loading rate, *Journal of Environmental Management* 204 (1) (2017) 674-683. <https://doi.org/10.1016/j.jenvman.2017.09.048>.
- [52] Oliveira, C. A., Penteadó, E. D., Tomita, I. N., Santos-Neto, Á. J., Zaiat, M., Silva, B. F., Gomes, P. C. F. L. Removal kinetics of sulfamethazine and its transformation products formed during treatment using a horizontal flow-anaerobic immobilized biomass bioreactor, *Journal of Hazardous Materials* 365 (2019) 34-43. <https://doi.org/10.1016/j.jhazmat.2018.10.077>.
- [53] Martins, G. S., Luchiari, N. C., Lamarca, R. S., Silva, B. F., Gomes, P. C. F. L., Removal of sulfamethoxazole and trimethoprim using horizontal-flow anaerobic immobilized bioreactor, *Scientia Chromatographica* 9 (4) (2017) 253-264. <http://www.iicweb.org/scientiachromatographica.com/files/v9n4a04.pdf>.
- [54] Rodríguez, A., Rosal, R., Perdigón-Melón, J. A., Mezcuca, M., Aguera, A., Hernando, M. D., Letón, P., Fernández-Alba, A. R., García-Calvo, E., Ozone-based technologies in water and wastewater treatment. In: Barceló, D., Petrovic, M. (Eds) *Emerging contaminants from industrial and municipal waste: removal technologies*, The Handbook of Environmental Chemistry, Springer Berlin Heidelberg, 2008. https://doi.org/10.1007/698_5_103.

- [55] Malato, S., Removal of emerging contaminants in waste-water treatment: removal by photo-catalytic processes. In: Barceló, D., Petrovic, M. (Eds) Emerging contaminants from industrial and municipal waste: removal technologies, The Handbook of Environmental Chemistry, Springer Berlin Heidelberg, 2008. https://doi.org/10.1007/978-3-540-79210-9_5.
- [56] Jovancic, P., Radetic, M., Advanced sorbent materials for treatment of wastewaters. In: Barceló, D., Petrovic, M., (Eds) Emerging contaminants from industrial and municipal waste: removal technologies, The Handbook of Environmental Chemistry, Springer Berlin Heidelberg, 2008. https://doi.org/10.1007/698_5_097.
- [57] Barceló, D., Petrovic, M., Conclusions and future research needs. In: Barceló, D., Petrovic, M. (Eds) Emerging contaminants from industrial and municipal waste: removal technologies, The Handbook of Environmental Chemistry, Springer Berlin Heidelberg, 2008. https://doi.org/10.1007/698_5_109.
- [58] EPA. Method 1694: Pharmaceuticals and Personal Care Products in Water, Soil, Sediment, and Biosolids by HPLC/MS/MS. December, 2007. https://www.epa.gov/sites/production/files/2015-10/documents/method_1694_2007.pdf.
- [59] EPA. Method 1698: Steroids and Hormones in Water, Soil, Sediment, and Biosolids by HRGC/HRMS. December, 2007. https://www.epa.gov/sites/production/files/2015-10/documents/method_1698_2007.pdf.
- [60] Leite, G. S., Afonso, R. J. C. F., Aquino, S. F., Caracterização de contaminantes presentes em sistemas de tratamento de esgotos, por cromatografia líquida acoplada à espectrometria de massas tandem em alta resolução, *Química Nova* 33 (3) (2010) 734-738. <https://doi.org/10.1590/S0100-40422010000300044>.
- [61] Silva, C. G. A., Collins, C. H., Aplicação de cromatografia líquida de alta eficiência para o estudo de poluentes orgânicos emergentes, *Química Nova* 34 (4) (2011) 665-676. <https://doi.org/10.1590/S0100-40422011000400020>.
- [62] Silva, B. F., Jelic, A., López-Serna, R., Mozeto, A. A., Petrovic, M., Barceló, D., Occurrence and distribution of pharmaceuticals in surface water, suspended solids and sediments of the Ebro river basin, Spain, *Chemosphere* 85 (8) (2011) 1331-1339. <https://doi.org/10.1016/j.chemosphere.2011.07.051>.
- [63] Stewart, M., Olsen, G., Hickey, C. W., Ferreira, B., Jelić, A., Petrović, M., Barceló, D., A survey of emerging contaminants in the estuarine receiving environment around Auckland, New Zealand, *Science of the Total Environment* 468-469 (2014) 202-210. <https://doi.org/10.1016/j.scitotenv.2013.08.039>.
- [64] Jardim, I. C. S. F. Extração em fase sólida: fundamentos teóricos e novas estratégias para preparação de fases sólidas, *Scientia Chromatographica* 2 (1) (2010) 13-25. <http://www.iicweb.org/scientiachromatographica.com/files/v2n1a2.pdf>.
- [65] Dimpe, K. M., Nomngongo, P. N., Current sample preparation methodologies for analysis of emerging pollutants in different environmental matrices, *Trends in Analytical Chemistry* 82 (2016) 199-207. <https://doi.org/10.1016/j.trac.2016.05.023>.
- [66] Gilart, N., Borrull, F., Fontanals, N., Marcé, R. M., Selective materials for solid-phase extraction in environmental analysis, *Trends in Environmental Chemistry* 1 (2014) e8-e18. <https://doi.org/10.1016/j.teac.2013.11.002>.
- [67] Evans, S. E., Davies, P., Lubben, A., Kasprzyk-Hordern, B., Determination of chiral pharmaceuticals and illicit drugs in wastewater and sludge using microwave assisted extraction, solid-phase extraction and chiral liquid chromatography coupled with tandem mass spectrometry, *Analytica Chimica Acta* 882 (2015) 112-126. <https://doi.org/10.1016/j.aca.2015.03.039>.
- [68] Vazquez-Roig, P., Andreu, V., Blasco, C., Picó, Y., SPE and LC-MS/MS determination of 14 illicit drugs in surface waters from the Natural Park of L'Albufera (València, Spain), *Analytical and Bioanalytical Chemistry* 397 (7) (2010) 2851-2864. <https://doi.org/10.1007/s00216-010-3720-x>.
- [69] Buszewski, B., Szultka, M., Past, present, and future of solid phase extraction: a review, *Critical Reviews in Analytical Chemistry* 42 (3) (2012) 198-213. <https://doi.org/10.1080/07373937.2011.645413>.
- [70] Van Nuijs, A. L. N., Tarcomnicu, I., Simons, W., Bervoets, L., Blust, R., Jorens, P. G., Neels, H., Covaci, A., Optimization and validation of a hydrophilic interaction liquid chromatography-tandem mass spectrometry method for the determination of 13 top-prescribed pharmaceuticals in influent wastewater, *Analytical and Bioanalytical Chemistry* 398 (5) (2010) 2211-2222. <https://doi.org/10.1007/s00216-010-4101-1>.
- [71] Gros, M., Petrovic, M., Barceló, D. Development of a multi-residue analytical methodology based on liquid chromatography-tandem mass spectrometry (LC-MS/MS) for screening and trace level determination of pharmaceuticals in surface and

wastewaters, *Talanta* 70 (4) (2006) 678-690.
<https://doi.org/10.1016/j.talanta.2006.05.024>.

[72] Babic, S., Pavlovic, D. M., Asperger, D., Perisa, M., Zrncic, M., Horvat, A. J. M., Kastelan-Macan, M., Determination of multi-class pharmaceuticals in wastewater by liquid chromatography–tandem mass spectrometry (LC–MS–MS), *Analytical and Bioanalytical Chemistry* 398 (3) (2010) 1185-1194.
<https://doi.org/10.1007/s00216-010-4004-1>.

[73] Pedrouzo, M., Borrull, F., Marcé, R. M., Pocurull, E., Ultra-high-performance liquid chromatography–tandem mass spectrometry for determining the presence of eleven personal care products in surface and wastewaters, *Journal of Chromatography A* 1216 (42) (2009) 6994-7000.
<https://doi.org/10.1016/j.chroma.2009.08.039>.

[74] Andrade-Eiroa, A., Canle, M., Leroy-Cancellieri, V., Cerda, V., Solid-phase extraction of organic compounds: a critical review (part I), *Trends in Analytical Chemistry* 80 (2016) 641-654.
<https://doi.org/10.1016/j.trac.2015.08.015>.

[75] Gomes, P. C. F. L., Tomita, I. N., Santos-Neto, Á. J., Zaiat, M., Rapid determination of 12 antibiotics and caffeine in sewage and bioreactor effluent by online column-switching liquid chromatography/tandem mass spectrometry, *Analytical and Bioanalytical Chemistry* 407 (29) (2015) 8787-8801.
<https://doi.org/10.1007/s00216-015-9038-y>.

[76] Rodriguez-Mozaz, S., Alda, M. J. L., Barceló, D., Advantages and limitations of on-line solid phase extraction coupled to liquid chromatography–mass spectrometry technologies versus biosensors for monitoring of emerging contaminants in water, *Journal of Chromatography A* 1152 (1-2) (2007) 97-115.
<https://doi.org/10.1016/j.chroma.2007.01.046>.

Influence of Ce(IV) ions amount on the electrochemical behavior of organic-inorganic hybrid coatings in 0.1 mol L⁻¹ NaCl solution

Fernando Santos da Silva¹, Hercílio Gomes de Melo², Assis Vicente Benedetti¹, Patrícia Hatsue Suegama^{3*}

¹ São Paulo State University (Unesp), Institute of Chemistry, 55 Prof. Francisco Degni St, Araraquara, São Paulo, Brazil

² University of São Paulo (USP), 2463 Professor Mello Moraes Av, Butantã, São Paulo, São Paulo, Brazil

³ Faculty of Exact Sciences and Technology (UFGD), Dourados Hw - Itahum, km 12, Mato Grosso, Brazil

*Corresponding author: Patrícia Hatsue Suegama, email address: patriciasuegama@ufgd.edu.br

ARTICLE INFO

Article history:

Received: January 9, 2019

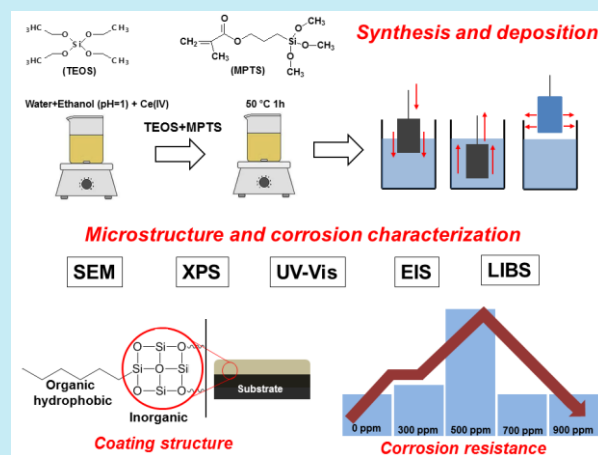
Accepted: May 14, 2019

Published: October 1, 2019

Keywords:

1. cerium
2. corrosion
3. organic-inorganic hybrid coating
4. EIS

ABSTRACT: In this work, the influence of ceric ions ($\text{Ce}(\text{SO}_4)_2$) addition to the hydrolysis solution on the corrosion protection afforded by organic-inorganic hybrid coating obtained from tetraethoxysilane (TEOS) and 3-methacryloxypropyl-trimethoxysilane (MPTS) to a carbon steel substrate in 0.1 mol L⁻¹ NaCl solution was studied. Open circuit potential (E_{oc}) and electrochemical impedance spectroscopy (EIS) experiments were carried out and showed that the protection afforded by the organic-inorganic hybrid coating was extremely dependent on the Ce^{4+} ions amount. These results were in close agreement with optical microscopy observation of the degrading surfaces, both procedures showing that more protective coating was produced when 500 ppm of Ce^{4+} ions were added to the organic-inorganic hybrid solution. The chemical state of the organic-inorganic hybrid coating investigated by X-ray photoelectron spectroscopy (XPS) indicated that the addition of Ce^{4+} ions enhances the polycondensation degree of the organic-inorganic hybrid coating leading to a denser siloxane (Si-O-Si) network. A strategy using laser-induced breakdown spectroscopy (LIBS) and UV-Vis spectrometry was set up in order to verify, respectively, the presence of Ce ions within the coating structure and its oxidation state. LIBS results confirmed the incorporation of Ce ions in the coating, which, according to UV-Vis measurements, are mainly in the (IV)-oxidation state.



1. Introduction

Organic-inorganic hybrid coating has been investigated as a new alternative for substitution of chromium-based coatings and paints for corrosion protection of several metallic substrates¹⁻¹⁰. The organic-inorganic hybrid coatings are environmentally friendly, have low cost, good adhesion, high corrosion resistance and are easily and rapidly prepared.

Organic-inorganic hybrid coating can be obtained by sol-gel process in two steps: initially, in the hydrolysis step, hydrolysable groups of the precursors are converted to silanol groups (Si-OH)². In the second step condensation reactions of silanol groups between themselves or with hydroxyl rich metallic surface lead to formation, respectively, of siloxane (Si-O-Si) and metal-siloxane (Me-O-Si) bonds. Thus, a highly adherent and cross-linked structure is obtained forming a physical barrier on the metal surface, which

prevent electrolyte from reaching the substrate. However, the efficiency of this barrier protection effect is limited due to formation of small pores, microcracks, and water uptake of the coating⁴⁻⁷. In order to improve the protection provided by these coatings the modification of the organic-inorganic precursor solution using corrosion inhibitors like nanoparticles and cerium ions has been proposed^{1,2,6-10}.

The use of ceric sulfate, in the modification of polymers and organic-inorganic hybrid materials by redox polymerization reaction is a widely used method with industrial importance¹¹⁻¹⁶. For organic-inorganic hybrid materials, it is proposed that silanol molecules (R1-Si-(OH)₃) and alcohol from the hydrolyzed precursors can complex with Ce⁴⁺ ions to produce free radicals, thus increasing the polymerization and the polycondensation degree of the siloxane (Si-O-Si) network¹⁷⁻²².

The effect of cerium ions in the performance of organic-inorganic hybrid coatings was previously described^{8-10,12,19-22}. Ferreira *et al.*⁸ have used rare earth (Ce, La) salts and bis-sulfur silane (BTESPT) as chromate substitutes for galvanized steel, resulting in improvement of corrosion resistance and paint adherence. The effect of cerium in the corrosion protection of galvanized steel by doping with cerium (III) nitrate silane solutions was discussed based in the self-healing effect due to the cerium oxide precipitation⁹. Montemor *et al.*¹⁰ investigated the electrochemical behavior of galvanized steel substrates pre-treated with bis-[triethoxysilylpropyl]tetrasulfide silane (BTESPT) solutions modified with SiO₂ or CeO₂ nanoparticles. The presence of nanoparticles reinforced the barrier properties of the silane coating and suggested a synergism between the activated nanoparticles and cerium ions, that reduced the corrosion activity. Suegama *et al.*¹⁹ have evaluated the effect of low amount of Ce⁴⁺ ions (\approx 50 ppm) addition on the polymerization of bis-[triethoxysilyl]ethane (BTSE) coating applied on carbon steel. The coating characterization showed a better surface finishing and a higher thickness for the coatings doped with Ce⁴⁺ ions enhancing the barrier properties provided by the coating alone. Palomino *et al.*²⁰ have studied the performance of bis-1, 2-(triethoxysilyl) ethane (BTSE) doped with a mixture of Ce⁴⁺ ions and silica nanoparticles as a pre-treatment to protect the AA 2024-T3 against corrosion. The addition of Ce⁴⁺ ions increased the degree of surface coverage and improved the anticorrosion properties of the

doped coating. Hammer *et al.*²¹ have investigated hybrid coatings prepared by tetraethoxysilane (TEOS), 3-methacryloxy propyltrimethoxysilane (MPTS), doped with Ce³⁺ and Ce⁴⁺ ions deposited onto 316L stainless steel. The XPS results indicate an increase in the network connectivity related to the active role of Ce⁴⁺ ions in the polymerization of siloxane groups and the improvement of the corrosion resistance of Ce⁴⁺ doped organic-inorganic hybrid coating. The effect of the addition of Ce⁴⁺ ions was also performed using structural analyzes of Si RMN²². The results showed that the T3 (Si(OSi)₃R') and Q4 (Si(OSi)₄) resonance bands were more intense in the hybrids modified with Ce⁴⁺ ions, indicating a structure with a denser Si-O-Si network, thus producing more resistive, thicker and less porous materials. According to the literature^{12,19-22}, the improved protection characteristics of the hybrid is attributed to the effect of Ce⁴⁺ ions in the polymerization rate of the organic phase and in the polycondensation of the siloxane structure, producing more condensed and crosslinked polymeric networks. Authors also reported that hydroxyl groups from alcohol molecules can form complexes with Ce⁴⁺ ions, which decomposes to form free radicals, contributing to the hybrid polymerization²².

This work aims at studying the influence of different amounts of Ce⁴⁺ ions added to tetraethoxysilane (TEOS) and 3-methacryloxy-propyl-trimethoxysilane (MPTS) organic-inorganic hybrid coating deposited on carbon steel and evaluating its corrosion resistance during relative long immersion times in NaCl 0.1 mol L⁻¹ using electrochemical impedance spectroscopy (EIS) and open circuit potential (E_{oc}) measurements. As far as authors are aware, there is no work carried out to identify the presence of Ce ions inside the organic-inorganic hybrid coating using Laser-induced breakdown spectroscopy (LIBS) as well the use of UV-Vis analysis to investigate the Ce oxidation state inside this coating.

2. Materials and methods

2.1. Metallic substrate and solutions

The metallic substrate used was a SAE 1020 carbon steel (20 × 22 × 1.2 mm) with the composition C (0.40 wt.%), Mn (0.30 wt.%), Si (0.03 wt.%) and Fe balance, determined using an EDX-720/800HS Energy Dispersive X-ray

Fluorescence Spectrometer, SHIMADZU. Initially the samples were ground with 320, 600 and 1200 grit silicon carbide emery paper, washed with distilled water and dried in purified air. Afterwards, they were sonicated in ethyl alcohol for 10 min and dried in hot air stream.

2.2. Coating preparation and coating thickness

The synthesis of the TEOS and MPTS organic-inorganic hybrid coating modified with 0, 300, 500, 700 or 900 ppm Ce^{4+} ions was performed via the sol-gel process in two steps. Initially, 6.8 mL of an ethanol/water solution (62/38% v/v) at pH 1.0 was used to solubilize the desired amount of cerium salt ($\text{Ce}(\text{SO}_4)_2$) under stirring, until a colorless solution was obtained. In the second step 6 mL of TEOS (Sigma Aldrich 99.8%) and 3.2 mL of MPTS (Fluka 99.8%) were added together to the solution prepared in the first step, and the mixture was stirred for 1 h at 50 °C. The solution of the organic-inorganic hybrid just before deposition on steel had a final pH 4. All coatings were applied by dip coating at a constant immersion / withdrawal rate of 14 cm min^{-1} with three dips, with intervals of 1 min between each one of them. The curing step consisted in heating at 50 °C for 24 h followed by 3 h at 160 °C. The coating thickness was measured by optical interference using a FILMETRICS F3-CS with 2 nm resolution. The thicknesses of TEOS/MPTS organic-inorganic hybrid coatings were measured at three different regions, and the average values were: 728 ± 2 nm (0 ppm); 748 ± 3 nm (300 ppm); 843 ± 8 nm (500 ppm); 736 ± 8 nm (700 ppm) and 789 ± 5 nm (900 ppm).

2.3. Electrochemical measurements

The protection of the substrate provided by the coatings was investigated in 0.1 mol L^{-1} NaCl solution using EIS and E_{OC} measurements. The measurements were performed during 120 h for the substrate and for different times for coatings containing the following cerium additions / ppm: 0 (144 h); 300 (192 h); 500 (688 h); 700 (144 h) and 900 (172 h). For these coatings, the testing time corresponds to an abrupt change of E_{OC} values, suggesting that the electrolyte has reached the substrate. EIS measurements were done in the frequency range from 100 kHz to 10 mHz, by applying a sinusoidal potential perturbation of 10 mV (rms) vs. E_{OC} , and were performed after 1 h, 8 h and every 24 h of immersion until visual failure

of the samples. Therefore, EIS measurements were conducted until the resistance of the coating was very low, and no more protection of the substrate was afforded. Equivalent Electric Circuit (EEC) fitting using the Z-view[®] software was employed for quantitative analysis of the EIS responses. Before the fitting procedure, the consistency of the experimental data was verified using the Kramers-Kronig Transform (KKT)²³. The fittings were carried out only for the experimental points in the frequency region where there was concordance with the KKT treatment.

2.4. Surface characterization and analytical techniques

2.4.1 SEM-EDS and AFM analysis

Morphological characterization using optical micrograph images was performed for all samples during the electrochemical measurements. Images of scanning electron microscopy and EDS analysis were obtained using a JEOL JSM-5310 coupled with energy dispersive X-ray spectroscopy analysis (SEM / EDS). The micrographs were acquired prior to and after 240 h immersion in the chloride medium for the sample protected with the nondoped organic-inorganic hybrid coating and after ≈ 400 h for the organic-inorganic hybrid coating with the Ce^{4+} quantity that showed the best anticorrosion protection. The accelerating voltage used to perform the EDS analysis was 15 keV.

The morphologies of TEOS / MPTS coatings prepared with 300 ppm of Ce^{4+} or Ce^{3+} ions were also analyzed by Atomic Force Microscopy (AFM) to compare the effects of the Ce ions oxidation state on the coating morphology. An AFM model Agilent 5500 was used to acquire the images in the intermittent mode and using a pyramidal tip. All images were done in 5 μm^2 area.

2.4.2 X-Ray Photoelectron spectroscopy (XPS) analysis

Structural characterization of the coatings was performed using a UNI-SPECS UHV instrument for organic-inorganic hybrid-coated samples without Ce and with the doped condition with the best anticorrosion performance. The samples were fixed on small flat discs on a XYZ manipulator and placed in the analysis chamber, which residual pressure was maintained below 10^{-8} Torr while data were being obtained. The Mg $K\alpha$ line was used

($h\nu = 1253.6$ eV) and the analyzer pass energy was set to 10 eV. XPS was used to investigate the core level of C 1s, O 1s, Si 2p. The intensities were estimated by calculating the area under each peak after smoothing and subtraction of the shaped background and fitting the experimental curve to a combination of Lorentzian and Gaussian lines of variable proportions.

2.4.3 Laser-induced breakdown spectroscopy (LIBS) analysis

LIBS was also used to analyze the organic-inorganic hybrid coatings without Ce^{4+} ions and doped with 1500 ppm of Ce^{4+} ions prepared in the same conditions of the other organic-inorganic hybrid coatings (subsection 2.2) and deposited onto copper substrate. This strategy was adopted, since iron from the substrate exhibits strong interference in the Ce analysis²⁴. The spectra of the samples were acquired with a LIBS 2500plus spectrometer (Ocean Optics, Dunedin, FL, USA), which uses a Q-switched Nd:YAG laser at 1064 nm (Quantel, Bozeman, MT, USA) operating at 75 mJ maximum power energy, 8 ns pulse width, and 10 Hz frame rate. The laser pulse was focused on the sample inside an ablation chamber. After the plasma was formed, the emission of excited species was carried out by an optical fiber bundle connected to seven spectrometers ranging from 188 to 980 nm, each one coupled with a 2048 nm element linear silicon CCD array, whose resolution was ~ 0.1 nm (FWHM). The distance from the sample to the collecting optical fiber bundle was approximately 7 mm. All measurements were performed in air, and the LIBS system was set to 50 mJ per laser pulse with a 2.1 ms integration time and a fixed delay time of 2 μs . 10 measurements were carried out on each sample.

2.4.4 UV-Vis measurements

To perform the UV-Vis measurements freestanding cerium nitrate ($\text{Ce}(\text{NO}_3)_3$) and ceric sulfate ($\text{Ce}(\text{SO}_4)_2$) doped organic-inorganic hybrid coatings (300, 500 and 900 ppm) were prepared by pouring the hydrolysis solution into a crucible and then curing as previously described (subsection 2.2). Afterwards, 3 g of each coating were ground and placed in test tubes with 3 mL of distilled water for 15 days. Then, the extract was filtered (pore size < 25 μm) and the solution analyzed in the UV-Vis region. Water was used as reference and spectra

were also obtained from solutions of 200 ppm of $\text{Ce}(\text{SO}_4)_2$ or $\text{Ce}(\text{NO}_3)_3$ in distilled water. Two solutions were also prepared by extracting Ce, in argon atmosphere, from the coating doped with Ce^{4+} or Ce^{3+} ions, and immediately analyzed. UV-Vis measurements of freestanding solid organic-inorganic hybrid coating were also carried out. Organic-inorganic hybrid coating with 0 and 500 ppm of Ce^{4+} ions were deposited onto glasses. For comparison UV-Vis measurements of the glass and crystals of $\text{Ce}(\text{SO}_4)_2$ were also performed. The spectra were obtained with an UV/VIS Lambda 265 (Perkin Elmer) or an UV/Vis/NIR (Perkin Elmer) spectrophotometer from 190 to 1100 nm with spectral resolution of 2 nm and using a polished four-face quartz cuvette with a light path length of 10 mm for measuring in solution. Special care was taken to obtain the spectra considering the complexity of the UV-Vis response of Ce^{4+} and Ce^{3+} ions systems that show, respectively, charge transfer and f-d transitions, which are strongly influenced by the environment. Therefore, only spectra obtained at the same conditions were compared.

3. Results and discussion

3.1. Electrochemical measurements

E_{OC} evolution after different immersion times for the uncoated and coated substrates are presented in Fig. 1. All samples protected with the organic-inorganic hybrid coating showed E_{OC} more positive than the bare substrate, indicating that the electrochemical response was modified. The sample doped with 500 ppm of Ce^{4+} ions provided the noblest potential (0.4 ± 0.1) V/(Ag/AgCl/KCl_{sat}) at initial immersion times, suggesting the formation of a denser cross linked coating, and the best protective character^{13,16,21}. This E_{OC} value also indicates that the barrier effect of the coating doped with 500 ppm of Ce^{4+} ions induced a higher ohmic drop compared to the bare substrate and other coatings. After 432 h, the E_{OC} abruptly decreases to -0.6 V/(Ag/AgCl/KCl_{sat}), very close to that E_{OC} of the substrate, suggesting that the electrolyte may have reached the coating/substrate interface. Other coatings showed at initial immersion times E_{OC} values close to -0.4 V/(Ag/AgCl/KCl_{sat}), and at times less than 200 h the E_{OC} values were almost the same of the substrate, indicating electrolyte uptake by the coating and coating degradation as verified by other studies²⁵.

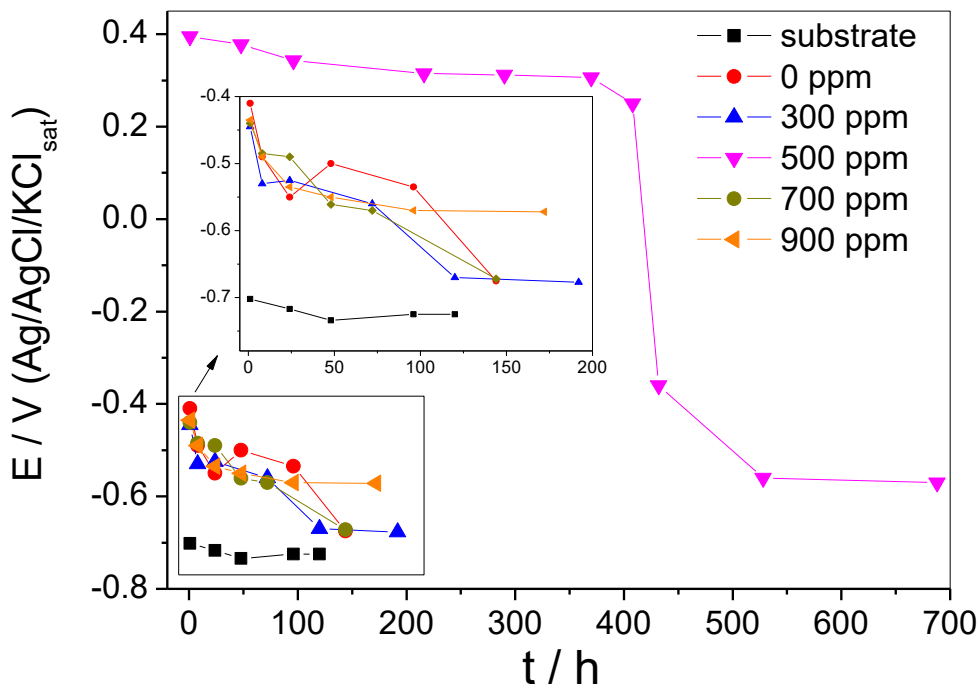
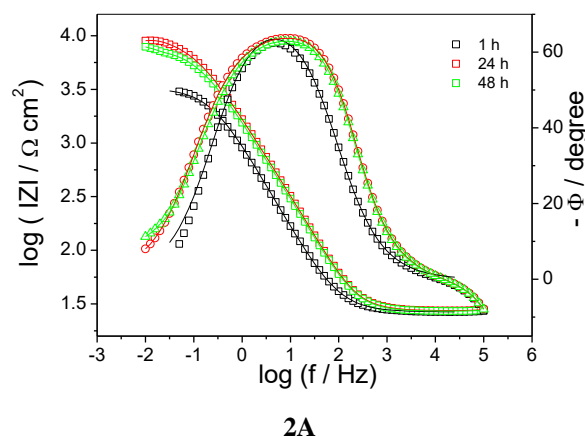


Figure 1. E_{oc} variation in 0.1 mol L^{-1} NaCl solution for bare carbon steel and for samples protected with TEOS / MPTS organic-inorganic hybrid coatings modified with different amounts of Ce^{4+} ions.

Fig. 2 shows the Bode plots for all studied samples. The phase angle diagrams for the bare substrate showed basically one time constant centered at around 5 Hz (Fig. 2A) due to iron oxidation. For the sample protected with the nondoped coating, two time constants can be clearly identified (Fig. 2B). The high frequency (HF) one is related to the organic-inorganic hybrid coating, and the other, in the low frequency (LF) domain, is attributed to the interfacial response (double layer charging in parallel with the charge transfer resistance)^{16,22,26}. For the coatings doped with Ce^{4+} ions (Fig. 2C-2F) a third-time constant appeared in the medium frequency (MF) range. This feature was associated to the presence of Ce species within the organic-inorganic hybrid coating, presenting a different relaxation behavior than that exhibited by the coating and the substrate. In the HF region, phase angles close to -90° were always obtained for short immersion times, indicating good barrier properties of the coating. Afterwards a slow decay was observed for longer immersion periods that can be related to coating degradation due to electrolyte uptake²⁷. The decaying rate is directly proportional to the coating

protection capability: the more protective the coating the slower the HF phase angle reduction. Concomitantly, a reduction of the LF impedance modulus occurs at variable rate depending on the sample, indicating the progress of corrosion processes at the interface.



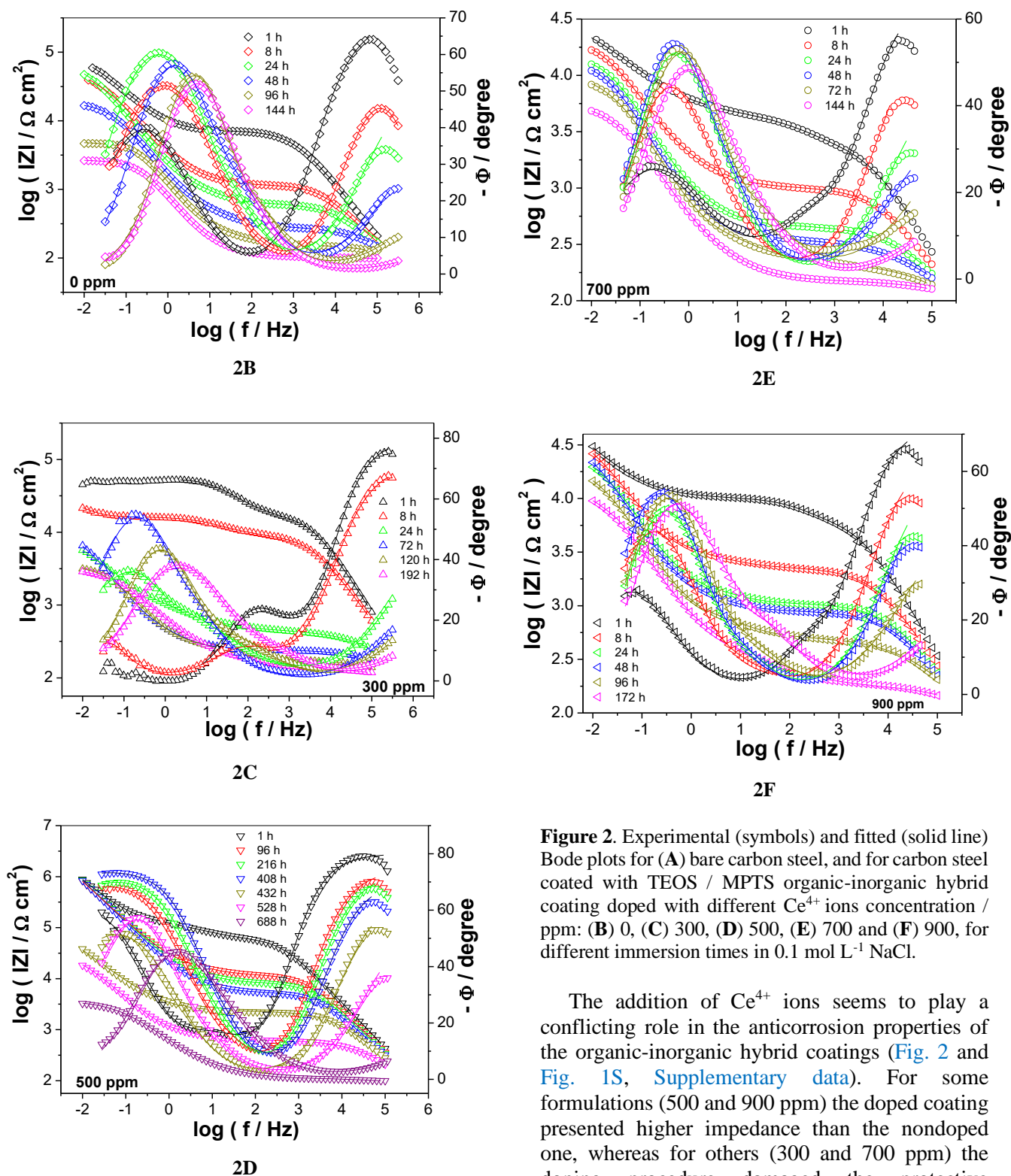


Figure 2. Experimental (symbols) and fitted (solid line) Bode plots for (A) bare carbon steel, and for carbon steel coated with TEOS / MPTS organic-inorganic hybrid coating doped with different Ce^{4+} ions concentration / ppm: (B) 0, (C) 300, (D) 500, (E) 700 and (F) 900, for different immersion times in $0.1 \text{ mol L}^{-1} \text{ NaCl}$.

The addition of Ce^{4+} ions seems to play a conflicting role in the anticorrosion properties of the organic-inorganic hybrid coatings (Fig. 2 and Fig. 1S, Supplementary data). For some formulations (500 and 900 ppm) the doped coating presented higher impedance than the nondoped one, whereas for others (300 and 700 ppm) the doping procedure damaged the protective properties of the coating.

In previous works^{10,21,22,28}, it has been reported that the addition of Ce^{4+} ions to the hydrolysis solution provides an increase of the silanol groups condensation rate to form a denser and cross-linked

coating. In addition, in organic chemistry, these ions are often used for the oxidation of alcohols^{15-18,29,30}. The proposed general mechanism for such reaction shows that Ce^{4+} ions form complexes with the ethanol molecules, which, when decomposed, form free radicals that react with each other leading to the polymerization of ethanol and / or silanol by a polymerization redox reaction^{16,19}. This redox polymerization process is characteristic of ethanol in the presence of Ce^{4+} ions. The complexes may react with each other via free radical reactions leading to polymerization, in a similar way as the generic mechanism previously presented¹⁶. The effect of Ce^{4+} ions in the coating formation would be twofold, besides increasing the polymerization rate it would also promote the formation of silanol groups as it shifts to the right the equilibrium of the hydrolysis reaction (silanol formation). Therefore, the effect of Ce^{4+} ions is to increase the reaction rate among silanol groups leading to the formation of more densely cross linked coating^{19,29-31}. The redox polymerization of Ce^{4+} ions also leads to the formation of Ce^{3+} ions^{19,29-31}. However, the amount of this latter ion being formed is insignificant, and it would not be reasonable to consider an inhibiting contribution effect due to the presence of Ce^{3+} ions in the organic-inorganic hybrid solution/coating in accordance with other authors^{2,22,28}. In addition, the molecule of MPTS can react with Ce^{4+} ions by redox polymerization due to the radical polymerization process (see [Supplementary data](#)). The MPTS molecule reacts with Ce^{4+} ions forming the radical species of MPTS and reducing Ce^{4+} to Ce^{3+} ions ([Fig. 1S, Supplementary data](#)). After that occurs successive additions of monomer to radical, and the termination stage occurs with mutual reactions of two radicals to form an inactive polymer and can occur by combination. It has been reported that the thickness of the organic-inorganic hybrid coating increases in the presence of cerium ions, which may result in higher impedance values for modified coating^{10,19-21}. Therefore, it would be expected a steady increase of the impedance modulus for increasing Ce^{4+} ions amounts added to the hydrolysis solution.

However, this was not verified in the present work where a thicker coating was obtained for the hydrolysis solution modified with 500 ppm of Ce^{4+} ions, which also presented the best anticorrosion behavior. It happens likely because the addition of Ce^{4+} ions to the hydrolysis solution above a certain amount may lead to the decrease in the rate of redox polymerization and crosslink formation^{21,29}.

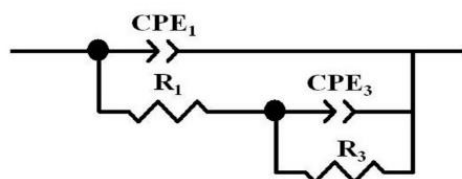
This results from the inactivation of the active initiator species due to excess Ce^{4+} ions concentration bringing about premature termination^{21,29}.

As evidenced in [Fig. 2B](#) and [2C](#) the addition of 300 ppm of Ce^{4+} ions to the hydrolysis solution produced an organic-inorganic hybrid coating with lower protection capabilities than the blank coating (organic-inorganic hybrid coating without Ce^{4+} ions). In addition, a complex impedance response was verified, particularly for short immersion periods, where an inductive loop was observed in the LF domain ([Fig. 1SA](#) and [1SB, Supplementary data](#)). The literature shows that an inductive LF response is obtained when iron dissolves in acidic electrolyte³²⁻³⁵. This has been ascribed to a dissolution path involving the formation of adsorbed species^{33,34}. When dipping the substrate in the hydrolysis solution, bonding of the silanol functionality to the carbon steel surface must compete with its dissolution by the acidic electrolyte. Hence, if the adsorption process is not very fast, acidic attack of the metal surface can take place during the coating deposition and remnants of the acidic hydrolysis solution may remain entrapped beneath the coating. This could lead to the attack of the substrate by the residual acid during the initial stages of immersion in the NaCl solution, as suggested by the shape of the Nyquist diagram after 1 h immersion ([Fig. 1S, Supplementary data](#)).

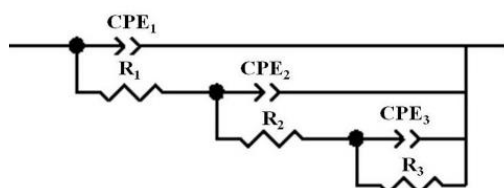
When larger amounts of Ce^{4+} ions (700 and 900 ppm) were used, a lesser protection of the substrate was also observed, as lower values of $|Z|_{(f=10\text{ mHz})}$ were obtained after 1 h of immersion (about 25 and 32 $k\Omega\text{ cm}^2$ – [Fig. 2E](#) and [2F](#)) when compared to the coating modified with 500 ppm ([Fig. 2D](#), $|Z|_{(f=10\text{ mHz})} = 100\text{ k}\Omega\text{ cm}^2$). These results are in accordance with the thicknesses determination that showed that the thickest layer was obtained when 500 ppm of Ce^{4+} ions was added to the hydrolysis solution. For higher concentrations (700 and 900 ppm) it is considered that a lower degree of polycondensation degree of the siloxane bonds might occur due to the large proportion of Ce^{4+} ions added to the hydrolysis solution^{16,22,29,36}. This means that the increase of cerium (IV) amount may provide more chances for premature termination of the growing chain radicals, and hence the polymerization degree is decreased¹⁴⁻¹⁶. The hydroxyalkyl free radicals, which are extremely reactive towards cerium (IV) species, can have an oxidative termination of their

primary free radicals generated in the initiation step¹⁶.

The impedance data were fitted using EECs to have a better understanding about the protective behavior of the coatings and their degradation. In the EIS diagrams of Fig. 2, symbols and lines correspond, respectively, to the experimental and fitted diagrams. EECs combine the use of elements such as resistors, constant phase elements, capacitors, inductors, and others. To be meaningful each passive element must have a physical-chemical association with an interfacial process. In addition, the fitting procedure must provide low chi-squared (χ^2) and low errors for each estimated value of the passive elements^{27,37}. The EEC of Fig. 3A, composed of two time constants, was used to fit the EIS data of the sample coated with nondoped TEOS / MPTS. The values for each fitted parameter for different immersion times are presented in Table 1S (Supplementary data). The good fit to the experimental results (Fig. 3B) suggests that it may physically represent the behavior of this sample.



(Figure 3A)



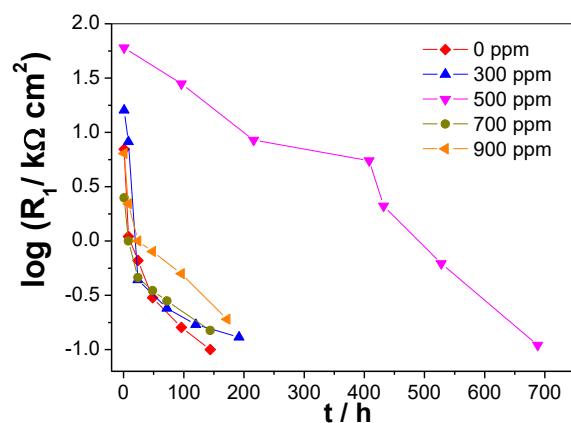
(Figure 3B)

Figure 3. Electrical equivalent circuits used to fit the impedance data for carbon steel coated with TEOS / MPTS with no doping (A) and doped with Ce^{4+} ions (B).

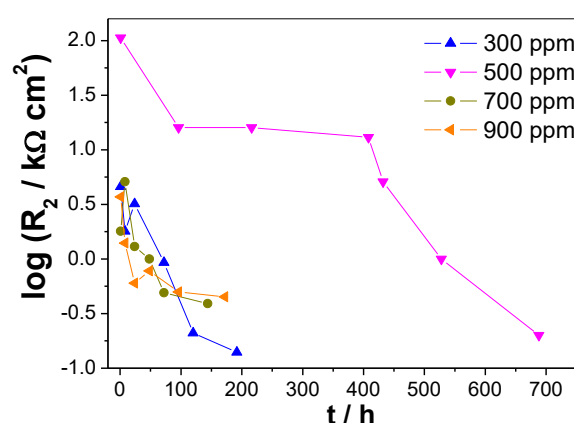
For the HF time constant, attributed to the organic-inorganic hybrid coating, CPE_1 is a constant phase element associated with the coating admittance ($\text{CPE}_1\text{-T}$) and a value of $\alpha_1 \neq 1$ ($\text{CPE}_1\text{-P}$) can be related to a nonuniform permittivity across the coating thickness due to electrolyte uptake^{33,38-40}. The subcircuit associated with the organic-inorganic hybrid coating is completed with

R_1 that represents the pore resistance. In the LF region, the time constant represented by the subcircuit CPE_3 in parallel with R_3 , is related to the double layer admittance and the charge transfer resistance. In this case, a value of $\alpha_3 \neq 1$ suggests a heterogeneous charge distribution at the surface due to surface roughness, adsorption of species or defects on the sample surface⁴⁰⁻⁴².

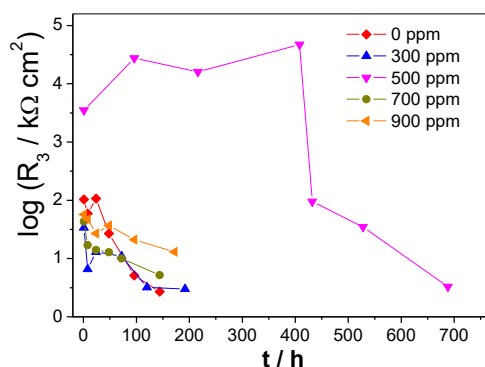
For the nondoped coating a gradual increase in the value of $\text{CPE}_1\text{-T}$ (related to the coating capacitance) is observed for increasing immersion times (Table 1S, Supplementary data), indicating progressive electrolyte uptake by the coating^{41,42}. Concomitantly the pore resistance R_1 decreases (Fig. 4A) indicating the enlargement / multiplication of conductivity pathways through the coating.



(Figure 4A)



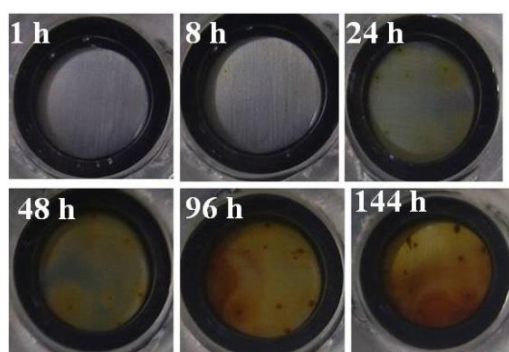
(Figure 4B)



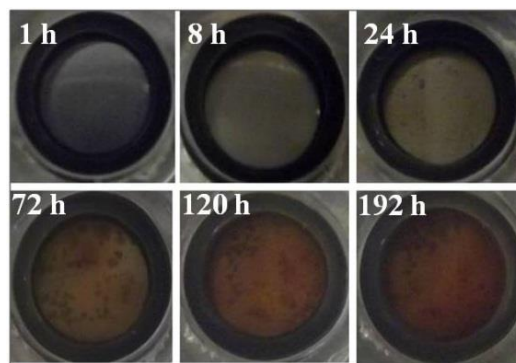
(Figure 4C)

Figure 4. Resistance values for the different time constants of the electrical equivalent circuits presented in Fig. 3 for doped and nondoped coating: (A) R_1 , pore resistance; (B) R_2 , resistance of the cerium oxide/ions within the organic-inorganic hybrid coating and (C) R_3 , charge transfer resistance.

Accordingly, pit formation can be observed after 24 h, which must be a consequence of coating disruption (Fig. 5A). This can be assisted by the hydrolysis of the siloxane bonds within the coating, further increasing its degradation. Sakai *et al.*⁴¹ also attributed the decrease of the pore resistance with immersion time to the shift of the chemical equilibrium of the hydrolysis reactions occurring with water. From 48 h a great decrease of R_3 was verified (Fig. 5C), indicating enhanced corrosion activity at the interface, which was confirmed by the photos taken of the electrode surface showing large amount of corrosion products (Fig. 5A).



(Figure 5A)



(Figure 5B)

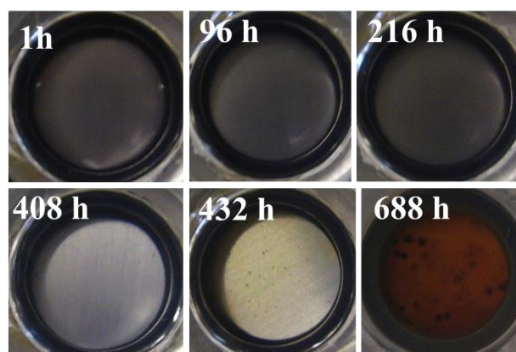


(Figure 5C)

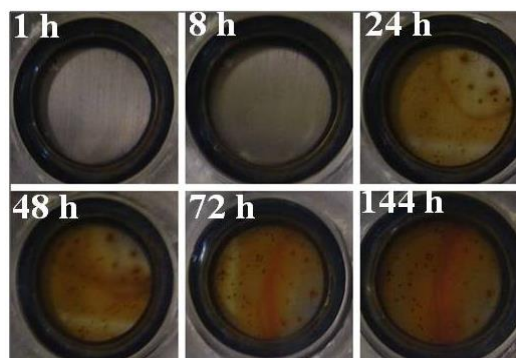


(Figure 5D)

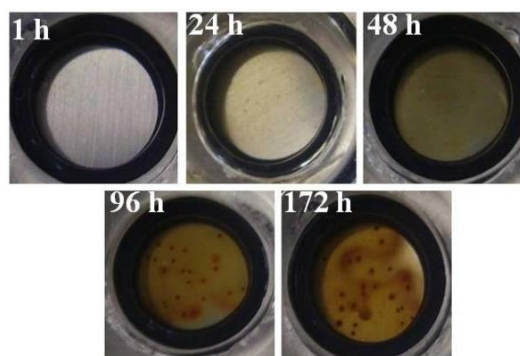


(Figure 5E)

Figure 5. Photos taken after the EIS measurements of samples protected with TEOS / MPTS organic-inorganic hybrid coating with different Ce^{4+} ions

concentrations / ppm: (A) 0, (B) 300, (C) 500, (D) 700 and (E) 900.

In the next paragraphs the influence of Ce^{4+} ions addition in the protective properties of the organic-inorganic hybrid coating will be discussed on the light of the EEC fitting procedures. For the samples protected with the coating doped with 300 to 900 ppm of Ce^{4+} ions the EEC of Fig. 3B adequately fitted the EIS experimental data (Tables 2S-5S, Supplementary data). For this EEC, the time constants at HF (CPE_1/R_1) and LF (CPE_3/R_3) are ascribed to the same phenomena as for the nondoped coating. On the other hand, the time constant at the MF (fitted with the CPE_2/R_2 subcircuit) is attributed to the presence of Ce incorporated into the organic-inorganic hybrid coating, which final oxidation state will be discussed in the second part of this manuscript. Several studies indicated that Ce species added to the hydrolysis solution may form oxides/hydroxides covering part of the metallic surface, and / or complexes located inside the coating, providing greater protection to the substrate⁴³⁻⁴⁵. Paussa *et al.*⁴³, using GDOES (glow discharge optical emission spectroscopy) measurements, reported the formation of a Ce compound layer on the substrate surface and inside a ZrO_2 sol-gel coating, improving the corrosion protection provided to the substrate, as verified by EIS experiments. Similar behavior was observed for epoxy coatings modified with pigments used to protect an Al-Zn alloy against corrosion²⁷. In this latter case, the impedance data were also fitted using an EEC with three time constants at which the MF one was assigned to the electrical / electrochemical behavior of the pigments present within the coating²⁷.

For all the coatings doped with Ce^{4+} ions the values of $\text{CPE}_1\text{-T}$ increase (Table 2S-5S, Supplementary data) and R_1 decrease (Fig. 4A) with immersion time, indicating that the protective properties of the coating are being lost due to electrolyte uptake. These changes occur at different rates depending on the Ce amount added to the hydrolysis solution. Among the studied samples, the one doped with 500 ppm of Ce^{4+} ions showed the slowest changes in these parameters (Table 3S, Supplementary data) when compared to the others. For this particular sample, the capacitive elements $\text{CPE}_1\text{-T}$ and $\text{CPE}_2\text{-T}$ slightly increase between 1 h and 408 h of test indicating slow electrolyte uptake by the coating, which seems to maintain its integrity (Fig. 5C), thus avoiding excessive

exposure of the substrate to the electrolyte. During this period, R_1 and R_2 values decrease by about one order of magnitude (Fig. 4A and 4B) indicating, respectively, enhanced electrolyte penetration through conductive pathways in the coating and dissolution of Ce ions. For this time span, $\text{CPE}_3\text{-T}$ decreases (Table 3S, Supplementary data) and R_3 (corresponding to the charge transfer resistance) presents very high values and keeps increasing up to 400 h (Fig. 4C), indicating, respectively, that the reaction rate at the interface is low and that it is progressively hindered. Considering the physical model for the EEC, it is hypothesized that dissolved Ce ions could migrate to cathodic sites precipitating^{20,43-45}. The blockage of the cathodic reactions would, consequently, avoid the metal oxidation and, apparently, impart some self-healing properties to the protective coating, as proposed by different authors^{46,47}.

For longer immersion times (432 h) $\text{CPE}_1\text{-T}$ increases by approximately one order of magnitude whereas $\text{CPE}_2\text{-T}$ becomes fifty times higher than at the beginning of the exposure period (Table 3S, Supplementary data). This indicates, respectively, that the protective properties of the coating have been seriously damaged and that much of the Ce ions entrapped within the coating has been dissolved. For this immersion time, visual corrosion of the substrate could be observed, which increased with immersion time (Fig. 5C).

For the other studied samples (doped with 300, 700 or 900 ppm) the same tendencies for the CPE and R were observed, but with higher degradation rates (see Fig. 4A, 4B and 4C, Fig. 5B, 5D and 5E and Tables 2S, 4S and 5S, Supplementary data), and with no clear sign of self-healing properties, which could be ascribed to very defective coatings (note the steep decrease of R_1 (Fig. 4A) and R_2 (Fig. 4B) for these samples). Finally, it must be stressed that, for all investigated samples, α values were between 0.9 and 0.6, indicating heterogeneities in the coating properties and heterogeneous charge distribution on the metallic surface.

Fig. 5 shows photos of the samples surfaces after each EIS measurement. Pitting is observed after 24 h immersion for the samples protected with the organic-inorganic hybrid without and with 300 ppm and 700 ppm of Ce^{4+} ions (Fig. 5A, 5B and 5D). On the other hand, localized corrosion was initiated after 96 h for the coating doped with 900 ppm (Fig. 5E) and after 432 h for the sample prepared with 500 ppm of Ce^{4+} ions (Fig. 5C).

These results were highly coherent with the EIS ones confirming that this latter formulation presents the best substrate protection against corrosion. They are also coherent with the thicknesses of the coatings presented in the experimental part.

The sample protected with the modified coating with the best electrochemical response (500 ppm of Ce^{4+} ions) and the unmodified one (reference) were observed by SEM. Fig. 6 presents SEM images of these samples surfaces prior to (A and C) and after (B and D) 240 h immersion in the test electrolyte. Before the corrosion test, the coatings were defect-free and completely covered the substrate surfaces (Fig. 6A and 6C). Before immersion, the maps of elements for these samples (Fig. 2SA and 2SB) show uniform distribution of C, O and Si all over the surface and Fe was not detected. On the other hand, after the completion of the corrosion test, the sample protected by the organic-inorganic hybrid coating without Ce showed cracks distributed throughout the surface (Fig. 6B), indicating a high degree of degradation. This can be attributed both to a low degree of polycondensation and to the hydrolysis of the siloxane bonds due to electrolyte uptake, generating these preferential pathways for the onset of the corrosion process at the substrate surface^{25,37} as also detected in the EIS experiments. The EDS microanalysis of this sample after 240 h of test (Fig. 2SC, Supplementary data) showed the presence of iron, especially near the cracks, confirming the existence of preferential corrosion sites. For the sample protected by the coating modified with 500 ppm of Ce^{4+} ions, cracks and surface defects were not observed, even after 240 h of immersion (Fig. 6D), indicating that the integrity of the coating was maintained, corroborating the good EIS results. EDS analysis (Fig. 2SD, Supplementary data) did not identify iron on this sample surface, confirming that the coating acted as an effective barrier, preventing the electrolyte to reach the substrate.

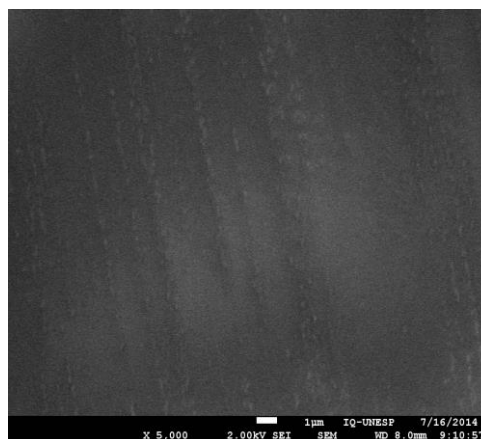


(Figure 6A)

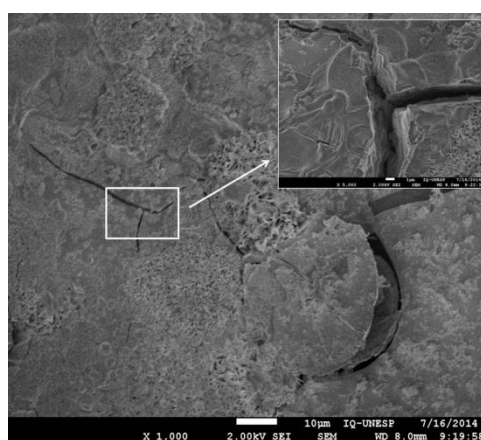


(Figure 6B)

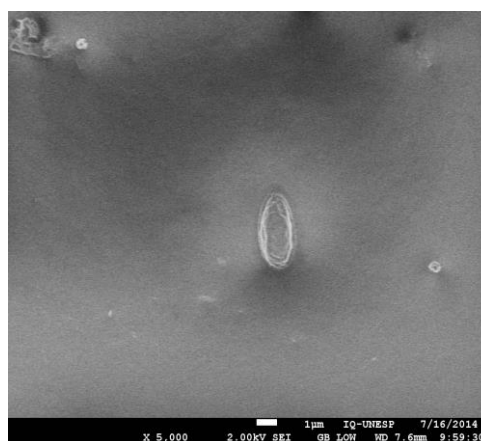


(Figure 6C)

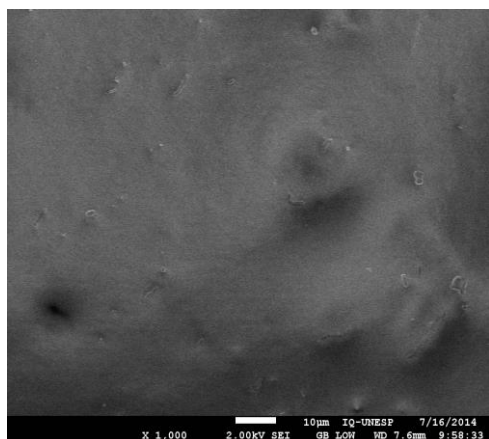


(Figure 6D)

Figure 6. SEM images for the coatings TEOS / MPTS doped with different Ce^{4+} ions concentration / ppm: (A) 0 and (B) 500 before immersion; (C) 0 and (D) 500 after 400 h immersion in 0.1 mol L^{-1} NaCl.

3.2. Strategy to identify Ce ions within the organic-inorganic hybrid coating

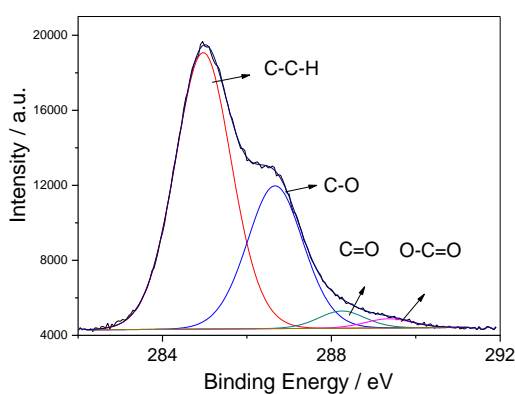
To make one step ahead in the interpretation of the role of Ce^{4+} ions in the corrosion protection afforded by these organic-inorganic hybrid coatings, it is necessary to have some insight about their effective presence within the coating structure as well as about their oxidation state, which is a complex task considering the low amount of this modifier added to the hydrolysis solution. Only few works^{21,45} have detected the presence of Ce in organic-inorganic hybrid coating, but its amount needs to be, in general, higher than that used in the present investigation. Paussa *et al.*⁴³, using GDOES measurements, reported the presence of a thin Ce layer on the substrate surface and inside the ZrO_2 coating. Cerium (III) and cerium (IV) species were detected in polysiloxane hybrid by the deconvolution of the complex Ce 3d spectrum of the XPS analysis^{20,21}. In general, the main problem for the XPS analysis is the amount of Ce ions in the sample, lower than the detection limit of the equipment. In addition, photooxidation of Ce ions during XPS measurements has also been reported²¹. Therefore, attempting to assess/identify the presence of Ce ions in the organic-inorganic hybrid coating, XPS, LIBS and UV-Vis techniques were used.

Figs. 7 and 8 show, respectively, the XPS spectra for the C1s, O1s and Si2p for samples coated with the organic-inorganic hybrid coating without and with 500 ppm of Ce^{4+} ions. Table 1 shows the binding energy values, peak areas and

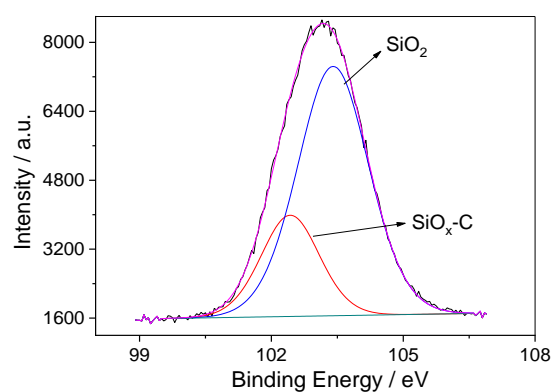
full width at half-maximum (FWHM) determinations. In the Si2p (Fig. 7C and 8C) and O1s (Fig. 7B and 8B) spectra, it is important to highlight the presence of two peaks that characterize the siloxane (Si-O-Si) structure and the polycondensation degree of the organic-inorganic hybrid coating⁴⁸⁻⁵¹. The first peak in the O1s spectrum ($\approx 533 \text{ eV}$) is assigned to the oxygen-silicon (Si-O-Si) bond; the second peak in the Si2p spectrum, at 103.7 eV , is related to the formation of connection strings (SiO_2) in the organic-inorganic hybrid structure⁴⁶⁻⁴⁹. However, the distortion in the SiO_2 binding energy was not accessed, the difference between dopant-modified and unmodified coatings is within the experimental error (Table 1), probably because the low Ce^{4+} ions concentration. But the peak intensity at 103.7 eV for both coatings can be compared: for the doped coating (Fig. 8), the intensity of this peak was 3.5%, a slightly higher value than that to the nondoped coating, suggesting an increase in the polycondensation degree of the organic-inorganic hybrid coating^{20,48,50}. A comparison of the effect of Ce obtained in this work with that of literature^{20,50} is impaired, since dopant concentration is $\sim 15\times$ smaller. This structure extends throughout the material, resulting in a denser and more effective barrier against corrosion, supporting the results of microscopic analyses and electrochemical measurements. For the C1s (Fig. 7A and 8A) spectra different chemical environments were observed for both samples. The coating without the dopant shows two sharp peaks at 285 eV and 287 eV related, respectively, to alkyl CCH and C-O structure connections, whereas for the doped sample only the peak at 285 eV is sharp, the other one is quite smooth and low. This different chemical environment for the nondoped sample can be attributed to a lower polycondensation degree of the organic-inorganic hybrid structure and/or to the presence of a larger amount of organic phase incorporated to the organic-inorganic hybrid structure. The presence of Ce ions was not detected in the XPS measurements, probably because its amount within the coating is lower than the detection limit of the equipment. In some studies, spectra resolved for Ce were only possible with the use of quantities greater than 1000 ppm ^{19,21}. For the same reason LIBS measurements were unsuccessful in detecting Ce in the coating composition when concentrations below 1000 ppm were used.

Table 1. Results of fitting XPS spectra for samples protected with the organic-inorganic hybrid coating with 0 and 500 ppm of Ce(IV). Estimated error in areas is lower than 2.5%.

	0 ppm			500 ppm		
	BE	FHWM	Area	BE	FHWM	Area
C1s	284.9	1.67	59.36	284.9	1.57	62.72
	286.2	2.00	14.02	286.6	1.56	32.34
	288.8	1.70	14.21	288.2	1.29	3.21
	289.0	1.73	12.42	289.3	1.30	1.73
O1s	530.7	1.42	3.18	530.7	1.41	2.32
	532.5	1.71	83.07	532.7	1.71	92.83
	533.7	1.94	13.76	534.1	1.87	4.84
Si2p	102.6	1.68	27.68	102.4	1.56	25.17
	103.3	1.81	72.32	103.4	1.90	74.83



(Figure 7A)



(Figure 7B)

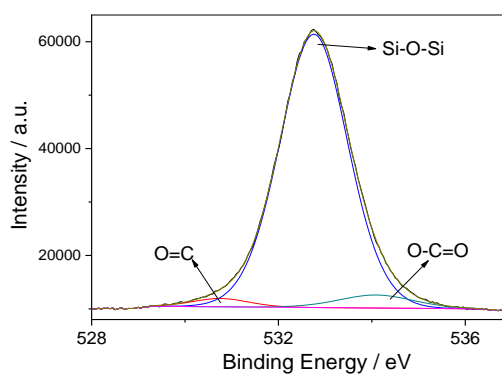


(Figure 7C)

Figure 7. X-ray photoelectron spectra for the C1s, O1s and Si2p for the organic-inorganic hybrid coating without Ce⁴⁺ ions: (A) C 1s, (B) O 1s and (C) Si 2p.

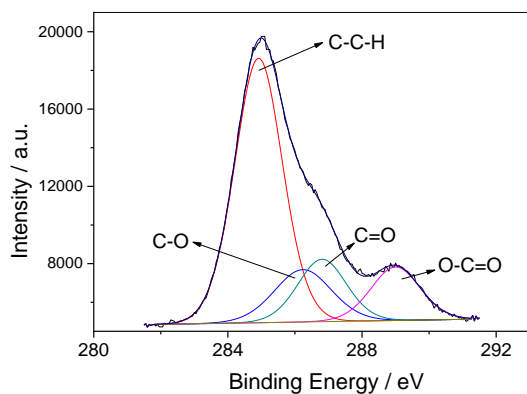


(Figure 8A)

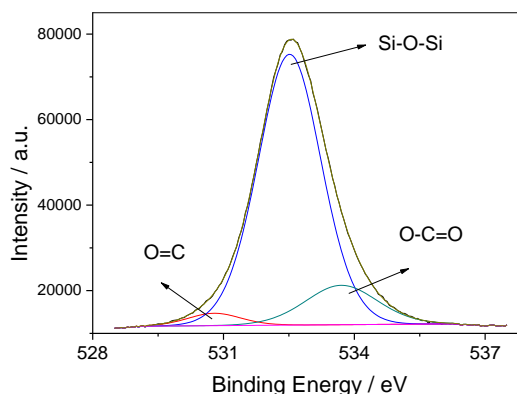


(Figure 8B)

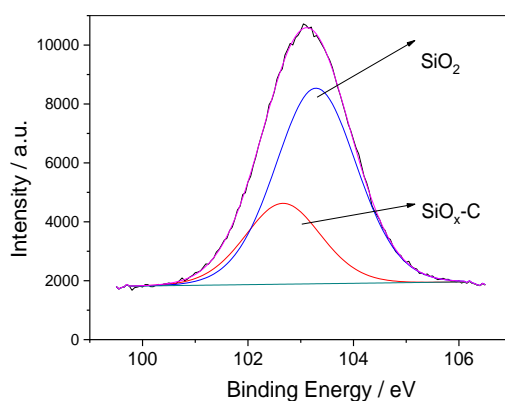


(Figure 8C)

Figure 8. X-ray photoelectron spectra for the C1s, O1s and Si2p for the organic-inorganic hybrid coating doped with 500 ppm of Ce⁴⁺ ions (A) C 1s, (B) O 1s and (C) Si 2p.

Fig. 9 shows LIBS spectra for the coatings without and with 1500 ppm of Ce⁴⁺ ions prepared in the same conditions as those previously reported (*subsection 2.2*) and deposited onto copper substrate to avoid the strong interference of iron in Ce analysis²⁴. To improve the sensibility for Ce detection, one spectrum was obtained with a shearing system

that increases the atomization process. The main lines at 570 nm and 590 nm observed in spectra of Fig. 9A and 9B can be attributed to Si and the lines at 594 nm (Fig. 9C) and 428 nm (Fig. 9D) are attributed to Ce²⁺, confirming the presence of this specie within the coating structure.

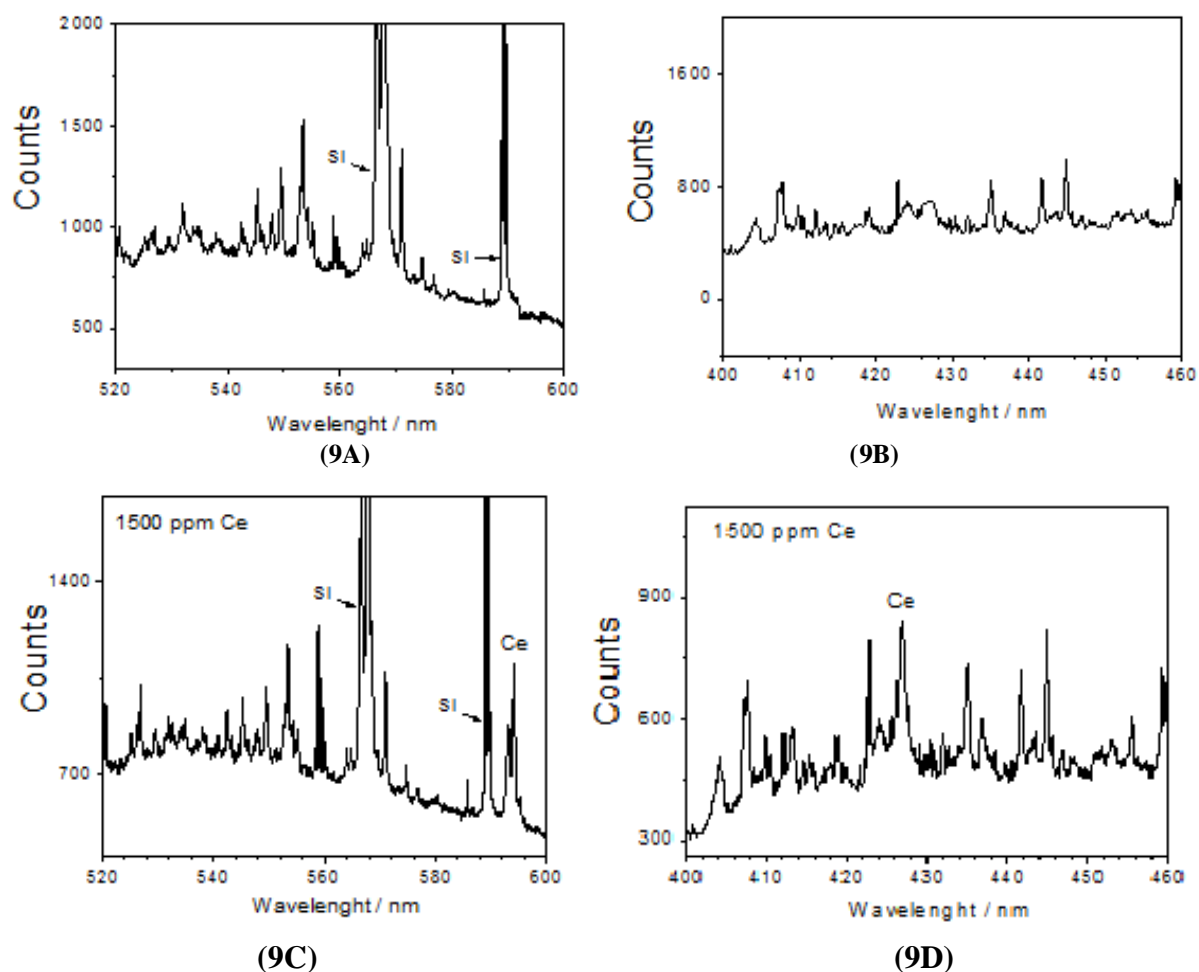


Figure 9. LIBS spectra obtained for pellets of free-standing organic-inorganic hybrid coating nondoped (A) and (B). Doped with 1500 ppm of Ce^{4+} ions (C) and (D).

Fig. 10 shows the UV-Vis spectra of cerium (III) nitrate, cerium (IV) sulfate aqueous solutions, and of Ce ions extraction from freestanding coating doped with 500 ppm of cerium (III) or cerium (IV) salts in naturally aerated deionized water (pH 6.5). Two main relatively wide bands were observed at around 280 nm and 250 nm attributed to the charge transfer transition from oxygen to the d-Ce(IV) orbital and to f-d Ce(III) transition, respectively^{52,53}. Three main information are

highlighted from these spectra: (a) Ce is present inside the doped freestanding coating and can be at least partially extracted with water, indicating that a certain amount of Ce is probably not strongly bonded to the organic molecules of the organic-inorganic hybrid coating; (b) Ce is mainly in the cerium (IV) oxidation state regardless if the doped coating were prepared using cerium (III) or cerium (IV) salts; (c) a small amount of cerium (IV) species is present in the cerium (III) nitrate salt.

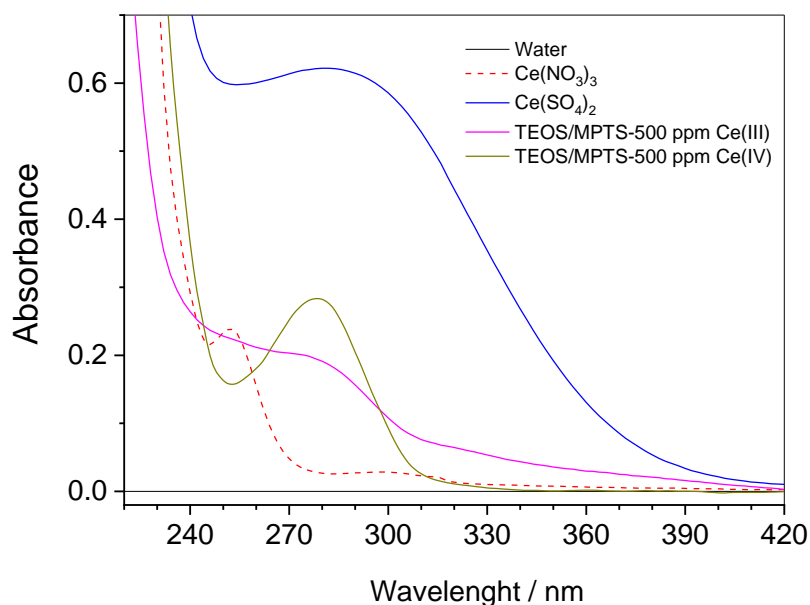


Figure 10. UV-Vis spectra of aqueous solution containing cerium (III) nitrate, cerium (IV) sulfate and solutions of cerium ions extraction, in the presence of oxygen, from the coating doped with 500 ppm of cerium (III) or cerium (IV) salts.

UV-Vis spectra were also obtained for aqueous solution resulting from Ce ions extraction from the organic-inorganic hybrid coating doped with different amounts of cerium (IV) species (Fig. 3S, Supplementary data). From these spectra, the intensity of the peaks follows the order: 900 ppm > 500 ppm > 300 ppm, indicating that the quantity of Ce ions extracted is proportional to its content in the doped coating. To have an idea about the amount of Ce^{4+} ions extracted from the freestanding coating, an analytical curve was constructed for Ce^{4+} ions (Fig. 4S, Supplementary data), the result was a straight line indicating that the amount of Ce ions liberated from the doped coating is proportional to its amount in the doped coating. Sequentially, 3 g of freestanding doped coating (TEOS / MPTS with 500 ppm cerium (IV) ions) was immersed in 3 mL of purified water (pH 6.5) and after extracting for 15 days, the solution was filtered and analyzed by UV-Vis spectrophotometry. The absorbance of the filtered solution was 0.27 corresponding to 35 ppm of Ce^{4+} ions, which means 35 μg cerium (IV) / g of freestanding doped coating. Based on the nominal

composition, the free-standing doped coating has 654 μg cerium (IV) / g, which means that around only 5% of Ce was extracted from the coating. These results also confirm that such amount of Ce is almost impossible to be detected by XPS or LIBS techniques.

Considering that the solution of Ce ions extracted from the freestanding coating doped with cerium (III) salt also showed the band at around 280 nm with similar shape to that acquired from the coating doped with Ce^{4+} ions, extraction of Ce ions from doped coating was performed in inert atmosphere by bubbling purified argon into the water before and during extraction (Fig. 11). For these experiments, the solution obtained by extracting Ce ions from the freestanding coating doped with cerium (III) salt shows a band at around 254 nm (characteristic of Ce^{3+} ions) and a stronger band at around of 276 nm characteristic of Ce^{4+} ions. However, for the solution obtained from the coating doped with cerium (IV) salt, only the band attributed to cerium (IV) was observed. This result suggests that, in both doped coating, Ce is mainly present as cerium (IV) species.

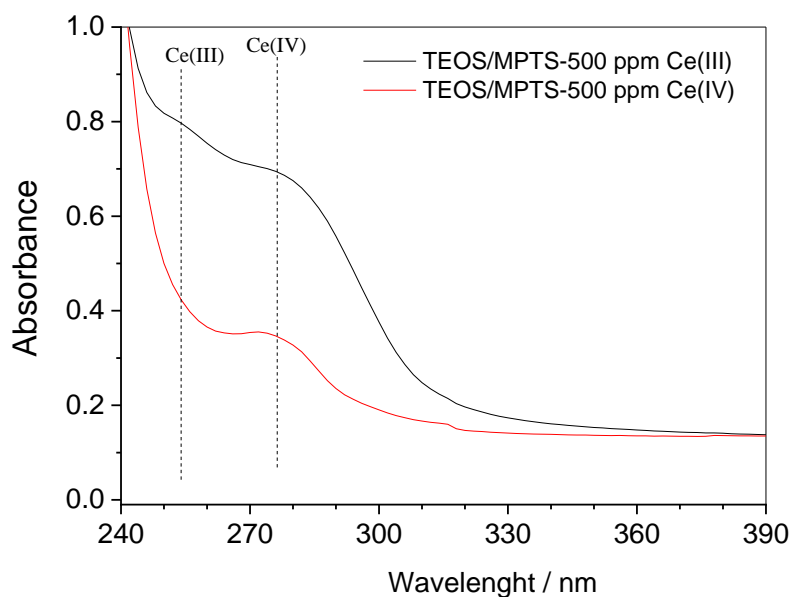
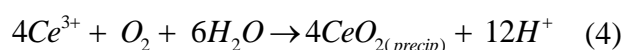
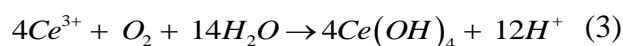
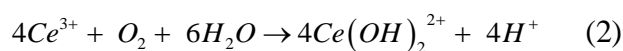
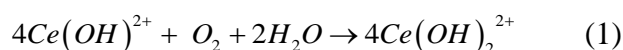


Figure 11. UV-Vis spectra of aqueous solutions of cerium ions extraction in the absence of oxygen from the coating doped with 500 ppm of cerium (III) or cerium (IV) salts.

For comparison with the experiments performed with the extraction from the freestanding coating doped with cerium, UV-Vis measurements were performed with solid organic-inorganic hybrid coating deposited onto glass (Fig. 5S, Supplementary data). For organic-inorganic hybrid coating doped with cerium (IV) ions and with cerium (III) ions one relatively wide band was observed in the range of 250 - 270 nm. In the similar wavelength range one band was observed and assigned to the UV-Vis spectrum of the $\text{Ce}(\text{SO}_4)_2$ crystals. Therefore, for the coating, Ce is mainly in the cerium (IV) oxidation state regardless if the doped coating was prepared using cerium (III) or cerium (IV) salts.

The results reported above indicated that cerium (IV) species react with ethanol and accelerate the radical formation and the polymerization process to form the organic-inorganic hybrid coating. Therefore, it would be expected a spectrum characteristic of cerium (III) species when the cerium was extracted from the doped coatings. Surprisingly, the main species observed in the extracted solution was cerium (IV) species independent on the oxidation state of the Ce ions added to the hydrolysis solution. The presence of cerium (IV) species into the lixiviated solution can be explained admitting the oxidation of cerium (III) to cerium (IV) species in the presence of oxygen, according to the equations^{52,53}:



AFM analysis (Fig. 6S) reinforces the presence of cerium (IV) inside the TEOS/MPTS organic-inorganic hybrid coating as following: an uniform and homogeneous surface without the presence of precipitates is observed for the organic-inorganic hybrid coating modified with cerium (IV) ions (Fig. 6SA, Supplementary data), while a surface with small precipitates at metal surface, possibly cerium oxides / hydroxides, is observed for the organic-inorganic hybrid coating doped with Ce^{3+} ions (Fig. 6SB, Supplementary data).

Trabelsi *et al.*⁹ have studied the effect of cerium (III)-doping of silane solutions in the protection of galvanized steel and also observed cerium (IV) species formation. Several possibilities can explain the presence of cerium (IV) species: (a) oxidation of $\text{Ce}(\text{OH})_3$ to CeO_2 as consequence of the

corrosion reactions caused by anodic areas formation on the steel surface; (b) generation of hydrogen peroxide as consequence of the oxygen reduction during cathodic reaction; (c) in solution oxidation of Ce^{3+} ions to $\text{Ce}(\text{OH})_2^{2+}$ ions and further precipitation of CeO_2 ; (d) dismutation solid state reaction of $\text{Ce}(\text{OH})_3$ to form CeO_2 and (e) a possible oxidation of Ce^{3+} ions to Ce^{4+} ions inside the film.

According to a parallel study of the cerium ions effect on the precursor solutions, Ce^{4+} ions would be reduced to Ce^{3+} ions during the polymerization redox reaction to form organic-inorganic coating (Fig. 1S, Supplementary data), and a fraction of Ce^{3+} ions could be re-oxidized to Ce^{4+} ions via one or more reactions represented in Eq. 1-4. The Ce^{4+} and Ce^{3+} ions may be trapped inside the coating and, as the coating may undergo some hydrolysis in contact with water / electrolyte, these ions are released / lixiviated from the coating and detected by the UV-Vis analysis. This process is reinforced by the AFM results described above. Therefore, Ce^{4+} ions may be present in the as-prepared organic-inorganic hybrid coating as trapped-like species. Briefly, it is proposed that part of Ce species present in the doped organic-inorganic hybrid coating is relatively free or trapped within the coating structure as soluble and can be partially removed by extraction with water or partial hydrolysis of the coating.

4. Conclusions

The influence of the addition of Ce^{4+} ions to the hydrolysis solution on the protective properties of a TEOS / MPTS organic-inorganic hybrid coating was investigated. The results demonstrated that when added at an appropriate amount (in the present case 500 ppm) the dopant can greatly improve the barrier and protective properties of the organic-inorganic hybrid coating, as demonstrated by EIS results.

XPS measurements have shown that the improvement of the barrier properties of the coating can be ascribed to the formation of a denser siloxane (Si-O-Si) network in the presence of cerium (IV) ions.

An experimental strategy designed using LIBS have evidenced the presence of Ce ions within the coating structure, whereas UV-Vis experiments evidenced that Ce is mainly present in the (IV)-oxidation state.

A mechanism was proposed where cerium (III) ions from the redox polymerization reaction may be oxidized back to cerium (IV) species mainly by the presence of oxygen.

6. Acknowledgements

The authors would like to thank CNPq (Process 305890/2010-7) and CAPES (Fernando Santos da Silva social demand scholarship). The authors thank Prof. Dr. Fabíola M. Verbi Pereira for her collaboration in the LIBS analysis and results interpretation.

7. References

- [1] Hammer, P., dos Santos, F. C., Cerrutti, B. M., Pulcinelli, S. H., Santilli, C. V., Carbon nanotube-reinforced siloxane-PMMA hybrid coatings with high corrosion resistance, *Prog. Org. Coat.* 76 (4) (2013) 601-608. <https://doi.org/10.1016/j.porgcoat.2012.11.015>.
- [2] Brinker, C. J., Scherer G. W. *Sol-Gel Science The Physics and Chemistry processing*, Academic Press, San Diego 1 (1990) 912. <https://www.elsevier.com/books/sol-gel-science/brinker/978-0-08-057103-4>.
- [3] Schubert, U., Husing, N., Lorenz, A., *Hybrid Inorganic-Organic Materials by Sol-Gel Processing of Organofunctional Metal Alkoxides*, *Chem. Mater.* 7 (11) (1995) 2010-2027. <https://doi.org/10.1021/cm00059a007>.
- [4] Lamaka, S. V., Montemor, M. F., Galio, A. F., Zheludkevich, M. L., Trindade, C., Dick, L. F., Ferreira, M. G. S., Novel hybrid sol-gel coatings for corrosion protection of AZ31B magnesium alloy, *Electrochim. Acta* 53 (14) (2008) 4773-4783. <https://doi.org/10.1016/j.electacta.2008.02.015>.
- [5] Van Ooij, W. J., Zhu, D., Stacy, M., Seth, A., Mugada, T., Gandhi, J., Puomi, P., *Corrosion Protection Properties of Organofunctional Silanes-An Overview*, *Tsinghua Sci. and Technol.* 10 (6) (2005) 639-664. [https://doi.org/10.1016/S1007-0214\(05\)70134-6](https://doi.org/10.1016/S1007-0214(05)70134-6).
- [6] Kron, J., Deichmann, K. J., Rose, K., *Self-healing properties of new surface treatments*, European Federation of Corrosion Publications, London, 2010. ISBN-13: 978-1906540364.
- [7] Wang, D., Bierwagen, G. P., *Sol-gel coatings on metals for corrosion protection*, *Prog. Org. Coat.* 64 (4) (2009) 327-338. <https://doi.org/10.1016/j.porgcoat.2008.08.010>.

- [8] Ferreira, M. G. S., Duarte, R. G., Montemor, M. F., Simões, A. M. P., Silanes and rare earth salts as chromate replacers for pre-treatments on galvanised steel, *Electrochim. Acta* 49 (17, 18) (2004) 2927-2935. <https://doi.org/10.1016/j.electacta.2004.01.051>.
- [9] Trabelsi, W., Cecilio, P., Ferreira, M. G. S., Montemor, M. F., Electrochemical assessment of the self-healing properties of Ce-doped silane solutions for the pre-treatment of galvanized steel substrates, *Prog. Org. Coat.* 54 (4) (2005) 276-284. <https://doi.org/10.1016/j.porgcoat.2005.07.006>.
- [10] Montemor, M. F., Ferreira, M. G. S., Cerium salt activated nanoparticles as fillers for silane films: Evaluation of the corrosion inhibition performance on galvanised steel substrates, *Electrochim. Acta* 52 (24) (2007) 6976-6987. <https://doi.org/10.1016/j.electacta.2007.05.022>.
- [11] Ozturk, T., Cakmak, I., Synthesis of block copolymers via redox polymerization: a critical review, *Iranian Polym. J.* 16 (8) (2007) 561-581. <http://journal.ippi.ac.ir/manuscripts/IPJ-2007-10-2427.pdf>.
- [12] Nagarajan, S., Srinivason, K. S. V., Block copolymerization initiated by Ce(IV)- poly(ethylene glycol) redox system-kinetics and characterization, *Europe Polym. J.* 30 (1) (1994) 113-119. [https://doi.org/10.1016/0014-3057\(94\)90240-2](https://doi.org/10.1016/0014-3057(94)90240-2).
- [13] Fernandez, M. D., Fernandez, M. J., Guzman, G. M., Study of the morphology of poly(methyl methacrylate) as polymerized by the redox system Ce(IV)-isopropyl alcohol, *J. Polym. Sci.* 27 (10) (1989) 3439-3450. <https://doi.org/10.1002/pola.1989.080271022>.
- [14] Cho, U. Y., Romero, J. R., Chemical and electrochemical oxidative dimerization of carbonyl compounds by cerium(IV) salts. A comparative study, *Tetr. Lett.* 36 (48) (1995) 8757-8760. [https://doi.org/10.1016/0040-4039\(95\)01921-4](https://doi.org/10.1016/0040-4039(95)01921-4).
- [15] Cho, L. Y., Madurro, J. M., Romero, J. R., Electrooxidation of β -Dicarbonyl Compounds Using Ceric Methanesulfonate as Mediator: Some Kinetics and Spectroscopic Studies, *J. Cat.* 186 (1) (1999) 31- 35. <https://doi.org/10.1006/jcat.1999.2541>.
- [16] Purgato, F. L. S., Romero, J. R., Electrooxidation of Hydroxyl Compounds Using Cerium Salts as Mediators: The Importance of Substrate Size for Catalyst Regeneration, *Journal of Catalysis* 209 (2) (2002) 394-400. <https://doi.org/10.1006/jcat.2002.3646>.
- [17] Aleixo, P. C., Cho, L. Y., Romero, J. R., Oxygen as an Oxidizing Agent in Electrocatalytic Oxidation of β -Dicarbonyl Compounds Using Ce^{IV} as a Mediator, *J. of Cat.* 192 (1) (2000) 248-251. <https://doi.org/10.1006/jcat.2000.2829>.
- [18] Lofrano, R. C. Z., Madurro, J. M., Romero, J. R., Preparation and properties of an electrode coated with a cerium poly(allyl ether p-benzenesulfonate) film for electroorganic reactions, *J. Mol. Catal. A: Chem.* 153 (1, 2) (2000) 237-242. [https://doi.org/10.1016/S1381-1169\(99\)00354-4](https://doi.org/10.1016/S1381-1169(99)00354-4).
- [19] Suegama, P. H., de Melo, H. G., Benedetti, A. V., Aoki, I. V., Influence of cerium (IV) ions on the mechanism of organosilane polymerization and on the improvement of its barrier properties, *Electrochim. Acta* 54 (9) (2009) 2655-2662. <https://doi.org/10.1016/j.electacta.2008.11.007>.
- [20] Palomino, L. M., Suegama, P. H., Aoki, I. V., Montemor, M. F., de Melo H. G., Electrochemical study of modified cerium-silane bi-layer on Al alloy 2024-T3, *Corr. Sci.* 51 (6) (2009) 1238-1250. <https://doi.org/10.1016/j.corsci.2009.03.012>.
- [21] Hammer, P., Schiavetto, M. G., Santos, F. C., Benedetti, A. V., Pulcinelli, S. H., Santilli, C. V., Improvement of the corrosion resistance of polysiloxane hybrid coatings by cerium doping, *J. Non-Cryst. Solids* 356 (44, 49) (2010) 2606-2612. <https://doi.org/10.1016/j.jnoncrsol.2010.05.013>.
- [22] Suegama, P. H., Sarmiento, V. H. V., Montemor, M. F., Benedetti, A. V., de Melo, H. G., Aoki, I. V., Santilli, C. V., Effect of cerium (IV) ions on the anticorrosion properties of siloxane-poly (methyl methacrylate) based film applied on tin coated steel, *Electrochim. Acta* 55 (18) (2010) 5100-5109. <https://doi.org/10.1016/j.electacta.2010.04.002>.
- [23] Orazem, M. E., Tribollet, B., *Electrochemical Impedance Spectroscopy*, John Wiley & Sons, New Jersey, 1st ed., 2008. ISBN: 111820994X.
- [24] Phuoc, T. X., Wang, P., McIntyre, D., Detection of rare earth elements in Powder River Basin sub-bituminous coal ash using laser-induced breakdown spectroscopy (LIBS), *Fuel* 163 (1) (2016) 129-132. <https://doi.org/10.1016/j.fuel.2015.09.034>.
- [25] Geenen, F. M., de Wit, J. H. W., An impedance spectroscopy study of the degradation mechanism for a model epoxy coating on mild steel, *Prog. Org. Coat.* 18 (3) (1990) 299-312. [https://doi.org/10.1016/0033-0655\(90\)80007-L](https://doi.org/10.1016/0033-0655(90)80007-L).

- [26] Sarmiento, V. H. V., Schiavetto, M. G., Hammer, P., Benedetti, A. V., Fugivara, C. S., Suegama, P. H., Pulcinelli S. H., Santilli C. V., Corrosion protection of stainless steel by polysiloxane hybrid coatings prepared using the sol-gel process, *Surf. & Coat. Technol.* 204 (16, 17) (2010) 2689-2701. <https://doi.org/10.1016/j.surfcoat.2010.02.022>.
- [27] Bonora, P. L., Deflorian, F., Fedrizzi, L., Electrochemical impedance spectroscopy as a tool for investigating underpaint corrosion, *Electrochim. Acta* 41 (7, 8) (1996) 1073-1082. [https://doi.org/10.1016/0013-4686\(95\)00440-8](https://doi.org/10.1016/0013-4686(95)00440-8).
- [28] Pepe, A., Aparicio, M., Duran, A., Cere, S., Cerium hybrid silica coatings on stainless steel AISI 304 substrate, *J. Sol-Gel Sci. Techn.* 39 (2) (2006) 131-138. <https://doi.org/10.1007/s10971-006-9173-1>.
- [29] Yaggi, C., Yildiz, U., Redox polymerization of methyl methacrylate with allyl alcohol 1,2-butoxylate-block-ethoxylate initiated by Ce (IV)/HNO₃ redox system, *Europe Poly. J.* 41 (1) (2005) 177-184. <https://doi.org/10.1016/j.eurpolymj.2004.08.008>.
- [30] Capelossi, V. R., Aoki, I. V., Influence of sonication on anticorrosion properties of a sulfur silane film doped with Ce (IV) on galvanized steel, *Prog. Org. Coat.* 76 (5) (2013) 812-820. <https://doi.org/10.1016/j.porgcoat.2013.01.012>.
- [31] Molander, G. A., Application of lanthanide reagents in organic synthesis, *Chem. Rev.* 92 (1) (1992) 29-68. <https://doi.org/10.1021/cr00009a002>.
- [32] Choi, Y-S., Nestic, S., Ling, S., Effect of H₂S on the CO₂ corrosion of carbon steel in acidic solutions, *Electrochim. Acta* 56 (4) (2011) 1752-1760. <https://doi.org/10.1016/j.electacta.2010.08.049>.
- [33] Keddad, M., Mattos, O. R. Takenouti H., Reaction Model for Iron Dissolution Studied by Electrode Impedance: II. Determination of the Reaction Model, *J. Electrochem. Soc.* 128 (2) (1981) 266-274. <https://doi.org/10.1149/1.2127402>.
- [34] Keddad, M., Mattos, O. R., Takenouti, H., Reaction Model for Iron Dissolution Studied by Electrode Impedance I. Experimental Results and Reaction Model, *J. Electrochem. Soc.* 128 (1) (1981) 257-266. <http://jes.ecsdl.org/content/128/2/257.short>.
- [35] Epelboin, I., Keddad, M., Mattos, O. R., Takenouti, H., The dissolution and passivation of Fe and Fe-Cr alloys in acidified sulphate medium: Influences of pH and Cr content, *Corr. Sci.* 19 (12) (1979) 1105-1112. [https://doi.org/10.1016/S0010-938X\(79\)80128-6](https://doi.org/10.1016/S0010-938X(79)80128-6).
- [36] Zhu, D., van Ooij, W. J., Corrosion protection of metals by water-based silane mixtures of bis-[trimethoxysilylpropyl]amine and vinyltriacetoxysilane, *Prog. Org. Coat.* 49 (1) (2004) 42-53. <https://doi.org/10.1016/j.porgcoat.2003.08.009>.
- [37] van Westing, E. P. M., Ferrari, G. M., de Wit, J. H. W., The determination of coating performance with impedance measurements-III. *in situ* determination of loss of adhesion, *Corros. Sci.* 36 (6) (1994) 979-994. [https://doi.org/10.1016/0010-938X\(94\)90198-8](https://doi.org/10.1016/0010-938X(94)90198-8).
- [38] Musiani, M., Orazem, M. E., Pèbèrec, N., Tribollet, B., Vivier, V., Constant-Phase-Element Behavior Caused by Coupled Resistivity and Permittivity Distributions in Films, *J. Electrochem. Soc.* 158 (12) (2011) C424-C428. <https://doi.org/10.1149/2.039112jes>.
- [39] Hirschorn, B., Orazem, M. E., Tribollet, B., Vivier, V., Frateur, I., Musiani, M. J., Constant Phase-Element Behavior Caused by Resistivity Distributions in Films I. Theory, *J. Electrochem. Soc.* 157 (12) (2010) C452-C457. <https://doi.org/10.1149/1.3499564>.
- [40] Hirschorn, B., Orazem, M. E., Tribollet, B., Vivier, V., Frateur, I., Musiani, M., Constant Phase-Element Behavior Caused by Resistivity Distributions in Films II. Applications, *J. Electrochem. Soc.* 157 (12) (2010) C458-C563. <https://doi.org/10.1149/1.3499565>.
- [41] Sakai, R. T., di L Cruz, F. M., de Melo, H. G., Benedetti, A. V., Santilli, C. V., Suegama, P. H., Electrochemical study of TEOS, TEOS/MPTS, MPTS/MMA and TEOS/MPTS/MMA films on tin coated steel in 3.5% NaCl solution, *Prog. Org. Coat.* 74 (2) (2012) 288-381. <https://doi.org/10.1016/j.porgcoat.2012.01.001>.
- [42] van Westing, E. P. M., Ferrari, G. M., de Witt, J. H. W., The determination of coating performance with impedance measurements-II. Water uptake of coatings, *Corros. Sci.* 36 (6) (1994) 957-977. [https://doi.org/10.1016/0010-938X\(94\)90197-X](https://doi.org/10.1016/0010-938X(94)90197-X).
- [43] Paussa, L., Rosero-Navarro, N. C., Bravin, D., Andreatta, F., Lanzutti, A., Aparicio, M., Durán, A., Fedrizzi, L. ZrO₂ sol-gel pre-treatments doped with cerium nitrate for the corrosion protection of AA6060, *Prog. Org. Coat.* 74 (2) (2012) 311-319. <https://doi.org/10.1016/j.porgcoat.2011.08.017>.
- [44] Silva, F. S., Suegama, P. H., Silva, W. P., Rinaldi, A. W., Domingues, N. L. C., Matsumoto, M. Y., Salazar, L. G., Effect of Different Dopants in Films TEOS/MPTS Used to Protect the Carbon Steel, *Mater. Sci. Forum* 805 (2015) 167-171.

<https://doi.org/10.4028/www.scientific.net/MSF.805.167>.

[45] Arnott, D. R., Ryan, N. E., Hinton, B. R. W., Auger and XPS studies of cerium corrosion inhibition on 7075 aluminum alloy, *Appl. of Surf. Sci.* 22-23 (1) (1985) 236-251. [https://doi.org/10.1016/0378-5963\(85\)90056-X](https://doi.org/10.1016/0378-5963(85)90056-X).

[46] Rosero-Navarro, N. C., Pellice, S. A., Duran, A., Aparicio, M., Effects of Ce-containing sol-gel coatings reinforced with SiO₂ nanoparticles on the protection of AA2024, *Corr. Sci.* 50 (5) (2008) 1283-1291. <https://doi.org/10.1016/j.corsci.2008.01.031>.

[47] Naderi, R., Fedel, M., Deflorian, F., Poelman, M., Olivier, M., Synergistic effect of clay nanoparticles and cerium component on the corrosion behavior of eco-friendly silane sol-gel layer applied on pure aluminum, *Surf. & Coat. Technol.* 224 (15) (2013) 93-100. <https://doi.org/10.1016/j.surfcoat.2013.03.005>.

[48] Nocun, M., Cholewa-Kowalska, K., Łaczka, M., Structure of hybrids based on TEOS cyclic forms of siloxane system, *J. Mol. Struct.*, 938 (1-3) (2009) 24-28. <https://doi.org/10.1016/j.molstruc.2009.08.034>.

[49] Materne, T., de Buyl, F., Witucki, G. L., *Organosilane technology in coating applications*, Dow Corning, Midland, 1st ed., 2004.

[50] Montemor, M. F., Ferreira, M. G. S., Analytical and microscopic characterisation of modified bis-[triethoxysilylpropyl] tetrasulphide silane films on magnesium AZ31 substrates, *Prog. Org. Coat.* 60 (3) (2007) 228-237. <https://doi.org/10.1016/j.porgcoat.2007.07.019>.

[51] Tabata, A., Fujii, S., Suzuoki, Y., Mizutani, T., Ieda, M., X-ray photoelectron spectroscopy (XPS) of hydrogenated amorphous silicon carbide (a-Si_xC_{1-x}:H) prepared by the plasma CVD method, *J. Phys. D: Appl. Phys.* 23 (3) (1990) 316-320. <https://doi.org/10.1088/0022-3727/23/3/008>.

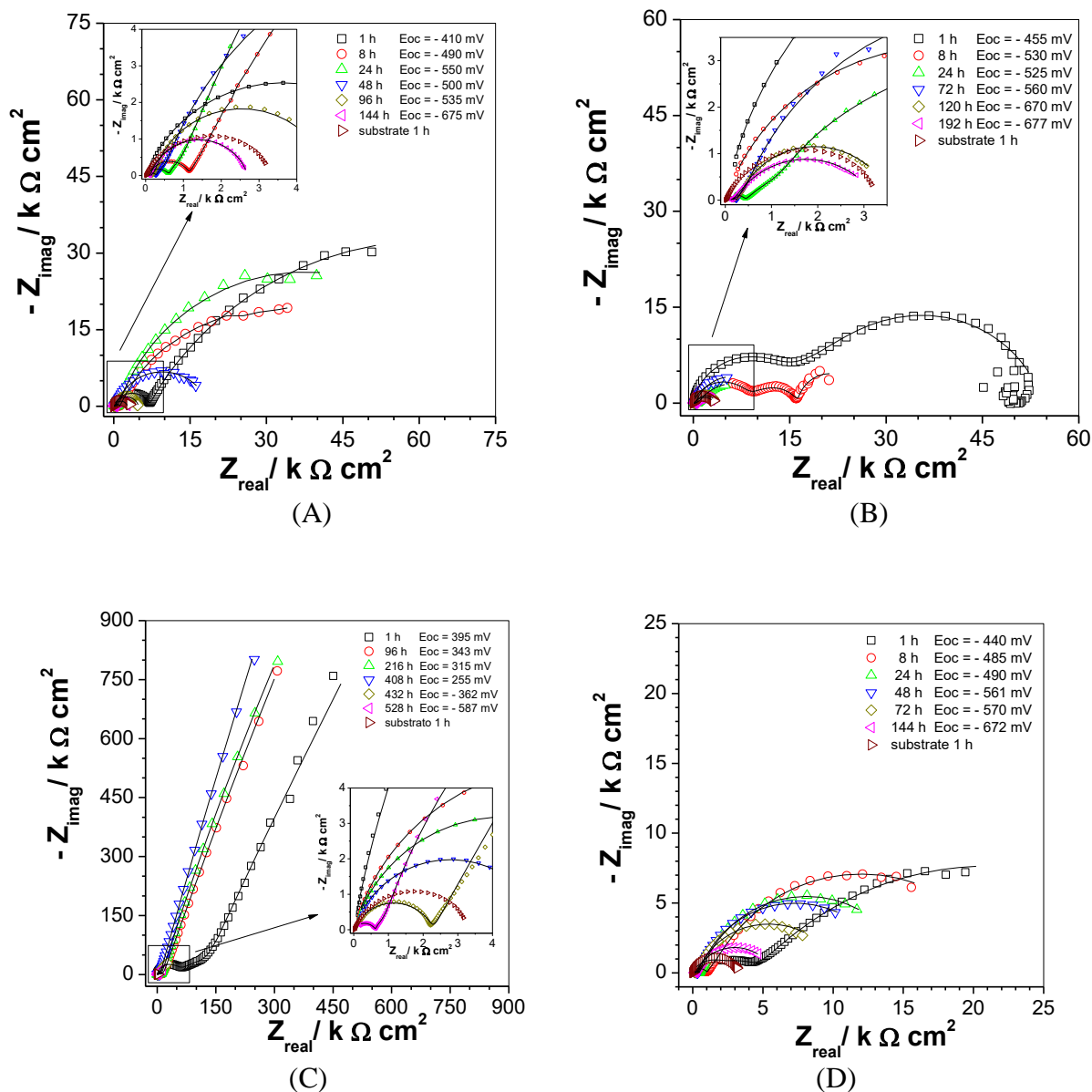
[52] Scott, H. A., Yu, P., O'Keefe, T. J., O'Keefe, M. J., Stoffer, J. O., The Phase Stability of Cerium Species in Aqueous Systems I. E-pH Diagram for the Ce-HClO₄-H₂O-Ce-HClO₄-H₂O System, *J. Electrochem. Soc.* 149 (2002) C623-C630. <https://doi.org/10.1002/chin.200309018>.

[53] Yu, P., Scott, H. A., O'Keefe, T. J., O'Keefe, M. J., Stoffer, J. O., The Phase Stability of Cerium Species in Aqueous Systems II. The Formula Systems. Equilibrium Considerations and Pourbaix Diagram Calculations, *J. Electrochem. Soc.* 153 (1) (2006) C74-C79. <https://doi.org/10.1149/1.1516775>

Supplementary data

Influence of Ce(IV) ions amount on the electrochemical behavior of organic-inorganic hybrid coatings in 0.1 mol L⁻¹ NaCl solution

Figure 1S shows the Nyquist plots for coated samples containing different amounts of Ce(IV).



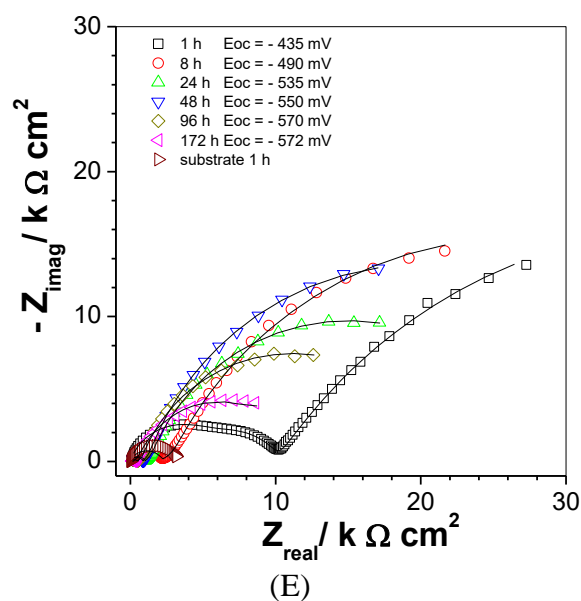
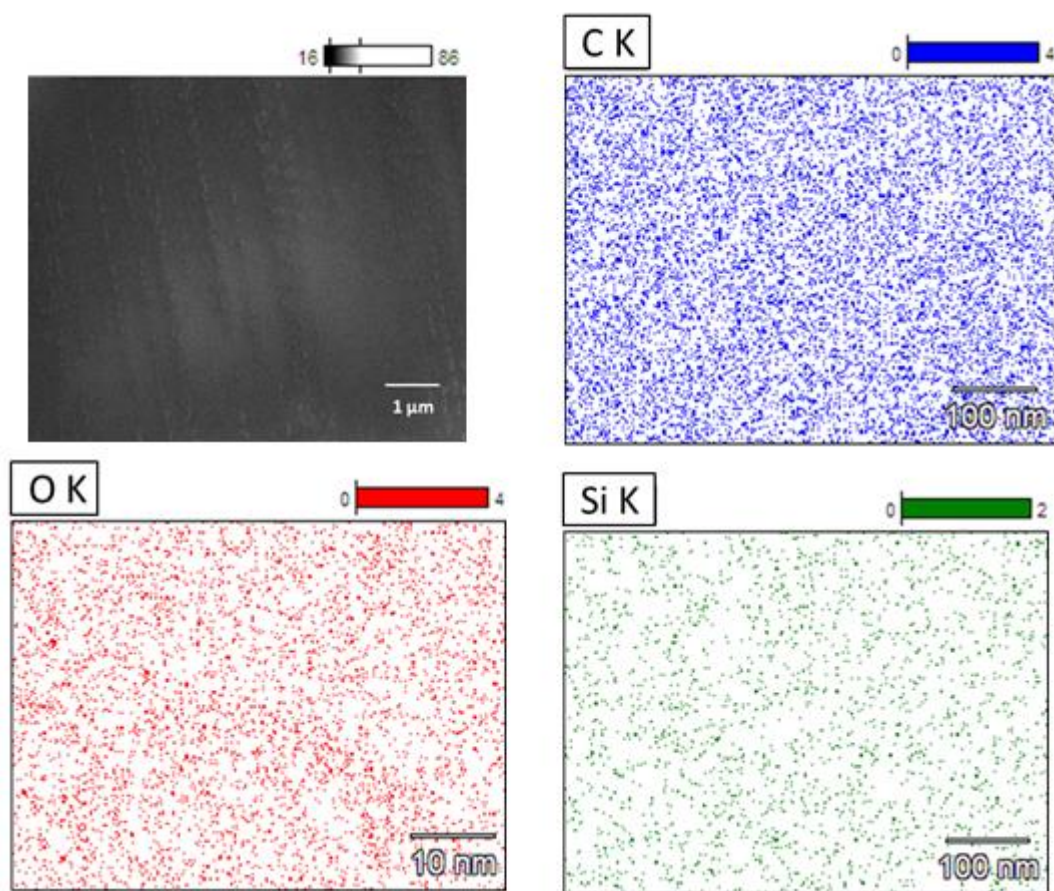


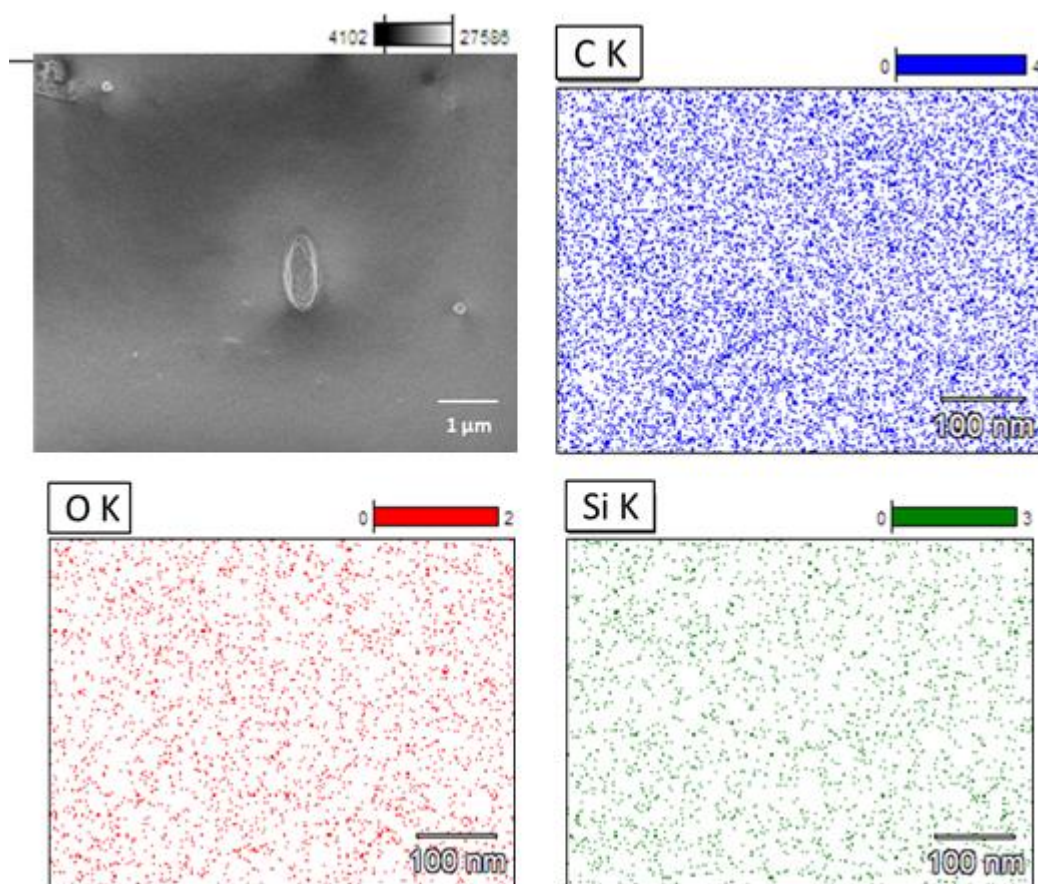
Figure 1S. Experimental (symbols) and fitted (solid line) complex plane plots for carbon steel coated with TEOS / MPTS doped with Ce(IV) ions: (A) 0 ppm, (B) 300 ppm, (C) 500 ppm, (D) 700 ppm and (E) 900 ppm with different immersion times in 0.1 mol L^{-1} NaCl.

Comparing the different diagrams, it can be verified that the coating doped with 500 ppm provides the highest impedance response, confirming the best protection of the substrate. For a given frequency, $f=10 \text{ mHz}$, the highest Z_{real} value was obtained for this sample (about $450 \text{ k}\Omega \text{ cm}^2$) while for the other samples the maximum value was near $50 \text{ k}\Omega \text{ cm}^2$ (300 ppm). Even after 408 h immersion this coating showed a Z_{real} ($f=10 \text{ mHz}$) around $200 \text{ k}\Omega \text{ cm}^2$, which is much higher than for the remainder of the samples at the beginning of their exposure period.

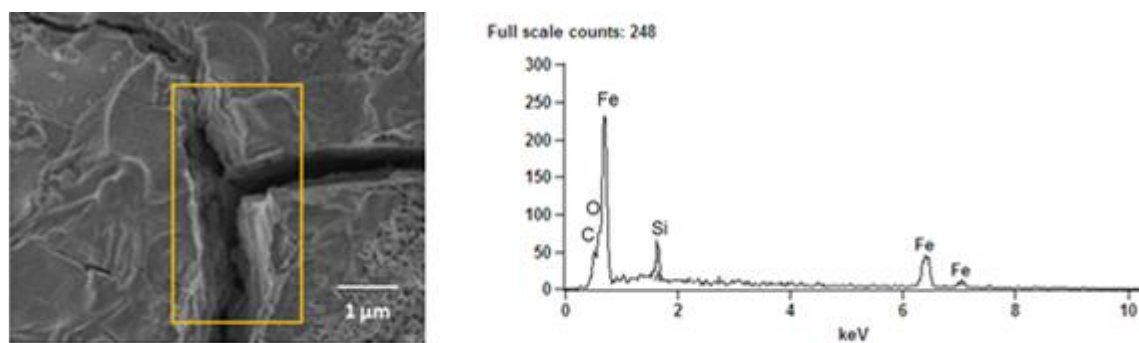
Figure 2S shows the maps of elements distribution for the hybrid coating with 0 and 500 ppm Ce^{4+} ions before immersion and EDS spectra after 240 h of immersion in 0.1 mol L^{-1} NaCl solution.



(A)



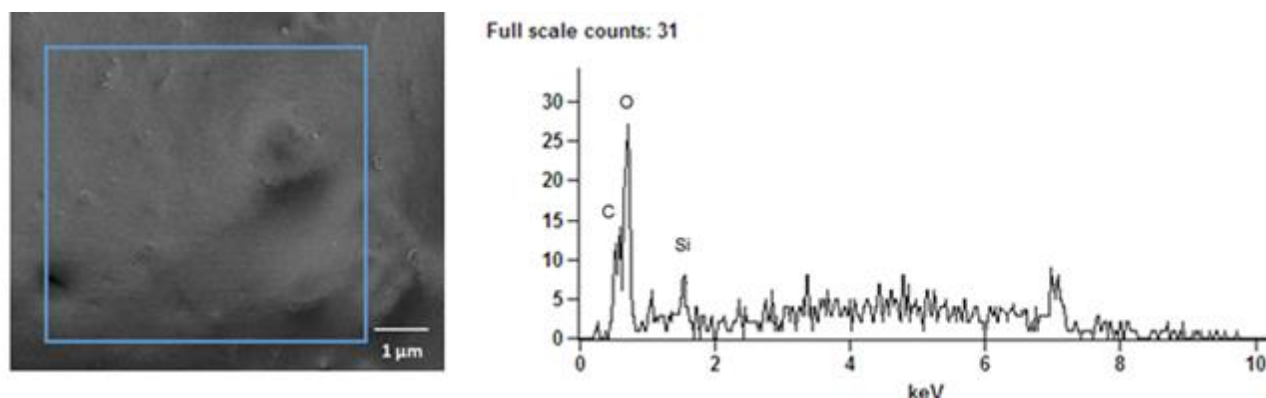
(B)



Quantitative Results for 0ppm Ce(IV) ions, EIS.

<i>Element Line</i>	<i>Weight %</i>
<i>C K</i>	14.57
<i>O K</i>	29.48
<i>Si K</i>	5.01
<i>Fe L</i>	50.94
<i>Total</i>	100.00

(C)



Quantitative results for 500 ppm Ce(IV) ions, EIS.

<i>Element</i>	<i>Weight %</i>
<i>Line</i>	
<i>C K</i>	32.25
<i>O K</i>	45.15
<i>Si K</i>	22.6
<i>Total</i>	100.00

(D)

Fig. 2S. Maps of elements distribution for the hybrid coating: (A) 0 ppm and (B) and 500 ppm Ce⁴⁺ ions before immersion and EDS spectra for samples with (C) 0 ppm and (D) 500 ppm Ce⁴⁺ ions after 240 h of immersion in 0.1 mol L⁻¹ NaCl solution.

As mentioned in the main part of the manuscript different techniques were used trying to get information about the presence of cerium in the hybrid film and its main oxidation state. In this way, XPS, LIBS and UV-Vis analysis were performed. Due to the low concentration of cerium species in the hybrid films both XPS and LIBS techniques failed in detecting these ions in the hybrid film. However, insight on the presence and nature of cerium species in the doped film were obtained using UV-Vis technique.

Figure 3S shows the spectra obtained for aqueous solution resultant of extraction of cerium species from doped hybrid coatings prepared with different concentrations of Ce(IV) species.

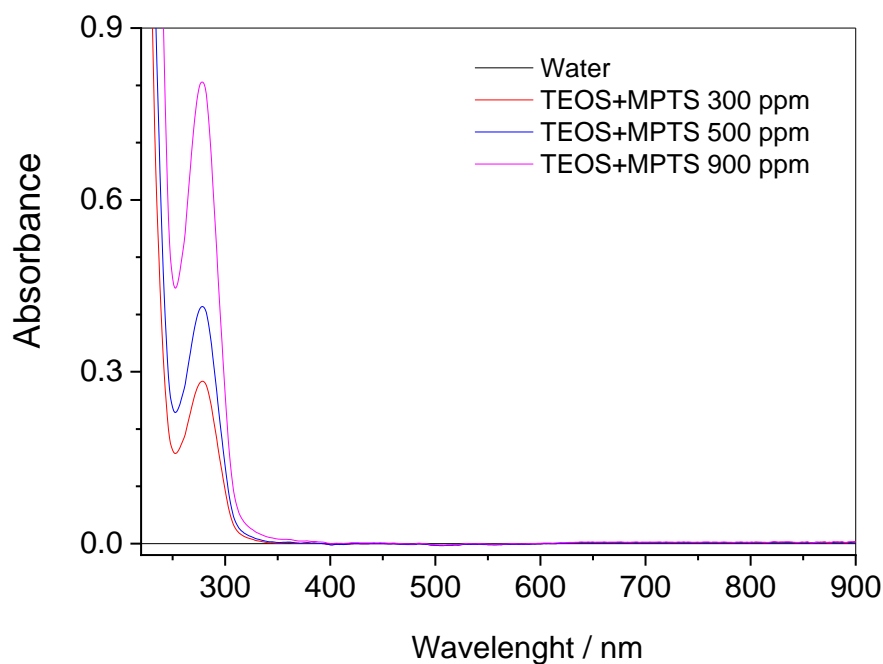


Figure 3S. Spectra obtained for aqueous solution resultant of extraction of cerium species from doped hybrid coatings prepared with different concentrations of Ce(IV) species.

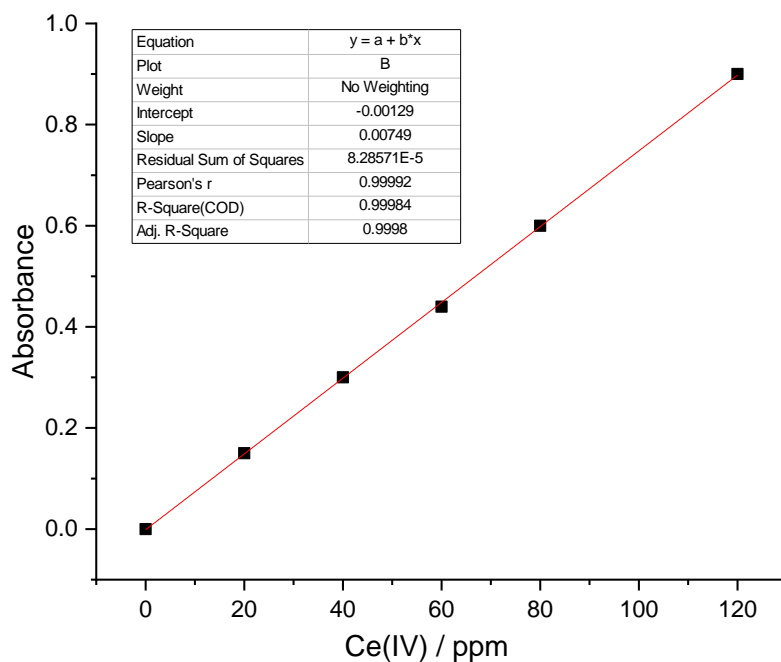


Figure 4S. Analytical curve for Ce(IV) ions ($\text{Ce}(\text{SO}_4)_2$) in aqueous solution at pH 6.5.

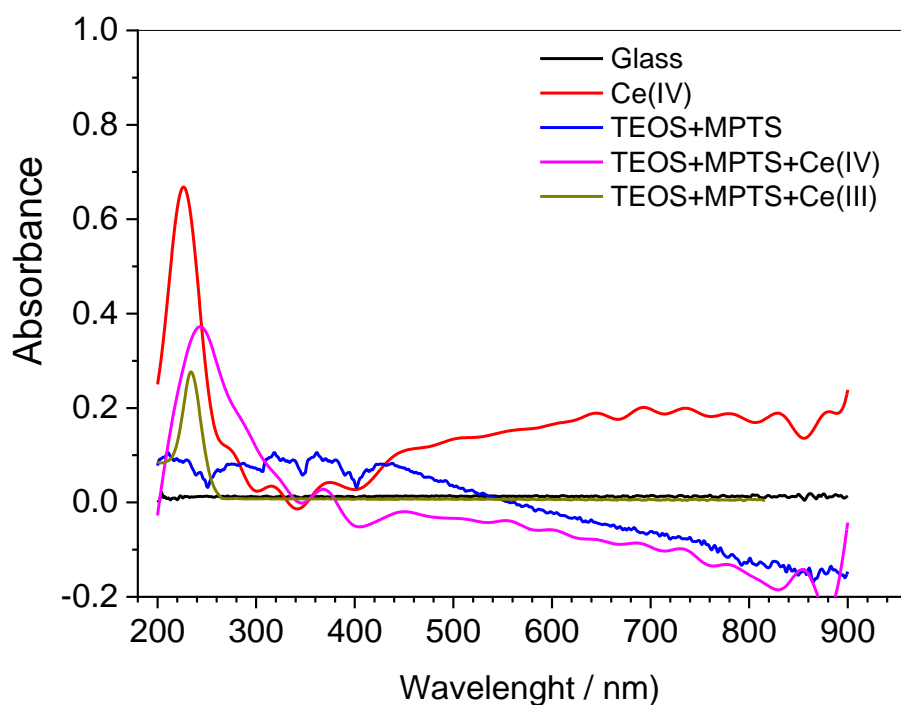


Figure 5S. Spectra obtained for cerium salt, glass and solid hybrid films with 0 ppm and 500 ppm of cerium deposited onto the glass.

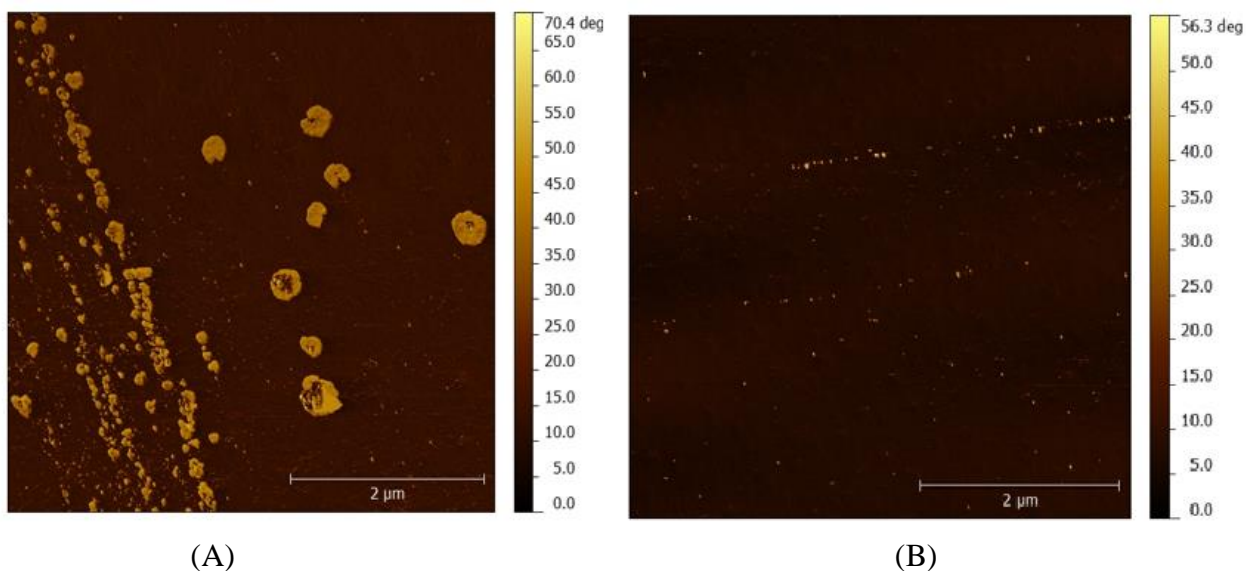


Figure 6S. AFM images from TEOS / MPTS hybrid films prepared with: (A) 300 ppm Ce(III) and (B) 300 ppm of Ce(IV).

Table 1S. Results of the fitting procedure of the experimental EIS data with the EEC presented in Fig. 4 for a carbon steel sample coated with TEOS / MPTS and 0 ppm Ce(IV) in 0.1 mol L⁻¹ NaCl solution.

Time / h	1	8	24	48	96	144
CPE ₁ -T / $\mu\text{Fcm}^{-2} \text{s}^{\alpha-1}$	0.13 (2)*	0.4 (4)	1.3 (12)	4.4 (2.4)	3.2 (6)	1.5 (11)
α_1	0.78 (0.2)	0.70 (0.5)	0.6 (1.7)	0.5 (3.6)	0.5	0.5
R ₁ / k Ω cm ²	7.0 (0.4)	1.1 (0.3)	0.66 (1.0)	0.30 (1.4)	0.16 (0.8)	0.10 (0.5)
CPE ₃ -T / $\mu\text{Fcm}^{-2} \text{s}^{\alpha-1}$	57 (0.5)	84 (0.4)	107 (1.0)	154 (1.6)	174 (1.8)	277 (1.2)
α_2	0.7 (0.6)	0.7 (0.3)	0.73 (0.5)	0.72 (0.8)	0.7 (0.7)	0.8 (0.5)
R ₃ / k Ω cm ²	103 (2.7)	59 (1.7)	107 (6.2)	27 (6.4)	5.1 (1.7)	2.7 (1.0)
$\chi^2 / 10^{-3}$	0.6	0.4	1.7	0.5	0.7	0.3

* The % errors associated with each estimative are given in parentheses.

Table 2S. Results of the fitting procedure of the experimental EIS data with the EEC Fig. 5 for carbon steel coated with TEOS / MPTS doped with 300 ppm of Ce(IV), in 0.1 mol L⁻¹ NaCl.

Time / h	1	8	24	72	120	192
CPE ₁ -T / $\mu\text{Fcm}^{-2} \text{s}^{\alpha-1}$	0.008 (2)*	0.03 (3.5)	0.86 (5.6)	1.1 (12)	1.8 (19)	2.0 (1.9)
α_1	0.9 (0.2)	0.80 (0.3)	0.58 (0.7)	0.56 (1.5)	0.53 (2.6)	0.5
R ₁ / k Ω cm ²	16 (0.9)	8.2 (2)	0.44 (0.3)	0.24 (0.3)	0.17 (0.6)	0.13 (0.3)
CPE ₂ -T / $\mu\text{Fcm}^{-2} \text{s}^{\alpha-1}$	0.05 (10)	1.3 (27)	508 (3)	649 (6)	288 (12)	184 (15)
α_2	1.0	0.7	0.50 (1.3)	0.73 (1.8)	0.68 (2.8)	0.65 (3)
R ₂ / k Ω cm ²	4.6 (16)	1.8 (9.6)	3.2 (11)	0.93 (18)	0.21 (8.4)	0.14 (11)
CPE ₃ -T / $\mu\text{Fcm}^{-2} \text{s}^{\alpha-1}$	0.72 (3)	5.5 (9.5)	302 (7.7)	368 (12)	509 (6.8)	342 (8.7)
α_3	0.7	0.7 (3.2)	0.92 (4.3)	0.89 (4.5)	0.82 (2)	0.65 (1.5)
R ₃ / k Ω cm ²	34 (2.7)	6.6 (5.3)	13 (6.2)	11 (2.0)	3.2 (0.7)	3.0 (0.5)
$\chi^2 / 10^{-3}$	0.20	0.20	0.17	0.60	0.41	0.12

* The % errors associated with each estimative are given in parentheses.

Table 3S. Results of the fitting procedure of the experimental EIS data with the EEC Fig. 5 for carbon steel coated with TEOS / MPTS doped with 500 ppm of Ce(IV), in 0.1 mol L⁻¹ NaCl.

Time / h	1	96	216	408	432	528	688
CPE ₁ -T / $\mu\text{Fcm}^{-2} \text{s}^{\alpha-1}$	0.016 (3)*	0.04 (1.5)	0.05 (1.7)	0.07 (1.7)	0.1 (3.6)	0.45 (4.5)	2.0 (2.4)
α_1	0.88 (0.4)	0.81 (0.2)	0.81 (0.2)	0.79 (0.2)	0.7 (0.4)	0.67 (0.5)	0.5
R ₁ / k Ω cm ²	60 (2)	8.5 (0.5)	8.5 (0.4)	5.5 (0.3)	2.1 (0.3)	0.62 (0.2)	0.11(0.2)
CPE ₂ -T / $\mu\text{Fcm}^{-2} \text{s}^{\alpha-1}$	2 (15)	6.2 (16)	6.2 (16)	7.2 (14)	107 (9)	221 (6.8)	279 (15)
α_2	0.65 (6.4)	0.8 (3.6)	0.8 (3.6)	0.84 (2.9)	0.76 (3)	0.75 (1)	0.7 (2.8)
R ₂ / k Ω cm ²	106 (11)	16 (29)	16 (29)	13 (28)	5.1 (23)	1.0 (16)	0.20 (25)
CPE ₃ -T / $\mu\text{Fcm}^{-2} \text{s}^{\alpha-1}$	7.64 (5)	4.7 (23)	4.7 (23)	4.5 (23)	96 (12)	136 (12)	200 (21)
α_3	0.83 (3)	0.79 (3.5)	0.79 (3.5)	0.81 (3.1)	0.8 (3.8)	0.85 (3.2)	0.7 (3.9)
R ₃ / k Ω cm ²	3510 (12)	27500 (11)	16000 (11)	47300 (27)	95 (3.2)	35 (1.8)	3.3 (1.3)
$\chi^2 / 10^{-3}$	1.69	0.13	0.13	0.11	0.39	0.26	0.18

* The % errors associated with each estimative are given in parentheses.

Table 4S. Results of the fitting procedure of the experimental EIS data with the EEC Fig. 5 for carbon steel coated with TEOS / MPTS doped with 700 ppm of Ce(IV), in 0.1 mol L⁻¹ NaCl.

Time / h	1	8	24	48	72	144
CPE ₁ -T / $\mu\text{F cm}^{-2} \text{s}^{\alpha-1}$	0.15(5.4)*	0.47 (4.3)	1.0 (6.6)	4.9 (0.5)	5.0 (3)	2.2 (1.0)
α_1	0.74 (0.6)	0.68 (0.5)	0.62 (0.9)	0.5	0.5	0.5
R ₁ / $\text{k}\Omega \text{cm}^2$	2.5 (1.8)	1.0 (0.3)	0.46 (0.3)	0.35 (0.1)	0.28 (0.6)	0.15 (0.1)
CPE ₂ -T / $\mu\text{F cm}^{-2} \text{s}^{\alpha-1}$	3.7 (13)	170 (1.6)	203 (8.5)	242 (5.5)	237 (3.6)	355 (4.8)
α_2	0.68 (3.1)	0.7	0.78 (2.0)	0.78 (1.3)	0.7	0.7 (1)
R ₂ / $\text{k}\Omega \text{cm}^2$	1.8 (4.5)	5.1 (11)	1.3 (24)	1.0 (15)	0.49 (9.6)	0.39 (11)
CPE ₃ -T / $\mu\text{F cm}^{-2} \text{s}^{\alpha-1}$	149 (0.4)	65 (4)	105 (16)	128 (10)	153 (5.7)	176 (10)
α_3	0.50 (1.0)	0.9 (3)	0.84 (4.5)	0.86 (3)	0.89 (1.8)	0.78 (2.4)
R ₃ / $\text{k}\Omega \text{cm}^2$	43 (4)	17 (3.7)	14 (1.8)	12.8 (0.8)	10 (1.5)	5.2 (0.6)
$\chi^2 / 10^{-3}$	0.13	0.41	0.20	0.15	1.8	0.10



* The % errors associated with each estimative are given in parentheses.

Table 5S. Results of the fitting procedure of the experimental EIS data with the EEC Fig. 5 for carbon steel coated with TEOS / MPTS doped with 900 ppm of Ce(IV), in 0.1 mol L⁻¹ NaCl.

Time / h	1	8	24	48	96	172
CPE ₁ -T / $\mu\text{F cm}^{-2} \text{s}^{\alpha-1}$	0.05 (3)*	0.18 (3)	0.25 (5)	0.32 (4.5)	1.4 (7.7)	2.7 (3)
α_1	0.81 (0.3)	0.73 (0.3)	0.72 (0.6)	0.70 (0.5)	0.58 (1.0)	0.5
R ₁ / $\text{k}\Omega \text{cm}^2$	6.4 (1.0)	2.2 (0.3)	1.0 (0.4)	0.8 (0.3)	0.50 (0.6)	0.19 (0.7)
CPE ₂ -T / $\mu\text{F cm}^{-2} \text{s}^{\alpha-1}$	1.4 (8)	89 (4.2)	95 (23)	130 (17)	133 (17)	186 (16)
α_2	0.74 (2)	0.7	0.79 (5.4)	0.79 (4.2)	0.73 (4.2)	0.64 (3.6)
R ₂ / $\text{k}\Omega \text{cm}^2$	3.7 (2.4)	1.4 (7.7)	0.6 (20)	0.78 (20)	0.5 (15)	0.45 (16)
CPE ₃ -T / $\mu\text{F cm}^{-2} \text{s}^{\alpha-1}$	207 (0.7)	123 (2.7)	166 (13)	165 (14)	217 (11)	214 (14)
α_3	0.64 (0.8)	0.73 (1)	0.77 (2.4)	0.79 (2.8)	0.81 (2.7)	0.79 (3.8)
R ₃ / $\text{k}\Omega \text{cm}^2$	57 (3.2)	47 (2)	27 (1)	37 (1.0)	21 (2)	13 (4)
$\chi^2 / 10^{-3}$	0.10	0.36	0.24	0.19	0.41	1.2

* The % errors associated with each estimative are given in parentheses.

Determination of trace amounts of selenium in natural spring waters and tea samples by catalytic kinetic spectrophotometry

Ramazan Gürkan¹, Nevalnur Zeynep Gürkan²

¹ University of Cumhuriyet, Faculty of Science, Department of Chemistry, Sivas, Turkey

² Near East University, Faculty of Medicine, Near East Blvd., Nicosia, Cyprus

*Corresponding author: Ramazan Gürkan, Phone: +90 (346) 219 2136, email address: rgurkan@cumhuriyet.edu.tr

ARTICLE INFO

Article history:

Received: March 6, 2019

Accepted: July 26, 2019

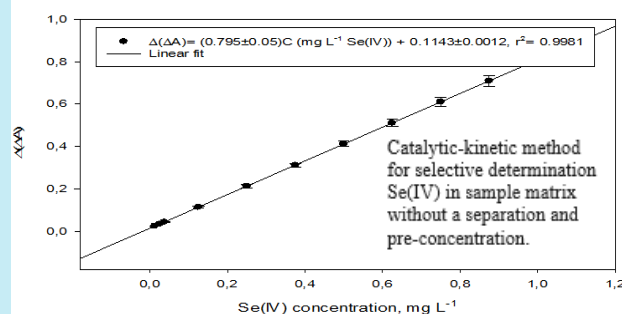
Published: October 1, 2019

Keywords:

1. inorganic selenium
2. phosphomolybdic acid
3. hypophosphite
4. catalytic kinetic spectrophotometry
5. natural spring water
6. tea samples

ABSTRACT: In this work, a new kinetic method is described for the determination of trace Se(IV) in natural spring waters and commercial tea samples. The method is based on the activation of Se(IV) onto the indicator reaction in acidic medium. The reaction was monitored using a fixed time approach of 20 min at 680 nm. The variables affecting the reaction rate were evaluated and optimized. The method allows the determination of Se(IV) in the range of 0.0125-1.0 mg L⁻¹ with a detection limit of 3.6 µg L⁻¹. The precision was in range of 0.63-3.15% (as RSD %) with a higher recovery than 98.6%. The method has been found to be selective against matrix effect. The method was applied to the speciation analysis of inorganic Se species present in the selected samples. The method was statistically validated by analysis of two certified samples and comparing the obtained results to those of HG-AAS analysis. Also, the total Se levels of the samples were determined by using both methods after conversion of Se(VI) into Se(IV) in ultrasonic bath in acidic medium for 30 min at 85-90 °C. The results were in good agreement with those of HG-AAS. The Se(VI) level of the samples was calculated from the difference between amounts of total Se and Se(IV).

-1.0 mL of standard Se(IV) solution - 0.125-10.0 µg mL⁻¹ range or aliquot of pretreated samples solutions
 -Addition of reactants of H₂SO₄, H₂PO₂⁻, PMA and Hg²⁺
 -Preheating in thermostatic bath (70 °C, 20 min)
 -Cooling down to room temperature
 -Absorbance against blank at 680 nm



1. Introduction

Selenium is an essential trace element with only a small difference between toxic and essential levels. It has been reported that selenium has an anticancer effect, protecting the human body from free radicals and preventing heavy metal toxic effects¹, but it is also a potential toxicant². Selenium concentration in fresh waters is usually around 20 µg L⁻¹. The selenium content of surface waters is greatly influenced by pH, being high in acidic (pH < 3.0) and in alkaline waters (pH > 7.5). Traces of selenium ranging from 0.01 to 10 µg L⁻¹ are commonly found in community drinking water.

The guideline level of selenium in drinking water set by the World Health Organization (WHO) was 10 µg L⁻¹³. As bioavailability and absorption strongly depend on chemical form in which the element is present, rapid, accurate and precise analytical methodologies for the qualitative and quantitative speciation analysis of selenium in foodstuffs are now becoming more and more necessary⁴. In addition to food, beverages may act as another important potential ingestion way to elements in our daily life⁵. As a popular nonalcoholic and healthy beverage, tea is massively consumed in the world⁶. The regular consumption of tea may contribute to the daily



dietary requirements of several essential elements. Considering the enormous consumption of tea and the investigation focusing on selenium, there is great importance to study inorganic selenium speciation in tea samples as well as in natural waters⁷.

There are many analytical techniques with their self-advantages and disadvantages, such as capillary electrophoresis online coupled with hydride generation-atomic fluorescence spectrometry (CE/HG AFS)², inductively coupled plasma mass spectrometry (ICP MS) after a separation and preconcentration procedure^{4,7}, spectrophotometry with and without preconcentration^{8,9}, graphite furnace atomic absorption spectrometric (GF AAS) after preconcentration with coprecipitation¹⁰, electrothermal atomic absorption spectrometry (ET AAS)¹¹, inductively coupled plasma optical emission spectrometry with hydride generation (HG ICP OES)¹², atomic absorption spectrometry with hydride generation (HG AAS)¹³, and high performance liquid chromatography with UV detection (HPLC)¹⁴⁻¹⁷ in literature for speciation analysis of inorganic selenium species.

In routine analysis, the spectrophotometric method is a versatile and cost-effective analytical tool that is easy to use, simple and requires no expert user in this area for underdeveloped and developing countries. However, the above-mentioned methods are time-consuming or less sensitive. Catalytic kinetic methods are noteworthy due to their significant advantages in determining many organic and inorganic components at trace levels without the need for prior separation and enrichment step with the choice of a good indicator, catalyst, inhibitor and activator.

Different catalytic kinetic methods have been reported for the determination of inorganic selenium species like Se(IV), Se(VI) and total selenium in waters¹⁸⁻²⁴, including micellar sensitized kinetic quantification of low levels of bisphenol A in foodstuffs by spectrophotometry²⁵. Significant number of methods for the determination of selenium in real samples have been based on the catalytic effect of Se(IV) on the reduction of absorbing chromogenic or fluorogenic dyes in visible region, 380-800 nm, such as Toluidine blue²⁶, Methylene blue²⁷, Gallocyanin²⁸, Semicarbazite²⁹, and Ponceau S³⁰. Some of these methods have high selection limits or suffer from many interfering species such as Te(IV) and As(V), have time-consuming and laborious processes, and

at the same time these methods are unstable. There are a limited number of catalytic kinetic methods that allow the determination of Se(IV), Se(VI) and total selenium in water samples³¹. Therefore, there is still a need to develop more sensitive and selective catalytic kinetic spectrophotometric methods for the determination and speciation of selenium in real matrix samples such as natural hot springs and tea samples.

In the present study, Se(IV) was used as an activator to increase the sensitivity and stability of the indicator system, Hg(II)-PMA-NaH₂PO₂-H₂SO₄. The variables affecting the reaction rate were evaluated in detail and optimized to give the best calibration sensitivity. The developed activation-controlled kinetics system has been successfully applied to speciation analysis of the inorganic selenium species present in natural spring water and tea samples. The proposed kinetic method is sufficiently sensitive, selective, very simple and practical to use. The existing kinetic method, without any pre-separation and enrichment, is as accurate and reliable as the sensitive and element selective HG AAS, which is commonly used for selenium analysis in real samples.

2. Materials and methods

2.1. Instrumentation

In the present study, a spectrophotometer equipped with a 1 cm light path quartz cell (Shimadzu model UV-Visible 1601 PC, Kyoto, Japan) was used for absorbance measurements at 680 nm. A thermostatic water bath was used to control the reaction temperature with accuracy of ± 0.5 °C. A stopwatch was used to record the reaction time. Shortly before the start of the indicator reaction with and without the activator, all the solutions were preheated to a temperature of 70 °C. A Sonicor model SC-121TH ultrasonic probe with total volume of 4 L was used for ultrasonic dissolution (optimal conditions, 35 kHz, 220 V, for 15 min at 65 °C). In addition, HG AAS (in terms of total Se analysis) was also used to check the accuracy of the method. For comparative purposes, the hydride for Se analysis was run with an atomic absorption spectrometer (HG AAS, Shimadzu AAS-6300, HVG-13 channels) forming under the following operating conditions: 4.0 (w/v) NaBH₄, 6-8 mol L⁻¹ HCl, carrier argon gas at a pressure of 0.32 MPa at a flow rate of 70 mL min⁻¹,

air at a flow rate of 7.0 L min^{-1} for fuel/burner acetylene at a flow rate of 15 L min^{-1} , 0.2 nm bandwidth, 194.0 nm wavelength and 10 mA lamp current.

2.2. Chemicals and solutions

All chemicals used were in analytical reagent purity. 1000 mg L^{-1} Se(IV) and Se(VI) solutions were prepared by dissolving the appropriate amounts of solid Na_2SeO_3 and Na_2SeO_4 in doubly distilled water and completing with water to the line. 100 mL of 1.5 mol L^{-1} H_2SO_4 solution was prepared by diluting the concentrated solution with water. 100 mL of 0.5 (w/v) PMA solutions was also prepared by dissolving 0.5 g of solid PMA in diluted NaOH and diluting with water. 100 mL of 0.5 mol L^{-1} hypophosphite solution was prepared by dissolving suitable amounts of solid NaH_2PO_2 in water, homogenizing thoroughly with water and soaking in water. 100 mL of 0.01 mol L^{-1} Hg(II) ion solution was prepared by dissolving a known amount of solid $\text{Hg}(\text{NO}_3)_2$ salt in analytical purity in water and diluting with water. The other reagents (HNO_3 , H_2O_2 , HCl and 1.5% (w/v) NaBH_4 in 0.2% (w/v) NaOH) used in dissolution of the samples, interference studies and selenium analysis steps by Hg AAS, were used by either direct or preparing solutions at known concentrations.

2.3. Preparation of samples for analysis

Natural cold- and hot-spring water samples were directly collected from the cold and hot spring (Kalin Town, Sivas, Turkey) and stored in a cool, dark place to protect them from heat and light. Water samples were acidified using dilute HNO_3 to prevent metal ions from adsorbing on the walls of the measurement containers. Samples were passed through a $0.45 \mu\text{m}$ pore size membrane filter to remove suspended solids prior to analysis. To determine the total selenium, samples were submitted to analysis under optimum reagent conditions, without any other pretreatment, except for prereduction with HCl. Where necessary, known volumes of masking reagents such as thiourea and NH_4F were added to the solution medium prior to analysis to control possible interference resulted from Te(IV), Cu(II), Bi(III) and Sn(IV) ions. At least, one blank solution for each sample was also analyzed to evaluate metal contamination with the reagents used.

Initially, the certified tea sample (about 0.1-0.2 g) was subjected to analysis for different sonication times (5-30 min), temperature (25 - $80 \text{ }^\circ\text{C}$) and H_2SO_4 concentration (0.2 - 5 mol L^{-1}) under 35 kHz ultrasonic power for the optimization of the ultrasonically assisted dissolution process. The certified value of sample was considered as base to assess the effectiveness of the procedure. Optimal values were found to be an acid concentration of 3.5 mol L^{-1} , sonication temperature of $65 \text{ }^\circ\text{C}$ and sonication time of 15 min after each optimization step. Real tea samples were solubilized in these conditions, converted to hydride, H_2Se after reduction with 1.5% (w/v) NaBH_4 in acidic medium (4.0 mol L^{-1} HCl) and detected with HG-AAS. Approximately 0.1 g of tea samples was taken in PTFE dissolution vessels for five repetitive analyzes, and each was mixed with 5 mL of concentrated acid and/or acid mixture (H_2SO_4 or H_2SO_4 - HNO_3 - H_2O_2 , 2:2:1 (v/v)). The flasks were covered with a watch glass, and then dissolved at 60 - $80 \text{ }^\circ\text{C}$ for 3-4 h. The acid and/or acid mixtures were intermittently added until the color of the solution became transparent, and the heating was continued. The excess acid was evaporated until a semi-dried mass remained; 2.0 mL of 0.2 mol L^{-1} HNO_3 was added to this after cooling and centrifuged for 10 min at 3500 rpm. Final volume was completed to a volume of 5.0-10 mL using 0.5 mol L^{-1} HNO_3 , and the known volumes of sample solution were analyzed by kinetic method. For the tea samples below the detection limit, the standard addition-based calibration curve approach was used when necessary, and the total selenium level of the sample was determined from difference after prereduction. The blank samples were analyzed in a similar way.

2.4. The catalytic kinetic procedure

A suitable volume (1.0 mL) of standard Se(IV) or sample solution in linearity range of 0.125 - $10.0 \mu\text{g mL}^{-1}$ was transferred to a centrifugation tube of 10 mL, and then 0.5 mL of 1.5 mol L^{-1} H_2SO_4 , 0.1 mL of 0.5 mol L^{-1} H_2PO_2^- , 1.5 mL of 0.5% (w/v) PMA and 0.75 mL of 0.01 mol L^{-1} Hg^{2+} solutions were sequentially added. After that, the volume was completed to 10 mL with water and incubated at $70 \pm 0.5 \text{ }^\circ\text{C}$ for a fixed time of 20 min. The thermostat was left in the equilibrium in the water bath. Finally, the solution was brought to room temperature by holding under the running

tap. The absorbance of the indicator solution at 680 nm for analysis of Se(IV) was measured against water using a 1-cm quartz cell and taken as an analytical signal. In a similar way, under optimal conditions, the absorbance was measured for the noncatalyzed solution without Se(IV) and the signal ΔA_C was taken into account. As a measure of calibration sensitivity, $\Delta(\Delta A)$: $\Delta A_C - \Delta A_0$ difference as a net analytical signal was plotted *versus* Se(IV) concentration, and a calibration curve was generated. The selenium contents of the samples were determined using this calibration curve.

3. Results and discussion

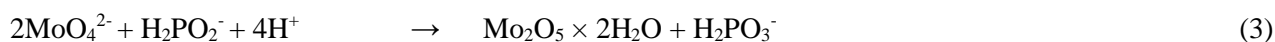
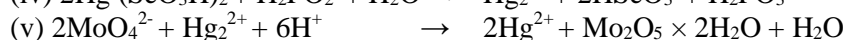
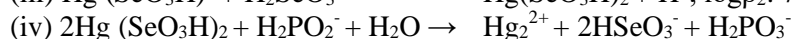
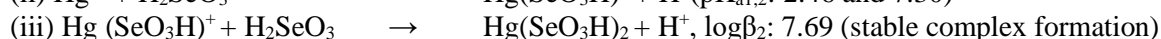
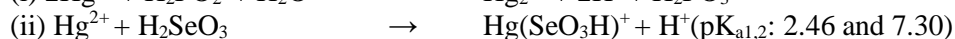
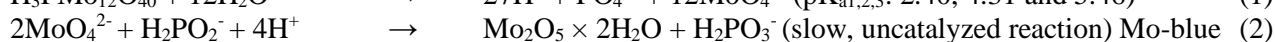
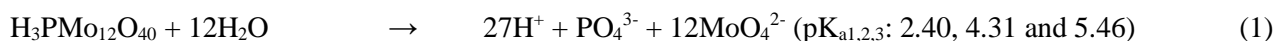
3.1. Absorption properties

Phosphomolybdic acid (PMA), a heteropoly acid with three acid ionization constants ($pK_{a1,2,3}$: 2.40, 4.32 and 5.46), is a dye which is commonly used for sensitive detection of low molecular mass compounds such as alkaloids, phenolic species and steroids for visualization of complex biological structures in TLC. PMA ($H_3PMO_{12}O_{40}$, FA: $1825.25 \text{ g mol}^{-1}$), also known as dodeca molybdic acid, is a yellowish-green compound, soluble in polar organic solvents such as water and ethanol. Conjugate unsaturated compounds reduce PMA to Mo-blue. Color intensity increases with the number of conjugated double bonds present in the dye molecule³². The PMA's implementation principle is based on the fact that many inorganic and organic materials form highly colored blue mixed oxide where the initial Mo(VI) is reduced to Mo(IV). Similar reaction products can be easily monitored by light and electron microscopy and can be measured by spectroscopic techniques, usually at a wavelength of 600-900 nm, depending on the nature of the reducing agent used^{33,34}. Different

investigators³⁵⁻⁴¹ reported different absorption spectra with different wavelengths for maximum absorption for the Mo-blue complex. In the present study, when sodium hypophosphite was used as a reducing agent for PMA, and when H_2SO_4 was added, intense blue color appeared. The shape and maximum absorption wavelength of the absorption spectra are changed by changing the concentration of acid in solution in the presence of Hg(II) and Se(IV) ions at constant concentrations. A comparison between these spectra showed that the maximum absorbance for a solution containing $0.075 \text{ mol L}^{-1} H_2SO_4$ in a final volume of 10 mL was observed at 680 nm. Increasing Hg(II) and Se(IV) concentrations at constant acid concentration also led to an increase in the absorbance at the characteristic absorption wavelength. For this reason, 680 nm was taken into account as working wavelength for further studies.

3.2. Indicator reaction

PMA was used as a redox indicator because of its ability to produce a product such as Mo-blue, which has a characteristic absorption effect on the visible region when reduced. Reduction of PMA in the presence of hypophosphite in acidic medium at room temperature is very slow. However, Se(IV) at trace levels activates selectively the catalytic effect of Hg(II) ions in acidic medium at 70 °C. This can be explained by the stable complex formation of Se(IV) in the catalytic cycle of Hg(II) ions in the acidic medium. According to Pearson's acid-base theory, Hg(II), which is soft Lewis acid, will interact with the soft base Se(IV) to form Hg-Se bond. The rate increase observed in the catalytic behavior of Hg(II) in the presence of trace Se(IV) was spectrophotometrically monitored at 680 nm. The catalytic reaction mechanism, based on the expected activation, can be predicted as follows:



(Fast, catalyzed reaction in presence of Se(IV)) at 680 nm.

3.3. Optimization of the analytical variables

The effect of reaction variables (acidity, concentration of reactants, temperature, time, and ionic strength of the medium) on the net reaction rate was extensively evaluated and optimized by monitoring each variable at a certain interval by keeping all other variables constant, based on optimization tool which is also well-known as univariate approach. In fact, in which there is not an interaction between variables, this approach is simpler, easy to use, more reliable, and moreover does not require an expert user (herein, a mathematician or statistician, which can statistically use multivariate models in optimization step) in his/her area to determine whether or not a variable is significant, and to establish relationships between variables as only one variable is used each time to obtain results. The optimum values of the variables for triplicate measurements of selenium at fixed concentration of 0.25 mg L^{-1} were determined to obtain the minimum detection limit and maximum sensitivity at each determination. The results were represented as error bars showing the mean and standard deviation of each replicate measurement sets in all figures.

3.3.1. Effect of acidity

The effect of acidity on the sensitivity, which is a measure of the rate difference between catalytic and noncatalytic reactions, was investigated in the range of 0.1-2.0 mL of $1.5 \text{ mol L}^{-1} \text{ H}_2\text{SO}_4$. The sensitivity, $\Delta(\Delta A)$, for the fixed-time of first 20 min at $70 \text{ }^\circ\text{C}$ in Fig. 1 was plotted against the volume of acid by keeping other reagent concentrations constant, and the maximum sensitivity was observed to be 0.5 mL. Sensitivity decreases at lower and higher acid volumes. This high acidity also indicates that the rate of the uncatalyzed reaction is more effective than the catalyzed reaction. At low concentrations, the activation power of Se(IV) may not be effective enough. As a result, 0.5 mL of $1.5 \text{ mol L}^{-1} \text{ H}_2\text{SO}_4$ concentration was considered to be sufficient for further studies.

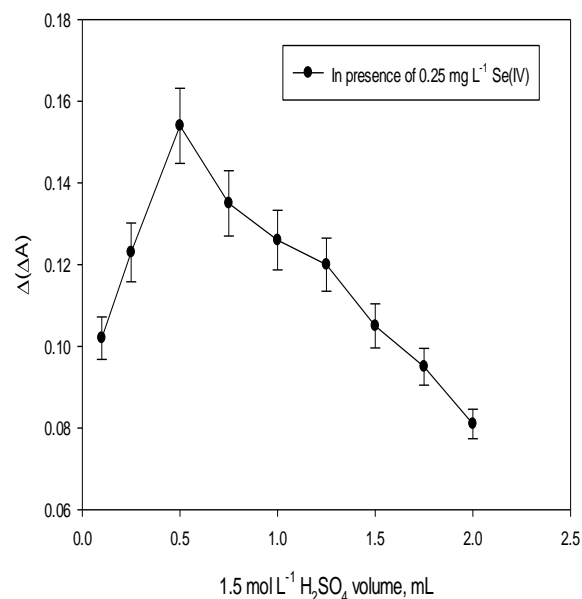


Figure 1. The effect of acidity on sensitivity. Optimal conditions: [Se(IV)]: $250 \text{ } \mu\text{g L}^{-1}$, [PMA]: 0.041 mol L^{-1} , $[\text{H}_2\text{PO}_2^-]$: $5.0 \times 10^{-3} \text{ mol L}^{-1}$, $[\text{Hg}^{2+}]$: $7.5 \times 10^{-4} \text{ mol L}^{-1}$, fixed-time: 20 min, temperature: $70 \text{ }^\circ\text{C}$ at 680 nm.

3.3.2. Effect of reducing agent volume

The effect of the hypophosphite concentration on the sensitivity was investigated using 0.5 mol L^{-1} hypophosphite at constant concentration, by keeping the other reagent concentrations constant at 680 nm in Fig. 2, and its volume was ranged from 0.025 to 1.25 mL for 20 min at $70 \text{ }^\circ\text{C}$. The volume of hypophosphite increased for both catalyzed and uncatalyzed reaction in range of 0.025-0.1 mL. At higher volumes, the sensitivity has decreased proportionally as the difference between the rate differences decreases. Therefore, a hypophosphite volume of 0.1 mL was considered as the optimal value.

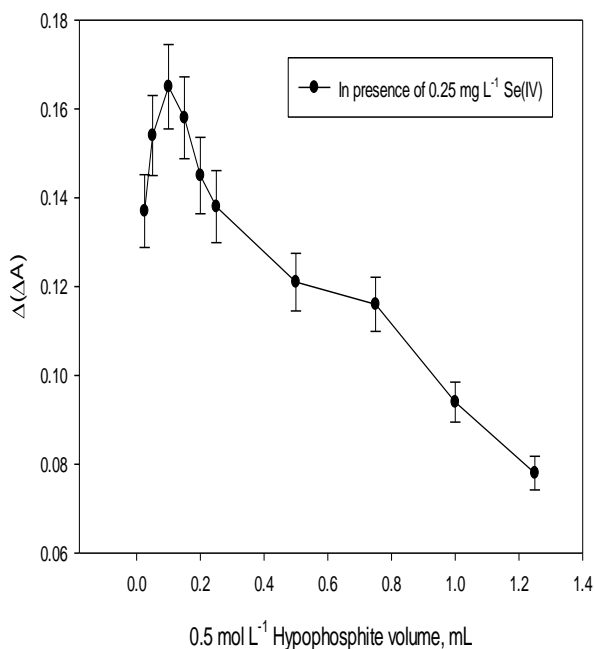


Figure 2. Effect of 0.5 mol L⁻¹ hypophosphite volume on sensitivity. Optimal conditions: [Se(IV)]: 250 μg L⁻¹, [PMA]: 0.041 mol L⁻¹, [H₂SO₄]: 0.075 mol L⁻¹, [Hg²⁺]: 7.5×10⁻⁴ mol L⁻¹, fixed-time: 20 min, temperature: 70 °C at 680 nm.

3.3.3. Effect of PMA volume

The effect of PMA volume on sensitivity was investigated in the range of 0.25-2.0 mL of 0.5% (w/v) in Fig. 3. The sensitivity for the fixed time of 20 min at 70 °C was plotted *versus* its volume, by keeping the other reagent concentrations constant at 680 nm, and the maximum sensitivity was observed to be 1.5 mL. In low volumes, sensitivity has increased up to 1.5 mL, while in higher volumes the slope gradually declines with a decreasing slope. This decrease in sensitivity is due to the fact that the noncatalytic reaction rate is faster than the catalytic reaction. High sensitivity at low volumes can be explained by the fact that the activation power of Se(IV) is more effective. Therefore, a PMA volume of 1.5 mL was considered as optimal for further studies.

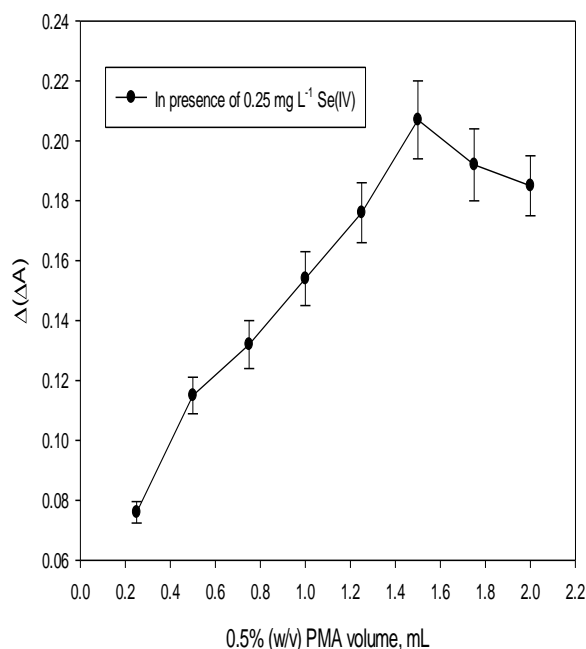


Figure 3. Effect of PMA volume on sensitivity. Optimal conditions: [Se(IV)]: 250 μg L⁻¹, [H₂SO₄]: 0.075 mol L⁻¹, [H₂PO₂⁻]: 5.0×10⁻³ mol L⁻¹, [Hg²⁺]: 7.5×10⁻⁴ mol L⁻¹, fixed-time: 20 min, temperature: 70 °C at 680 nm.

3.3.4. Effect of Hg(II) volume

The effect of Hg(II) volume on sensitivity was examined in the range of 0.1-2.0 mL of 0.01 mol L⁻¹. The sensitivity for the fixed time of 20 min at 70 °C was plotted *versus* Hg(II) volume in Fig. 4, by keeping the other reagent concentrations constant at 680 nm, and the maximum sensitivity was observed to be 0.75 mL. Sensitivity increased up to 0.75 mL at low volumes with increasing slope, declined with a decreasing slope in range of 0.75-1.5 mL, and remained constant in range of 1.5-2.0 mL. This decrease in sensitivity may be due to the fact that the non-catalytic reaction rate is faster than the catalytic reaction. Another explanation is that after the Hg(II)-complex formed in the presence of Se(IV) is reduced to Hg(I)-complex by hypophosphite, the reduced complex or Hg₂²⁺ ions can be converted to metallic Hg and Hg(II) by disproportionation. High sensitivity at low concentrations can be explained by the fact that the activation power of Se(IV) is more effective. Therefore, an Hg(II) volume of 0.75 mL was considered as optimal for further studies.

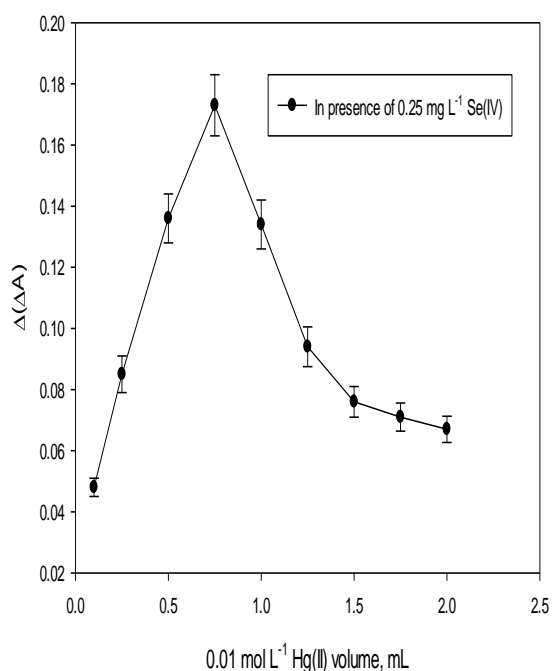


Figure 4. Effect of $0.01 \text{ mol L}^{-1} \text{ Hg(II)}$ volume on sensitivity. Optimal conditions: $[\text{Se(IV)}]: 250 \mu\text{g L}^{-1}$, $[\text{H}_2\text{SO}_4]: 0.075 \text{ mol L}^{-1}$, $[\text{PMA}]: 0.041 \text{ mol L}^{-1}$, $[\text{H}_2\text{PO}_2^-]: 5.0 \times 10^{-3} \text{ mol L}^{-1}$, fixed-time: 20 min, temperature: $70 \text{ }^\circ\text{C}$ at 680 nm .

3.3.5. Effect of temperature on sensitivity

At optimal conditions, the effect of temperature on the sensitivity was investigated in range of $40\text{--}85 \text{ }^\circ\text{C}$ in Fig. 5 because no significant difference in sensitivity was observed in room conditions. Both the catalytic and noncatalytic reaction rates increased with increasing temperature in range of $40\text{--}70 \text{ }^\circ\text{C}$, in which the rate of catalytic reaction was more pronounced. Sensitivity decreased at temperatures higher than $70 \text{ }^\circ\text{C}$. This reduction may be due to the fact that the noncatalytic reaction rate is relatively faster. For this reason, a temperature of $70 \text{ }^\circ\text{C}$ was considered as optimal for further studies. To check for possible signal fluctuations at this temperature, the analysis was carried out in a water bath, where the temperature was thermostatically controlled with an accuracy of $\pm 0.2 \text{ }^\circ\text{C}$.

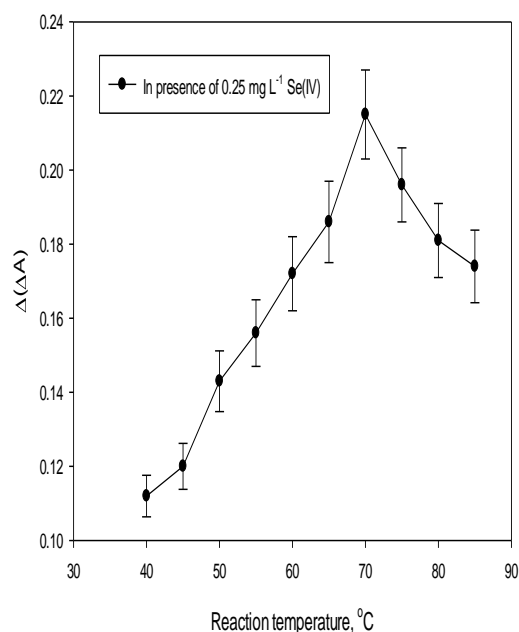


Figure 5. Effect of reaction temperature on sensitivity. Optimal conditions: $[\text{Se(IV)}]: 250 \mu\text{g L}^{-1}$, $[\text{H}_2\text{SO}_4]: 0.075 \text{ mol L}^{-1}$, $[\text{PMA}]: 0.041 \text{ mol L}^{-1}$, $[\text{H}_2\text{PO}_2^-]: 5.0 \times 10^{-3} \text{ mol L}^{-1}$, $[\text{Hg}^{2+}]: 7.5 \times 10^{-4} \text{ mol L}^{-1}$, fixed-time: 20 min at 680 nm .

3.3.6. Effect of reaction time on sensitivity

Under optimum reagent conditions, the effect of reaction time on sensitivity was studied in time interval of $5\text{--}40 \text{ min}$ at $70 \text{ }^\circ\text{C}$ in Fig. 6. The catalytic and noncatalytic reaction rates were monitored at 680 nm , and the sensitivity increased with increasing time in 5 min intervals; however, the catalytic reaction rate was more pronounced in this time interval. Sensitivity was decreased at longer times than 20 min . This decrease can be caused by acceleration in the noncatalytic reaction rate, so as to lead to a decrease in the signal difference. So, for more advanced applications, a reaction time of 20 min was considered as optimal.

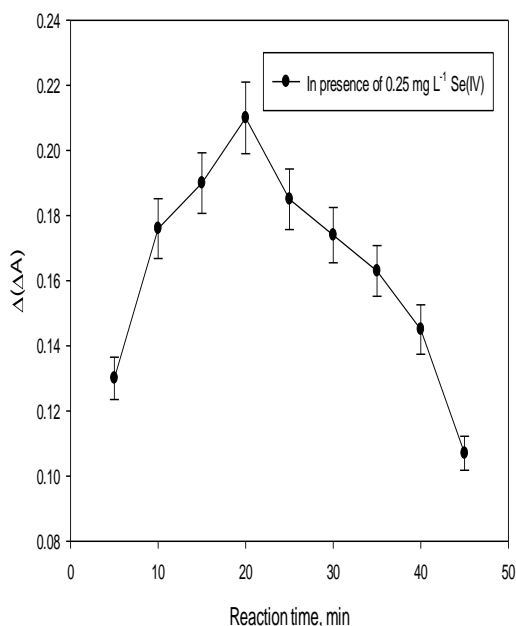


Figure 6. Effect of reaction time on sensitivity. Optimal conditions: [Se(IV)]: $250 \mu\text{g L}^{-1}$, [PMA]: 0.041 mol L^{-1} , [H₂SO₄]: 0.075 mol L^{-1} , [H₂PO₂⁻]: $5.0 \times 10^{-3} \text{ mol L}^{-1}$, [Hg²⁺]: $7.5 \times 10^{-4} \text{ mol L}^{-1}$, temperature: $70 \text{ }^\circ\text{C}$ at 680 nm .

3.3.7. Effect of inert salt concentration as a function of ionic strength on sensitivity

The effect of ionic strength on the catalyzed and uncatalyzed reaction was investigated in the volume range of $0.1\text{-}1.0 \text{ mL}$ of 0.5 mol L^{-1} KNO₃ and K₂SO₄ solutions in Fig.7. In the presence of KNO₃, at low volumes up to 0.5 mL , the sensitivity did not change, but it began to decline with increasing slope at higher volumes. However, even at low volumes in the presence of K₂SO₄, it was observed that the sensitivity decreased with increasing slope. This indicates that the ionic strength of the environment should be controlled in real complex specimens with high ionic strength. Another solution is to conduct sample analysis with a standard addition calibration curve based on the addition of the known standards of Se(IV).

$$\Delta(\Delta A) = (0.80 \pm 0.05) \times C_{\text{Se(IV)}} [\mu\text{g mL}^{-1}] + (0.014 \pm 0.001) \quad (n: 5, r^2: 0.9981) \quad (4)$$

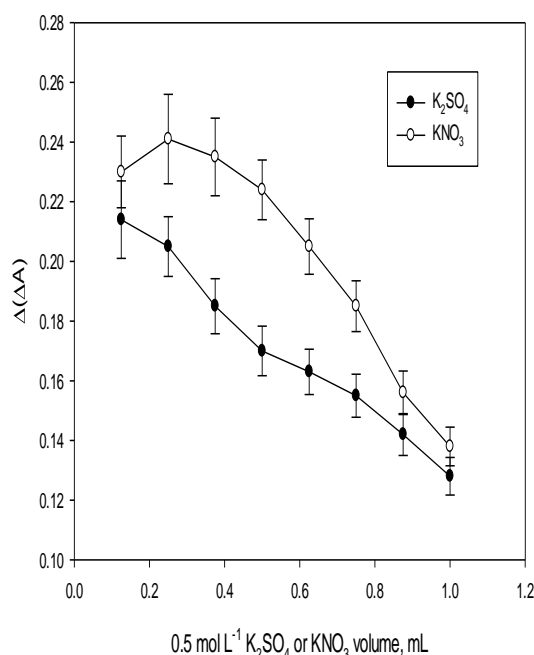


Figure 7. Effect of ionic strength of the medium on sensitivity. Optimal conditions: [Se(IV)]: $250 \mu\text{g L}^{-1}$, [H₂SO₄]: 0.075 mol L^{-1} , [PMA]: 0.041 mol L^{-1} , [H₂PO₂⁻]: $5.0 \times 10^{-3} \text{ mol L}^{-1}$, [Hg²⁺]: $7.5 \times 10^{-4} \text{ mol L}^{-1}$, fixed-time: 20 min , temperature: $70 \text{ }^\circ\text{C}$ at 680 nm .

3.4. Analytical figures of merit

3.4.1. Calibration curve, detection limit, accuracy and precision

Monitoring the net absorbance change according to optimal reagent conditions, different Se(IV) standard calibration solutions for $\Delta(\Delta A) = (\Delta A_C - \Delta A_0)$ were sampled. The results show that the analytical signal against the concentration of Se(IV) in the range of $0.0125\text{-}1.0 \mu\text{g mL}^{-1}$, $\Delta(\Delta A)$, lies in a sufficiently wide linear range with a regression coefficient of 0.9981 in Fig. 8. In this calibration interval the least squares equation is as follows:

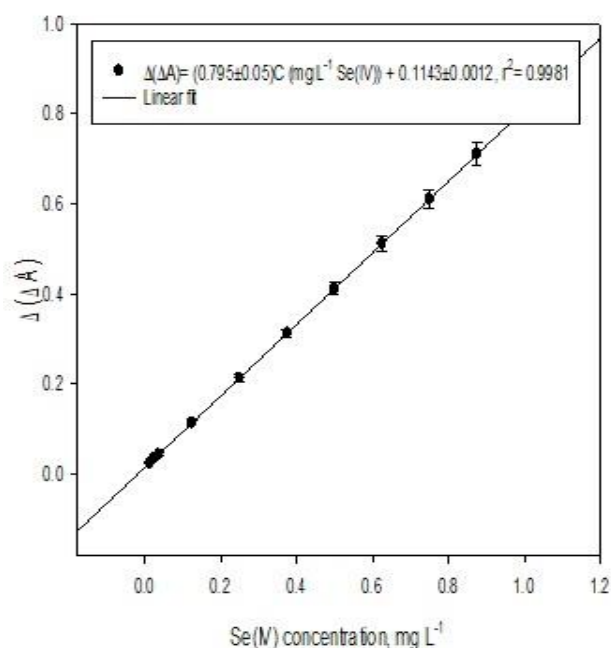


Figure 8. The calibration curve. Optimal conditions: [Se(IV)]: 250 $\mu\text{g L}^{-1}$, [H₂SO₄]: 0.075 mol L⁻¹, [PMA]: 0.041 mol L⁻¹, [H₂PO₂⁻]: 5.0 × 10⁻³ mol L⁻¹, [Hg²⁺]: 7.5 × 10⁻⁴ mol L⁻¹, 0.5 mL of 0.5 mol L⁻¹ KNO₃, fixed time: 20 min, temperature: 70 °C at 680 nm.

Table 1. The accuracy and precision of the five replicate measurement results of Se(IV) at different concentrations. Optimal conditions: [H₂SO₄]: 0.075 mol L⁻¹, [PMA]: 0.041 mol L⁻¹, [H₂PO₂⁻]: 5.0 × 10⁻³ mol L⁻¹, [Hg²⁺]: 7.5 × 10⁻⁴ mol L⁻¹, fixed time: 20 min, temperature: 70 °C.

	By fixed time approach of 20 min at 680 nm				
	Added	Found ± SD ^a	Recovery %	RE % ^b	RSD % ^c
Se(IV)	25	24.65 ± 0.80	98.6	-1.40	3.25
($\mu\text{g L}^{-1}$)	100	99.35 ± 1.48	99.4	-0.65	1.49
	250	251.90 ± 1.76	100.8	0.76	0.70
	750	748.65 ± 2.80	99.8	-0.18	0.37

^aThe average plus standard deviation of five repeated measurements (n: 5).

^bThe percent relative error (RE %).

^cThe percent relative standard deviation (RSD %).

3.4.2. Selectivity

To determine the selectivity of the kinetic method against interferents, the effect of possible interfering species on the rate of catalytic reaction was investigated by changing the concentration of interfering ions to keep the concentration of Se(IV) constant at 250 $\mu\text{g L}^{-1}$ in Table 2. The tolerance limit has been defined as the concentration of interfering species that does not cause more than ± 5.0% of relative error. The results are summarized in detail in Table 2. They indicate that all other

The limits of detection and quantification of the present kinetic method (LOD and LOQ) was calculated by taking 3- and 10-folds of the standard deviation of the signal for the ten replicate measurements of the blank solution without analyte, and found to be 3.6 and 12 $\mu\text{g L}^{-1}$, respectively. Five replicate measurements were performed for different concentrations ranging from 0.0125 to 1.0 $\mu\text{g mL}^{-1}$ and the percent recovery, relative error (RE) and relative standard deviation (RSD) values were found by substituting the analytical signals at the calibration equation. The detailed information is presented in Table 1. From the results, it can be stated that the proposed method is accurate and precise.

interfering species, except for Te(IV), Bi(III), Cu(II) and Sn(IV) ions, do not significantly affect the analytical signal when selenium at the level of 250 $\mu\text{g L}^{-1}$ was determined in a final volume of 10 mL under optimum reagent conditions. The effect of the Te(IV), Cu(II) and Bi(III) ions has been increased to a tolerance ratio ranging from 35 to 70 with addition of thiourea. The interference of Sn(IV) was improved to a tolerance ratio of 50-fold with the addition of NH₄F. Similar errors resulting from positive and negative interactions between analyte and matrix in real samples can be

minimized by using the calibration curve approach based on spiking at three concentration levels around quantification limit.

Table 2. The effect of potential interfering species on the determination of 250 $\mu\text{g L}^{-1}$ Se(IV) by the current kinetic method. Optimal conditions: $[\text{H}_2\text{SO}_4]$: 0.075 mol L^{-1} , $[\text{PMA}]$: 0.041 mol L^{-1} , $[\text{H}_2\text{PO}_2^-]$: 5.0×10^{-3} mol L^{-1} , $[\text{Hg}^{2+}]$ 7.5×10^{-4} mol L^{-1} , fixed time: 20 min, temperature: 70 °C.

Interfering species	Tolerance ratio, $[\text{C}_{\text{iyon}}/\text{C}_{\text{Se(IV)}}]$
NH_4^+ , Na(I), K(I), Li(I), Ca(II), Mg(II), Sr(II) and Ba(II)	> 1500
Cr(III), Zn(II), Al(III), $\text{C}_2\text{O}_4^{2-}$, F^- , thiosemicarbazide, CH_3COO^- and Cl^-	600-1200
Borate, citrate, tartrate, thiourea, SO_4^{2-} , Ni(II), Cd(II), HCO_3^- , ClO_3^- and Ce(III)	350-500
Pb(II), Sn(II), Mn(II), As(III), NO_3^- , HPO_4^{2-} and ClO_4^-	135-300
SCN^- , W(VI), Se(VI), Co(II) and Sb(III)	75-125
SO_3^{2-} , Mn(II), Fe(II), NO_2^- , IO_3^- , Cu(I) and Br^-	35-70
Cr(VI), $\text{S}_2\text{O}_3^{2-}$, Hg(I), CN^- , I^- and V(IV)	25-35
Fe(III), V(V), Ce(IV), As(V) and Sb(V)	15-25
Te(IV) ^b , Bi(III) ^c and Cu(II) ^c	5-10 (35, 50-75)
Sn(IV) ^d	3 (> 50)

^a C represents the concentration in $\mu\text{g L}^{-1}$.

^b The interference of Te(IV) may be greatly suppressed by addition of 1.5 mL of 0.01% (w/v) thiourea solution as a masking agent.

^c The interference of Cu(II) and Bi(III) ions may be greatly suppressed by addition of 1.2 mL of 0.02% (w/v) thiourea solution as masking agent.

^d The interference of Sn(IV) may be greatly suppressed by addition of 1.0-2.0 mL 0.025% (w/v) NH_4F as masking agent.

3.4.3. Analytical applications of the method

At initial, the method was applied to samples taken from hot- and cold-spring waters after submitting to certain pretreatments. Samples were treated by using directly kinetic method for analysis of Se(IV). Then, for total selenium analysis, samples were treated by boiling with 4.0-5.0 mol L^{-1} HCl at 85-90 °C for 30 min, for prereduction of Se(VI) to Se(IV). The total Se contents of samples were calculated from the difference between total Se and free Se(IV)

amounts obtained by using the kinetic method with and without prereduction. To ensure the accuracy and precision of the method, total selenium levels were also monitored after conversion to hydride with NaBH_4 in HCl medium after acidification. From the results obtained by both methods in Table 3, it can be concluded that the current method is as accurate and precision as the routine HG AAS method.

Table 3. Determination and speciation analysis of inorganic Se(IV), Se(VI) and total selenium levels in hot- and cold-spring waters by both kinetic method and HG AAS (n: 4).

Sample s	By the present kinetic method											By HG AAS				
	Spiking level ($\mu\text{g L}^{-1}$)		^a Found ($\mu\text{g L}^{-1}$)			^b Recovery %		^d RE %		^d RSD %		^a Found ($\mu\text{g L}^{-1}$)	^c Reco- very%	^d RE %	^d RSD%	
	Se(IV)	Se(VI)	Se(IV)	Se(VI)	Total Se	Se(IV)	Se(VI)	Total Se	Se(IV)	Total Se	Se (IV)	Total Se	Total Se			
Hot- spring water	–	–	5.2 ± 0.3	9.3	14.5 ± 0.5	–	–	–	–	–	5.4	3.6	16.1 ± 0.3	–	–	1.6
	10	100	15.3 ± 0.6	109.5	124.7 ± 0.5	96 ± 3	99 ± 4	99 ± 3	-2.7	-0.6	6.8	8.9	125.7 ± 2.6	99.6	-0.4	2.1
	100	10	105.4 ± 2.9	19.4	125 ± 3	100 ± 1	96 ± 1	99 ± 1	-0.3	-2.2	7.5	7.9	126.3 ± 2.5	100.2	0.2	2.0
	100	100	105.4 ± 2.9	109.5	215 ± 3	99 ± 2	99 ± 4	99 ± 3	-0.6	-1.4	8.4	6.5	215.7 ± 3.6	99.8	-0.2	1.7
Cold- spring water	–	–	4.5 ± 0.1	11.2	15.7 ± 0.1	–	–	–	–	–	4.0	4.7	15.4 ± 0.3	–	–	2.1
	10	100	14.4 ± 0.1	111.3	115.8 ± 0.1	96 ± 3	99 ± 4	99 ± 3	-2.7	-0.6	6.8	8.9	125.5 ± 3.2	100.1	0.9	2.6
	100	10	106 ± 0.1	21.3	115.7 ± 0.1	100 ± 1	96 ± 1	99 ± 1	-0.3	-2.2	7.5	7.9	125.8 ± 2.9	99.7	-0.3	2.3
	100	100	114.1 ± 0.1	111.3	215.9 ± 0.1	99 ± 2	99 ± 4	99 ± 3	-0.6	-1.4	8.4	6.5	215.7 ± 3.6	99.8	-0.2	1.7

^a The average ± standard deviation of replicate measurement results found using both kinetic method and HG AAS.

^b The spiking recoveries for analysis of Se(IV), Se(VI) and total selenium by the present kinetic method were defined by the following equation: $\text{spiking recovery\%} = \frac{C_{\text{found}} - C_{\text{real}}}{C_{\text{added}}} \times 100$. Here, C_{found} , C_{real} and C_{added} are the concentration of analyte after the addition of a known amount of standard in the real sample, the concentration of the analyte in the real sample and the concentration of a known amount of standard spiked to the real sample, respectively.

The present kinetic method for validation was applied to two separate SRMs given in Table 4 after sample preparation to analysis with two different wet dissolution approaches and conversion of Se(VI) to Se(IV) by boiling sample solutions at 85-90 °C with 4.0-4.5 mol L⁻¹ HCl. To ensure the accuracy of the method, two certified samples were also analyzed by HG AAS, which is an independent comparison method after pre-reduction with NaBH₄, by thoroughly dissolving and homogenizing the samples in H₂SO₄ by under ultrasonic effect. The results were quite consistent with the certified values of selenium. The kinetic method after wet digestion with H₂SO₄ appears to be somewhat questionable in terms of both accuracy and precision. This indicates that the selenium present in the sample matrix cannot be

fully solubilized and released. It can be said that the result obtained with the other digestion approach is highly compatible with that of the HG AAS, and the results obtained with both methods are quite consistent with the certified values in terms of accuracy and precision. The kinetic procedure was applied to two different SRMs given in Table 4. The results are in good agreement with the selenium values. The relative standard deviations for solid samples were in the range of 5.8-8.7% as a measure of precision. The precision (as RSD%, n: 5) for both SRMs varies between 5.0-6.62%. On the other hand, the precision of HG AAS analysis results was in range of 4.57-5.07%.

Table 4. Total selenium levels found in the selected CRMs by the present kinetic method and HG AAS (n: 5)

Samples	By the present kinetic method						By HG AAS			The statistically observed t- and F-values ^a		
	After wet digestion with H ₂ SO ₄			After wet digestion with mixture of HNO ₃ , H ₂ SO ₄ and H ₂ O ₂			After ultrasonic dissolution in H ₂ SO ₄ medium					
Certified value	Found	RS D %	RE %	Found	RSD %	RE %	Found	RSD %	RE %	t-value	F-value	
GBW 07605 Tea	0.072 μg g ⁻¹	0.068 ± 0.004 μg g ⁻¹	6.6	-5.9	0.070 ± 0.004 μg g ⁻¹	5.4	-2.9	0.071 ± 0.004 μg g ⁻¹	5.1	-1.4	0.82, 0.30	1.56, 1.11
LGC 6010 Hard drinking water	9.3 μg L ⁻¹	9.5 ± 0.5 μg L ⁻¹	5.7	+2.1	9.4 ± 0.5 μg L ⁻¹	5.0	+1.1	9.4 ± 0.4 μg L ⁻¹	4.6	+1.1	0.23, 0.25	1.58, 1.19

^a The statistical t- and F-values observed in the detection of determinate and indeterminate errors for the present kinetic and independent HG-AAS methods for 8 degrees of freedom at 95% confidence level where the critical t- and F-values are 2.31 and 6.39, respectively.

Because of the importance of selenium consumption by foods and beverages such as tea for healthy life, the present method was applied to different brand black and green tea samples after two different digestion approaches. The sensitive and selective method commonly used for total Se analysis such as HG AAS to ensure the accuracy of the method was used in parallel after the ultrasonic-based dissolution approach in H₂SO₄ medium, and the results were found to be highly consistent with those of the present kinetic method. The results were extensively presented in Table 5. A report in literature has shown that the total Se and Se(IV) levels in four commercial tea leaves supplied from different regions of China varied from 191 to 724 μg kg⁻¹ and from 173 to 613 μg kg⁻¹ respectively¹⁶, which are consistent with our results (ranging from 281 to 708 μg kg⁻¹). Another research group in Turkey has determined a total selenium level of 68 μg kg⁻¹ with a standard deviation of 5 μg kg⁻¹ in a black tea sample supplied from the market from Turkey¹⁰. In a similar way, from analysis of the samples by means

of ICP OES, it has been observed that total selenium levels are 280/1250 μg kg⁻¹ and 1093/1668 μg kg⁻¹ respectively in Turkish green and black tea samples with and without lemon. It is clear that lemon addition synergistically increases the selenium concentration in both the black teas and green teas⁴². Selenium is a trace mineral that is essential to good health but required only in small amounts. Selenium is incorporated into proteins to make selenoproteins, which are important antioxidant enzymes. The antioxidant properties of selenoproteins help prevent cellular damage from free radicals. Free radicals are natural by-products of oxygen metabolism that may contribute to the development of chronic diseases such as cancer and heart disease. Other selenoproteins help to regulate thyroid function and play a role in the immune system. In this sense, it can be concluded that citric acid in lemon leads to an improvement in antioxidant property of selenium or selenoprotein in tea.

Table 5. Total Se levels found in different tea samples by the present kinetic method and HG AAS (n: 5).

Samples	By the present kinetic method						By HG AAS		
	After wet digestion with H ₂ SO ₄			After wet digestion with mixture of HNO ₃ , H ₂ SO ₄ and H ₂ O ₂			After ultrasonic dissolution in H ₂ SO ₄ medium		
	Added (µg L ⁻¹)	^a Found (µg L ⁻¹)	^b Recovery (%)	Added (µg L ⁻¹)	^a Found (µg L ⁻¹)	^b Recovery (%)	Added (µg L ⁻¹)	^a Found (µg L ⁻¹)	^b Recovery (%)
Black tea1	–	28 ± 2	–	–	32 ± 2	–	–	31 ± 3	–
	10	38 ± 2	97.0	10	42 ± 2	97.0	10	40 ± 2	97.0
	50	77 ± 5	97.4	50	81 ± 5	98.0	50	81 ± 5	99.8
Black tea2	–	32 ± 3	–	–	34 ± 2	–	–	35 ± 2	–
	10	42 ± 3	98.0	10	44 ± 4	97.0	10	45 ± 3	94.0
	50	82 ± 5	99.6	50	84 ± 5	99.0	50	85 ± 6	99.6
Green tea1	–	63 ± 5	–	–	67 ± 4	–	–	68 ± 4	–
	25	89 ± 6	97.0	25	91 ± 6	97.0	25	93 ± 7	97.0
	50	114 ± 8	98.0	50	117 ± 8	98.0	50	118 ± 8	98.0
Green tea2	–	56 ± 4	–	–	58 ± 4	–	–	58 ± 4	–
	25	90 ± 6	97.0	25	90 ± 6	97.0	25	90 ± 6	97.0
	50	116 ± 9	98.0	50	116 ± 9	98.0	50	116 ± 9	98.0
Green tea3	–	71 ± 6	–	–	72 ± 6	–	–	72 ± 5	–
	25	95 ± 6	97.0	25	98 ± 6	97.0	25	98 ± 6	97.0
	50	128 ± 9	98.0	50	121 ± 8	98.0	50	121 ± 8	98.0

^aThe average ± standard deviation of replicate measurement results found using both kinetic method and HG AAS

^bThe spiking recoveries for analysis of total Se by both the present kinetic method and HG-AAS were defined by the following equation: spiking recovery% = $(C_{\text{found}} - C_{\text{real}}) / C_{\text{added}} \times 100$ here, C_{found} , C_{real} and C_{added} are the concentration of analyte after the addition of a known amount of standard in the real sample, the concentration of the analyte in the real sample and the concentration of a known amount of standard spiked to the real sample, respectively.

4. Conclusions

A spectrophotometry in visible region with selection of an indicator suitable for analyte is a comparatively low cost, robust and easy-to-operate analytical technique that is readily available in most analytical research laboratories. In the selected kinetic mode, it is a fast, reproducible and versatile technique with analytical frequency of nine samples (three samples plus six calibrations standard) per 20 min. Because the developed method is based on a Se-activated indicator reaction and the final intermediate product is stable for fixed time of 20 min even at a temperature of 70 °C, this detection tool can be efficiently used for the fast, accurate and reliable analysis of selenium species. In addition, the method allows a detection of low levels of Se(IV) up to 3.6 µg L⁻¹ in a linear working range of 80-fold without need to a separation/preconcentration step. So, the determination of inorganic selenium species in other sample matrices can be performed even at low concentrations without any matrix effect. Finally, the method can be considered as an alternative to expensive, time-consuming/tedious and complex analytical techniques such as ICP MS, ICP OES, ET AAS or GF AAS, HG AAS, HG AFS, and HG AFS in combination with CE or LC. Moreover, these detection techniques require expert-users in his/her area as well as poor

precision and low recovery at low concentrations. Also, the detection limit of the method is especially comparable to most of the similar spectrophotometric and kinetic spectrophotometric methods reported in the literature in terms of linear working range, sensitivity, selectivity and reproducibility. The only disadvantage of the method is that the indicator reaction takes place at high temperature (70 °C) and long time (20 min) limiting sampling rate related to kinetic analysis of samples.

6. Acknowledgements

The authors are grateful to the Commission of Scientific Research Projects, University of Cumhuriyet, Sivas, Turkey for partial financial support through project number of F-228.

Authors have no financial relationship with the organization that sponsored the research.

7. References

- [1] Ochsenkühn-Petropoulou, M., Tsopeles, F., Speciation analysis of selenium using voltammetric techniques, *Anal. Chim. Acta* 467 (1-2) (2002) 167-178. [https://doi.org/10.1016/S0003-2670\(02\)00091-0](https://doi.org/10.1016/S0003-2670(02)00091-0).
- [2] Lu, C. Y., Yan, X. P., Capillary electrophoresis on-line coupled with hydride generation-atomic

- fluorescence spectrometry for speciation analysis of selenium, *Electrophoresis*, 26 (1) (2005) 155-160. <https://doi.org/10.1002/elps.200406102>.
- [3] World Health Organization (WHO), Selenium in drinking-water. WHO Press, World Health Organization, Geneva, Switzerland, 2011. https://www.who.int/water_sanitation_health/dwq/chemicals/selenium.pdf.
- [4] Huerta, V. D., Sánchez, M. L. F., Sanz-Medel, A., An attempt to differentiate HPLC-ICP-MS selenium speciation in natural and selenised *Agaricus* mushrooms using different in natural and selenised *Agaricus* mushrooms using different, *Anal. Bioanal. Chem.* 384 (4) (2006) 902-907. <https://doi.org/10.1007/s00216-005-0174-7>.
- [5] Yuan, C., Gao, E., He, B., Jiang, G., Arsenic species and leaching characters in tea (*Camellia sinensis*), *Food Chem. Toxicol.* 45 (12) (2007) 2381-2389. <https://doi.org/10.1016/j.fct.2007.06.015>.
- [6] Jha, A., Mann, R. S., Balachandran, R., Tea: A refreshing beverage, *Indian Food Ind.* 15 (1996) 22-29.
- [7] Huang, C., Hu, B., He, M., Duan, J., Organic and inorganic selenium speciation in environmental and biological samples by nanometer-sized materials packed dual-column separation preconcentration on-line coupled with ICP-MS, *J. Mass Spectrom.* 43 (3) (2008) 336-345. <https://doi.org/10.1002/jms.1321>.
- [8] Altunay, N., Gürkan, R., Güneş, M., Ultrasound assisted extraction and spectrophotometric determination of trace selenium in water, food and vegetable samples, *Anal. Methods.* 8 (46) (2016) 8208-8218. <https://doi.org/10.1039/C6AY02638A>.
- [9] Ahmed, M. J., Islam, M. T., Nime, M. J., A highly selective and sensitive spectrophotometric method for the determination of selenium using 2-hydroxy-1-naphthaldehyde-orthoaminophenol, *Anal. Methods.* 7 (18) (2015) 7811-7823. <https://doi.org/10.1039/C5AY01311A>.
- [10] Tuzen, M., Saygi, K. O., Soylak, M., Separation and speciation of selenium in food and water samples by the combination of magnesium hydroxide co-precipitation-graphite furnace atomic absorption spectrometric determination, *Talanta* 71 (2007) 424-429. <https://doi.org/10.1016/j.talanta.2006.04.016>.
- [11] Panhwar, A. H., Tuzen, M., Kazi, T. G., Ultrasonic assisted dispersive liquid-liquid microextraction method based on deep eutectic solvent for speciation, preconcentration and determination of selenium species (IV) and (VI) in water and food samples, *Talanta* 175 (2017) 352-358. <https://doi.org/10.1016/j.talanta.2017.07.063>.
- [12] Santos, E. J., Oliveira, E., Evaluation of Arsenic and Selenium in Brazilian Soluble Coffee by Inductively Coupled Plasma Optical Emission Spectrometry with Hydride Generation, Brazil. *Arch. Biol. Technol.* 44 (3) (2001) 233-238. <https://doi.org/10.1590/S1516-89132001000300003>.
- [13] Anthemidis, A. N., Determination of Selenium (IV) in Natural Waters by HG-AAS Using an Integrated Reaction Chamber Gas-Liquid Separator, *Spectrosc. Lett.* 39 (6) (2006) 699-711. <https://doi.org/10.1080/00387010600934519>.
- [14] Arain, M. A., Khuhawar, M. Y., Bhangar, M. I., Liquid chromatographic determination of selenium in vegetables and tea leaves as 2,1,3-benzoseleniazole, *J. Chem. Soc. Pak.* 21 (2) (1999) 137-140. <https://www.jcsp.org.pk/ViewByVolume.aspx?v=72&i=VOLUME 21, NO2, JUN 1999>.
- [15] Yoshida M, Kimura Y, Abe M, Ando T, Tachi H, Fukunaga K. Quantitative evaluation of selenium contained in tea by high performance liquid chromatography, *J. Nutr. Sci. Vitaminol. (Tokyo)*. 47 (3) (2001) 248-252. <https://doi.org/10.3177/jnsv.47.248>.
- [16] Zhou, Q., Lei, M., Li, J., Wang, M., Zhao, D., Xing, A., Zhao, K., Selenium speciation in tea by dispersive liquid-liquid microextraction coupled to high-performance liquid chromatography after derivatization with 2,3-diaminonaphthalene, *J. Sep. Sci.* 38 (9) (2015) 1577-1583. <https://doi.org/10.1002/jssc.201401373>.
- [17] Zhou, Q., Lei, M., Li, J., Wang, M., Zhao, D., Xing, A., Zhao, K., Selenium speciation in tea by dispersive liquid-liquid microextraction coupled to high-performance liquid chromatography after derivatization with 2,3-diaminonaphthalene, *J. Sep. Sci.* 38 (9) (2015) 1577-1583. <https://doi.org/10.1002/jssc.201401373>.
- [18] Keyvanfard, M., Sharifian, A., Kinetic spectrophotometric method for the determination of selenium(iv) by its catalytic effect on the reduction of spadns by sulphide in micellar media, *J. Anal. Chem.* 61 (6) (2006) 596-600. <https://doi.org/10.1134/S1061934806060153>.
- [19] Gürkan, R., Ulusoy, H. I., The investigation of a novel indicator system for trace determination and speciation of selenium in natural water samples by kinetic spectrophotometric detection, *Bull. Korean Chem. Soc.* 31 (7) (2010) 1907-1914. <https://doi.org/10.5012/bkcs.2010.31.7.1907>.

- [20] Ensafi, A. A., Lemraski, M. S., Highly Sensitive Spectrophotometric Reaction Rate Method for the Determination of Selenium Based on the Catalytic Reduction of Sulfonazo by Sulfide, *Anal. Lett.* 37 (12) (2004) 2469-2483. <https://doi.org/10.1081/AL-200029374>.
- [21] Gürkan, R., Ulusoy, H. I., Akçay, M., Bulut, P., A novel indicator system for catalytic spectrophotometric determination and speciation of inorganic selenium species (Se(IV), Se(VI)) at trace levels in natural lake and river water samples, *Rare Metals* 30 (5) (2011) 477-487. <https://doi.org/10.1007/s12598-011-0416-0>.
- [22] Chen, Y.-H., Zhang, Y.-N., Tiana, F.-S., Determination of selenium via the fluorescence quenching effect of selenium on hemoglobin catalyzed peroxidative reaction, *Luminescence* 30 (3) (2015) 263-268. <https://doi.org/10.1002/bio.2723>.
- [23] Gurkan, R., Akçay, M., Kinetic spectrophotometric determination of trace amounts of selenium based on the catalytic reduction of maxilon blue-SG by sulfide, *Microchem. J.* 75 (2003) 39-49. [https://doi.org/10.1016/S0026-265X\(03\)00049-3](https://doi.org/10.1016/S0026-265X(03)00049-3).
- [24] Keyvanfard, M., Kinetic-Spectrophotometric Determination of Trace Amounts of Vanadium (V) Based on its Catalytic Effect on the Oxidation of Victoria Blue B by Potassium Bromate in Micellar Medium, *World Appl. Sci. J.* 6 (5) (2009) 624-629. [https://www.idosi.org/wasj/wasj6\(5\)/8.pdf](https://www.idosi.org/wasj/wasj6(5)/8.pdf).
- [25] Temel, N. K., Gürkan, R., A micellar sensitized kinetic method for quantification of low levels of bisphenol A in foodstuffs by spectrophotometry, *Anal. Methods* 9 (7) (2017) 1190-1200. <https://doi.org/10.1039/C6AY03064E>.
- [26] Martinez-Lozano, C., Perez-Ruiz, T., Tomas, V., Abellan, C., Flow injection spectrophotometric determination of selenium based on the catalyzed reduction of Toluidine Blue in the presence of sulphide ion, *Analyst* 114 (1989) 715-717. <https://doi.org/10.1039/AN9891400715>.
- [27] Gökmen, I. G., Abdelkader, E., Determination of selenium in biological matrices using a kinetic catalytic method, *Analyst* 119 (4) (1994) 703-708. <https://doi.org/10.1039/AN9941900703>.
- [28] Ensafi, A. A., Dehaghi, G. B., Kinetic-spectrophotometric determination of trace amounts of selenium with catalytic reduction of gallocyanine by sulfide, *Anal. Lett.* 28 (2) (1995) 335-347. <https://doi.org/10.1080/00032719508000326>.
- [29] Safavi, A., Afkhami, A., Catalytic spectrophotometric determination of selenium, *Anal. Lett.* 28 (6) (1995) 1095-1105. <https://doi.org/10.1080/00032719508002681>.
- [30] Safavi, A., Sedghi, H. R., Shams, E., Kinetic spectrophotometric determination of trace amounts of selenium and vanadium, *Fresenius J. Anal. Chem.* 365 (6) (1999) 504-510. <https://doi.org/10.1007/s002160051513>.
- [31] Chand, V., Prasad, S., Trace determination and chemical speciation of selenium in environmental water samples using catalytic kinetic spectrophotometric method, *J. Hazard. Mater.* 165 (1-3) (2009) 780-788. <https://doi.org/10.1016/j.jhazmat.2008.10.076>.
- [32] Burstein, S., Reduction of phosphomolybdic acid by compounds possessing conjugated double bonds, *Anal. Chem.* 25 (3) (1953) 422-424. <https://doi.org/10.1021/ac60075a012>.
- [33] Zarzycki, P. K., Bartoszek, M. A., Radziwon, A. I., Optimization of TLC detection by phosphomolybdic acid staining for robust quantification of cholesterol and bile acids, *JPC-J. Planar Chrom-Modern TLC* 19 (107) (2006) 52-57. <https://doi.org/10.1556/JPC.19.2006.1.9>.
- [34] Zarzycki, P. K., Bartoszek, M. A., Improved TLC detection of prostaglandins by post-run derivatization with phosphomolybdic acid, *JPC-J. Planar Chrom-Modern TLC* 21 (5) (2008) 387-390. <https://doi.org/10.1556/JPC.21.2008.5.12>.
- [35] Sims, R. P. A., Formation of heteropoly blue by some reduction procedures used in the micro-determination of phosphorous, *Analyst* 86 (1961) 584-590. <https://doi.org/10.1039/AN9618600584>.
- [36] Theodore, G. T., Determination of aqueous phosphate by ascorbic acid reduction of phosphomolybdic acid, *Anal. Chem.* 58 (1) (1986) 223-229. <https://doi.org/10.1021/ac00292a054>.
- [37] Zatar, N. A., Abu-Eid, M. A., Eid, A. F., Spectrophotometric determination of nitrite and nitrate using phosphomolybdenum blue complex, *Talanta* 50 (4) (1999) 819-826. [https://doi.org/10.1016/S0039-9140\(99\)00152-6](https://doi.org/10.1016/S0039-9140(99)00152-6).
- [38] Sicilia, D., Rubio, S., Perez-Bendito, D., Kinetic determination of antimony(III) based on its accelerating effect on the reduction of 12-phosphomolybdate by ascorbic acid in a micellar medium, *Anal. Chem.* 64 (13) (1992) 1490-1495. <https://doi.org/10.1021/ac00037a031>.
- [39] Tosi, E. A., Cazzoli, A. F., Tapiz, L. M., Phosphorous in oil. Production of molybdenum blue

derivative at ambient temperature using non-carcinogenic reagents, *J. Am. Oil Chem. Soc.* 75 (1998) 41-44. <https://doi.org/10.1007/s11746-998-0007-x>.

[40] Nalumansi, I., Mbabazi, J., Ssekaalo, H., Ntale, M., Effect of various reductants on the spectral characteristics of the reduced phosphopolyoxomolybdate anion, and its application to orthophosphate anion quantification in selected Ugandan waters, *Int. J. Curr. Trends in Engin. Technol.* 1 (2) (2015) 59-66. <http://www.ijctet.org/assets/upload/463IJCTET123.pdf>.

[41] Shukor, Y., Adam, H., Ithnin, K., Yunus, I., Shamaan, N.A., Syed, M.A., Molybdate reduction to molybdenum blue in microbe proceeds via a phosphomolybdate intermediate, *J. Biol. Sci.* 7 (8) (2007) 1448-1452. <https://doi.org/10.3923/jbs.2007.1448.1452>.

[42] Derun, E. M., Kipcak, A. S., Ozdemir, O.D., Piskin, M. B. Cr, Fe and Se Contents of the Turkish Black and Green Teas and the Effect of Lemon Addition, *Int. Scholar. Sci. Res. Innov.* 6 (11) (2012) 1018-1021. <https://publications.waset.org/7515/pdf>.

Rapid and selective extraction of trace amount of Pb(II) in aqueous samples using a magnetic ion-imprinted polymer and detection by flame atomic absorption spectrometry

Saeed Babae[✉], Seyed Ghorban Hosseini[✉], Mohammad Mirzaei[✉]

Faculty of Chemistry and Chemical Engineering, Malek Ashtar University of Technology, Iran.

*Corresponding author: Saeed Babae, Phone: +98 2122987672, email address: safnba@gmail.com

ARTICLE INFO

Article history:

Received: March 12, 2019

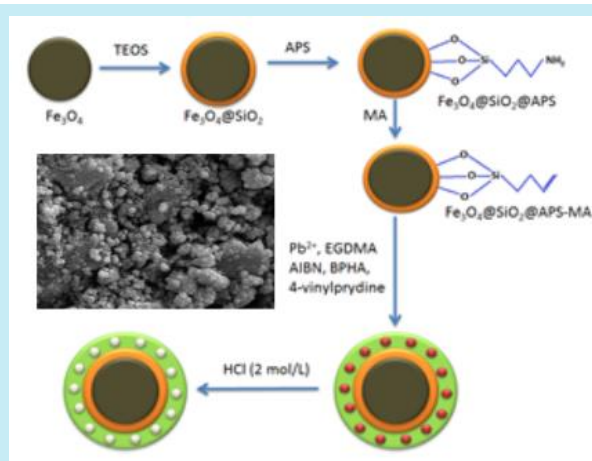
Accepted: June 26, 2019

Published: October 1, 2019

Keywords:

1. extraction
2. magnetic
3. ion imprinting polymer
4. lead
5. n-benzoyl-n-phenyl hydroxylamine

ABSTRACT: A magnetic Pb(II) ion-imprinted polymer was synthesized using magnetic Fe₃O₄@SiO₂ nanospheres as supporter, n-benzoyl-n-phenyl hydroxylamine as ligand, 4-vinyl pyridine as monomer, ethylene glycol dimethacrylate as crosslinker and 2,2'-azobis(isobutyronitrile) as the initiator. The template was removed from the polymer using 4 mL of HCl (2 mol L⁻¹). The chemical structure, morphology-particle size, elemental analysis, thermal behavior and magnetic properties of the sorbent were evaluated using Fourier-transform infrared spectroscopy, scanning electron microscopy & ImageJ software - Energy dispersive X-ray system, thermal gravimetric analysis and vibrating sample magnetometry. Various parameters such as pH, equilibrium extraction time, temperature and the eluent were optimized. The results showed the sorbent adsorption capacity was 92.3 mg g⁻¹ in pH 6.0 media, equilibrium time of 7 min at 40 °C. Calibration linearity was 2-150 µg L⁻¹ with detection limit of 0.3 µg L⁻¹. The prepared sorbent had high selectivity and was successfully applied to the removing of lead in real samples.



1. Introduction

It is clear that heavy metals contamination represents serious hazards to the ecosystem and especially to humans because of the complex toxicological effects on living beings¹. Lead has been accepted as an important toxic heavy metals resulting from mining, acid battery factories², metal plating³, printing⁴, textile⁵, photographic materials⁶, ceramic and glass industries as well as explosive manufacturing⁷. Through the joined system of water-plant-animal-human, Pb(II) is transferred into human body and causes to various severe health problems in vital organs of humans, such as damage to kidney, liver, blood

composition, central nervous system (CNS) due to binding sites on cerebellar phosphokinase C at trace amounts and also retarding the reproductive system in mental function⁸⁻¹⁰. The maximum permitted amount of lead ions by world health organization (WHO) in drinking water fixed as 10.0 µg L⁻¹ and for the U.S. environmental protection agency (USEPA) is 15.0 µg L⁻¹¹¹. Consequently, the developments of reliable and highly sensitive techniques to the determination and then removal of lead in water samples as the pollutant sources are crucially necessary.

Nowadays flame atomic absorption spectrometry (FAAS) because of its analytical abilities has been confirmed for trace analysis of

metal ions but lead concentration in environmental waters is usually lower than FAAS detection limit¹². Therefore, a separation and enrichment pretreatment is necessary before to Pb(II) determination at the $\mu\text{g L}^{-1}$ levels. Several methods have been developed for Pb^{2+} ions separation-preconcentration, such as liquid-liquid extraction¹³, liquid-phase microextraction¹⁴, solid phase extraction (SPE)¹⁵, coprecipitation¹⁶ and cloud point extraction¹⁷ which among them SPE is more common due to the higher enrichment factor, minimal costs, environment friendly and simple automation.

Different solid phases have been applied as sorbents which among them, molecularly imprinted polymers (MIPs) have been widely utilized for selective separation of organic and also inorganic compounds from aqueous samples¹⁸. Similar sorbents to MIPs are ion imprinted polymers (IIPs) that produced by chelating metal ions with the relevant ligands and then polymerizing with a monomer. Ion imprinted polymers (IIPs) are more attractive for separation of inorganic ions due to their high selectivity, high preconcentration factor and chemical stability¹⁹. In this manner Liu²⁰ synthesized a surface-imprinted mesoporous sorbent for Pb(II) ion by the post-synthesis method and the adsorption capacity reached to 36.6 mg g^{-1} . Ghoohestani²¹ synthesized Pb(II)-IIP by polymerization of chitosan on the surface of MCM-41 with adsorption capacity of 57.7 mg g^{-1} . Fan²² synthesized silica-supported sorbent functionalized with Schiff base by coupling a surface imprinting technique with a sol-gel process for removal of Pb(II) ions with adsorption capacity of 54.9 mg g^{-1} .

In present study, a novel magnetic Pb-IIP containing of n-benzoyl-n-phenyl hydroxylamine was synthesized on the surface of $\text{Fe}_3\text{O}_4@\text{SiO}_2$ by a surface imprinting technique for the selective and efficient preconcentration of lead ions in various aqueous samples. The adsorption experiments coupled with FAAS system was used to the analyte quantification at $\mu\text{g L}^{-1}$ levels.

2. Materials and methods

2.1 Reagents and materials

Ferric chloride, sodium acetate, ammonium hydroxide and tetraethyl orthosilicate (TEOS) were used for synthesis of $\text{Fe}_3\text{O}_4@\text{SiO}_2$ nanoparticles and for the functionalization.

Triethylamine (TEA) and 3-aminopropyltriethoxysilane (APS) were applied for the preparation of the imprinted polymer, utilized from 4-vinyl pyridine (VP), n-benzoyl-n-phenyl hydroxylamine (BPHA), ethylene glycol dimethacrylate (EGDMA), maleic anhydride (MA) and α, α' -azobisisobutyronitrile (AIBN). $\text{Pb}(\text{NO}_3)_2$ were used as source of Pb(II). Stock solutions were prepared daily from Pb^{2+} standard solution of 1000.0 mg L^{-1} by serial dilutions. Other chemicals were provided from Merck Company (Darmstadt, Germany). Deionized water was used for preparation of all solutions.

2.2 Apparatus

The measurements were performed using flame atomic absorption spectrometer (Varian, Model Spectra A-20 Plus) with hollow cathode lamp (10 mA current, spectral bandwidth and wavelength of 0.5 and 283.3 nm respectively). The infrared spectra of the IIP samples were obtained using a Shimadzu 8400S FTIR spectrometer. A scanning electron microscopy along with ImageJ software (Ver. 5.1.1)-energy dispersive X-ray (Joel-JSMT 300A) were used for morphology-particle size-elemental analysis. TGA studies were carried out with Stanton Redcroft-STA-780 system applying heating rate of 10 C min^{-1} in a temperature range of 50-600 °C, under air atmosphere with a flow rate of 50 mL min^{-1} . Magnetic properties were analyzed using a vibrating sample magnetometer (Microsense-EZ VSM). The pH was determined using a Metrohm pH meter (M. Lab-827) with a combined glass-calomel electrode.

2.3 Synthesis of magnetic nanospheres (MNSs)

The MNS was synthesized by a solvothermal reduction method²³. Typically, 1.35 g $\text{FeCl}_3 \cdot 6\text{H}_2\text{O}$ was dissolved in ethylene glycol (40 mL) to form a clear solution, followed by the addition of sodium acetate (3.6 g) and polyethylene glycol (1.0 g). The mixture was vigorously treated by ultrasonic bath for 30 min. After that it was refluxed at 180 °C for 8 h, and then allowed to cool down to room temperature. The black product was washed several times with ethanol and deionized water. Then it was dried at 60 °C for 6 h.

2.4 Synthesis of SiO₂ coated MNSs (Fe₃O₄@SiO₂)

These nanospheres were prepared according to a previously reported method with minor modifications²⁴. Typically, 0.5 g of the MNS was dispersed in 60 mL ethanol and 10 mL of deionized water, and treated by sonication for 15 min, followed by the addition of 1.0 mL ammonium hydroxide (25%) and 3.0 mL TEOS sequentially. The mixture was reacted for 12 h at room temperature under continuous stirring. The resultant product was collected by an external magnetic field and rinsed six times with ethanol and water. Subsequently, 8.0 g Fe₃O₄@SiO₂ were mixed with 100 mL of HCl (2 mol L⁻¹) and refluxed for 6h. the activated microspheres were recovered and washed several times. Finally, the obtained activated Fe₃O₄@SiO₂ was dried under vacuum at 60 °C for 3 h.

2.5 Synthesis of functional Fe₃O₄@SiO₂ microspheres

Two grams of Fe₃O₄@SiO₂ activated microspheres were added to 50 mL of anhydrous toluene, followed by an addition of moderate TEA and 12 mL APS. The mixture was incubated at 110 °C for 12 h in nitrogen atmosphere. Then the Amino modified microspheres (Fe₃O₄@SiO₂-APS) were magnetically separated, rinsed with toluene and vacuum dried at 25 °C. To prepare the Fe₃O₄@SiO₂-APS-MA particles, 1.5 g Fe₃O₄@SiO₂-APS and 2.5 g MA were added to 50 mL DMF, then the mixture reacted for 24 h at room temperature. The solid separated with magnetic field, rinsed with DMF and ethanol and then dried under vacuum at 25 °C for 2 h.

2.6 Synthesis of Pb²⁺ imprinted-polymer magnetic adsorbent (MIIP)

First, 2 mmol of Pb(NO₃)₂ was dissolved in 25 mL DMF under ultrasonic oscillation. Then 4 mmol BPHA, 8 mmol 4-vinyl pyridine and 25 mL methanol were added to the solution and stirred overnight at room temperature²⁵. After that, 0.5 g Fe₃O₄@SiO₂-APS-MA, 8 mmol EGDMA and 0.1 g AIBN were added to the solution and reacted at 60 °C for 24 h under nitrogen atmosphere. The final product was collected with magnetic field and washed with DMF and methanol. The lead ions in polymer were removed by an HCl solution (2 mol L⁻¹). The removal of the

template was determined by FAAS. Schematic diagram of this procedure is shown in Fig. 1.

Magnetic non-ion imprinted polymer (MNIIP) were prepared by same process exception of Pb(NO₃)₂ addition for the purpose of contrast test.

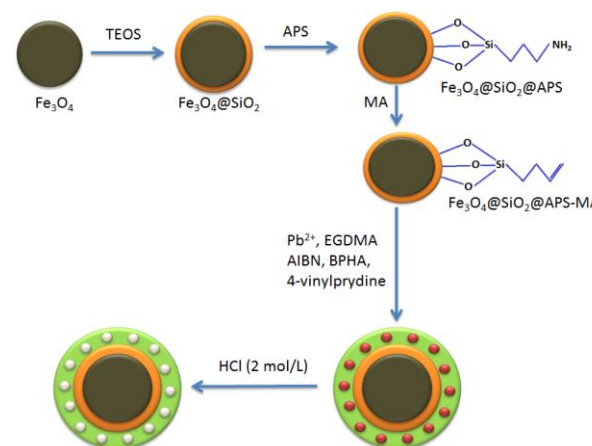


Figure 1. A schematic diagram for synthesis of magnetic IIP.

2.7 Determination procedure

The pH of sample solution containing Pb(II) was adjusted to 6 by drop-wise additions of 0.1 mol L⁻¹ of NaOH or HCl. Then 0.2 g of the sorbent was added into 100 mL of the solution and shake for 7 min via 40 °C. After adsorption equilibrium, these magnetic nanoparticles were separated by a magnet and the adsorbed Pb²⁺ ions were eluted with 4 mL HCl (2 mol L⁻¹) for 15 min. Now, the analyte in the supernatant and the eluent were determined by FAAS.

Percent extraction of lead (E%) and adsorption capacity (q) of magnetic ion-imprinted polymer (MIIP) was calculated via the following formulas (Eq. 1 and 2):

$$E\% = 100 (C_i - C_e) / C_i \quad (1)$$

$$q = (C_i - C_e) V/m \quad (2)$$

Where: C_i (mg L⁻¹) and C_e (mg L⁻¹) are the Pb²⁺ concentrations before and after adsorption in the solution respectively. V (L) is the volume of added solution, m (g) is the mass of MIIP in dry form.

2.8 Sample preparation

Environmental and wastewater samples were collected from Tehran, Polur (Anahita Co.) and an ammonium perchlorate factory in Iran respectively.

Prior to sampling, the bottle was cleaned with deionized water, diluted nitric acid and deionized water in succession. The samples were filtered through a cellulose filter membrane (0.45 μm) and their pH was adjusted before the determination.

3. Results and discussion

3.1 Characterization of MIIP

3.1.1 Structure investigation with FT-IR

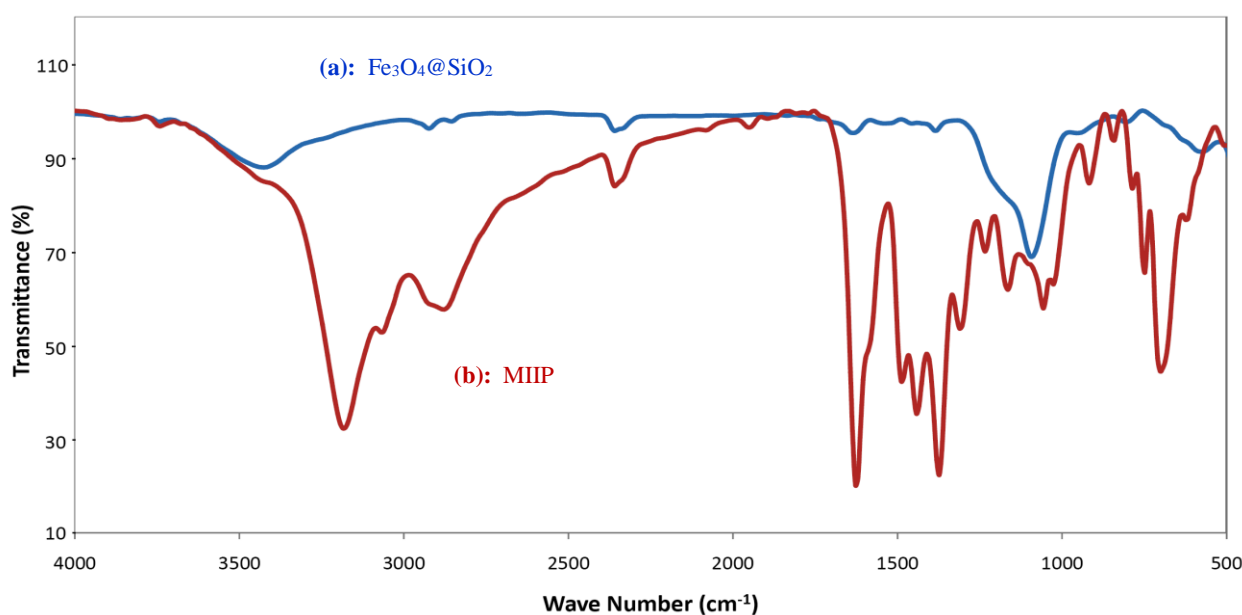


Figure 2. FT-IR spectra of (a) $\text{Fe}_3\text{O}_4@\text{SiO}_2$ and (b) MIIP.

3.1.2 Morphology analysis

The morphology and particle size histograms of the synthesized adsorbents were analyzed via SEM system and ImageJ software. The results of the MNIIP and MIIP nanoparticles are shown in Fig. 3(a, b). SEM image of Fig. 3a shows a homogenous and smooth surface for MNIIP nanospheres with particle size range of 30-40 nm that obtained from ImageJ software usage. As shown in SEM image

The FT-IR spectra of $\text{Fe}_3\text{O}_4@\text{SiO}_2$ and MIIP showed in Fig. 2. The peak at 1150 cm^{-1} is corresponding to Si-O-Si stretching that observed in both of samples, which indicates SiO_2 is encapsulated correctly inside the MIIP. The carbonyl peak at 1730 cm^{-1} , O-H peak at 3205 cm^{-1} and C-N peak at 1450 and 1380 cm^{-1} showed the presence of ligand (BPHA) in the MIIP structure.

of Fig. 3b, in the presence and then removing of Pb(II), a porous structure was resulted for MIIP which was attributed to imprinted cavities. This rough structure of this surface on the surface of MIIP is favor to mass transfer and the formation of three-dimensional recognition sites. In this manner the particle size range of MIIP was obtained 20-30 nm.

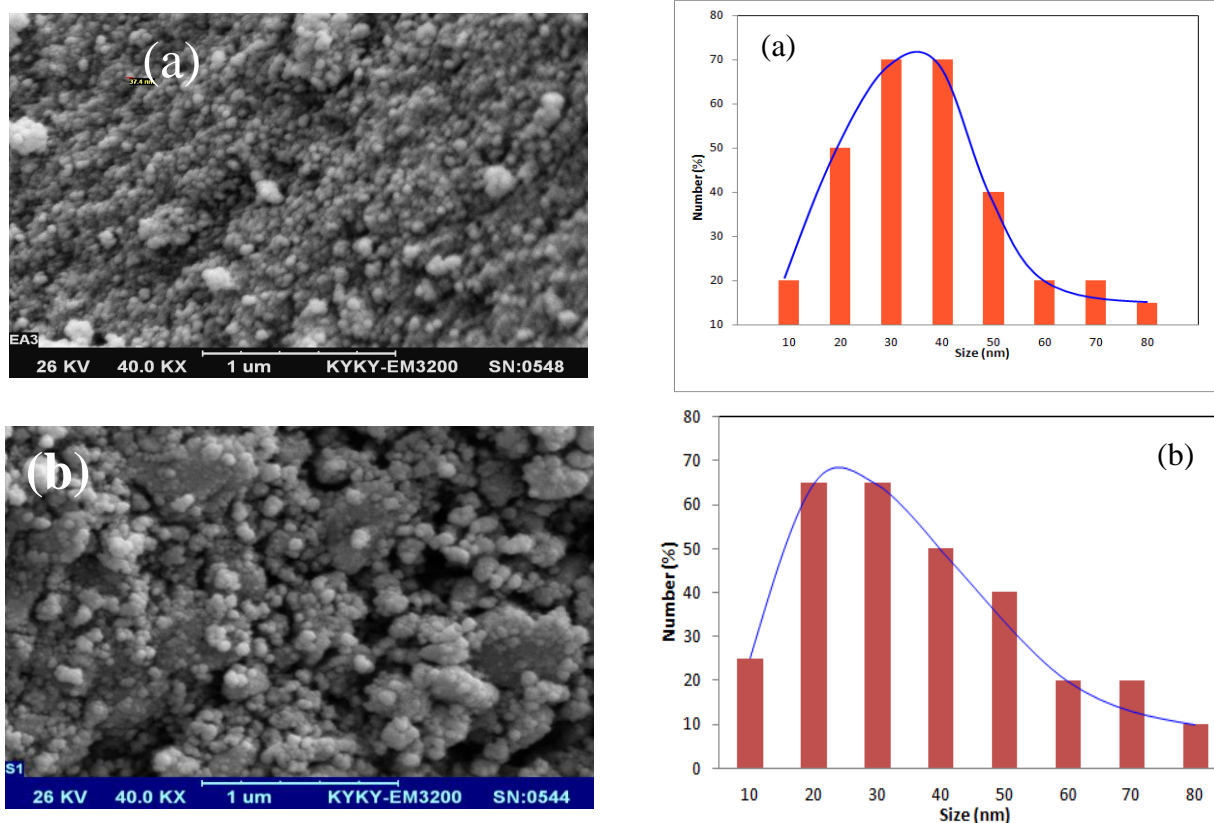


Figure 3. The SEM-Particle size analysis of MNIIP (a) and MIIP (b) adsorbents.

3.1.3 Elemental analysis

The EDX spectrums of MIIPs after adsorption and then elution of Pb(II) are shown in Fig. 4(a, b) respectively. As seen in Fig. 4a the spectrum of the no leached MIIP revealed that significant amount

of the analyte was adsorbed in the sorbent from the initial solution. Also Fig. 4b related to the leached MIIP confirmed the elimination of lead in the sorbent after rinsing with the selected eluent.

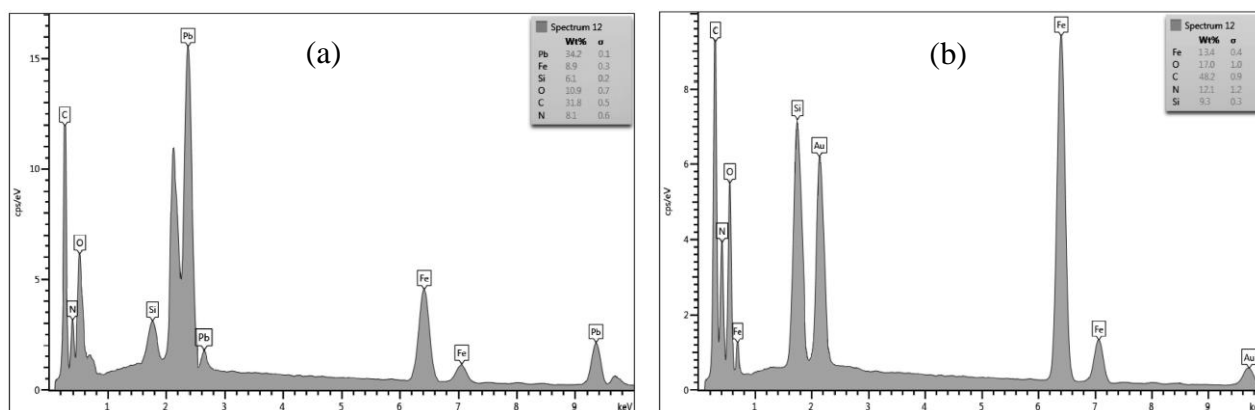


Figure 4. The EDX spectrums of the no leached (a) and leached (b) MIIPs.

3.1.4 Thermal studies by TGA

The amount of materials that modified the surface of nanoparticles can be valued by TGA. The TGA behavior of $\text{Fe}_3\text{O}_4@/\text{SiO}_2$ and MIIP are

shown in Fig. 5. The thermogram in Fig. 5a shows that the Fe_3O_4 has good thermal stability up to 500°C with only a little loss of about 3.9%. As shown in Fig. 5b, when the temperature was changed from 280 to 350°C , a 72.3% reduction in

weight of MIIP resulted that might be due to the decomposition of organic materials such as APS and polymeric layer. Hence, the results demonstrated the formation of an imprinted polymer. The remaining weight thermogram of MIIP can be attributed to Fe_3O_4 particles with higher thermal stability. The amount of capsulated $\text{Fe}_3\text{O}_4@/\text{SiO}_2$ in MIIP is 23.8% that is appropriate for showing magnetic properties.

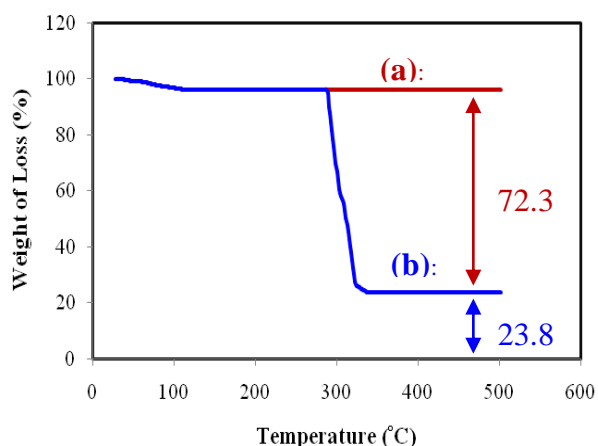


Figure 5. TGA thermograms of (a): $\text{Fe}_3\text{O}_4@/\text{SiO}_2$ and (b): MIIP.

3.1.5 Magnetism analysis

The magnetic properties of the, $\text{Fe}_3\text{O}_4@/\text{SiO}_2$, Pb(II)-MIIP and Fe_3O_4 were characterized using vibrating sample magnetometry (VSM) technique in the magnetic field of -10,000 to +10,000 Oersted at 25 °C. As shown in Fig. 6, the hysteresis curve of these samples is fully reversible that means nanomaterials have superparamagnetic properties and could be easily and quickly separated from a suspension. The saturation magnetization value of Fe_3O_4 , $\text{Fe}_3\text{O}_4@/\text{SiO}_2$ and MIIP was about 59, 23 and 9 emu g^{-1} , respectively. The value of saturation magnetization was decreased by increasing modifying steps. The decrease in magnetization value can be attributed to the existence of IIP on the surface of the $\text{Fe}_3\text{O}_4@/\text{SiO}_2$ nanoparticles. Also, this relationship can be seen in the comparison between $\text{Fe}_3\text{O}_4@/\text{SiO}_2$ and Fe_3O_4 . However, the MIIP with less magnetite encapsulation possesses enough magnetic response to meet the need of magnetic separation.

Also, from inset of Fig. 6, it is seen that in the absence of an external magnetic field, a yellow homogeneous dispersion was existed. When an external magnetic field was applied, the yellow

particles were attracted to the wall of vial in a short time (about 50 s).

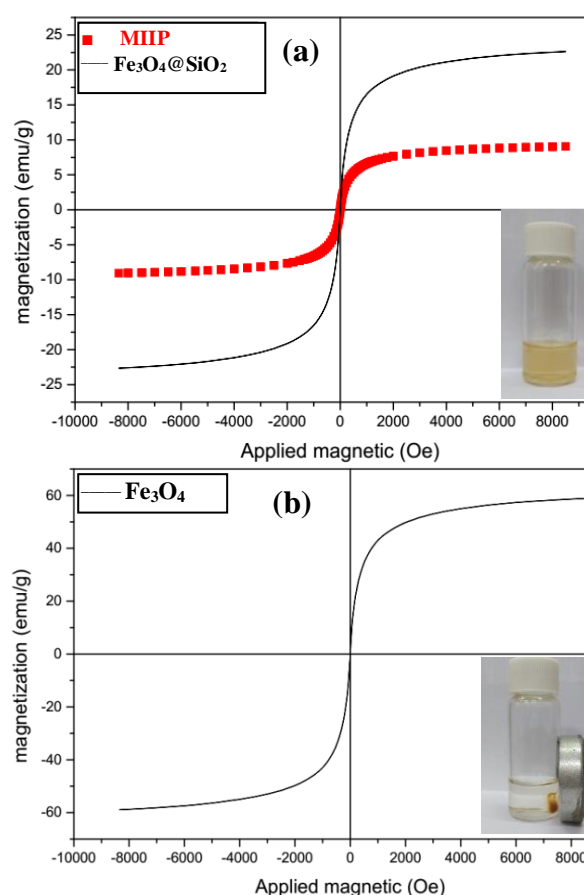


Figure 6. VSM curves of $\text{Fe}_3\text{O}_4@/\text{SiO}_2$, MIIP (a) and Fe_3O_4 (b) at 25 °C.

3.2 Optimization of extraction conditions

Adsorption of Pb(II) from solution was performed in a batch method. Effects of media pH, eluent solvent (type, volume and concentration), adsorption-desorption time, and equilibrium temperature were studied. Adsorbent addition was set to 0.2 g in 100 mL solution and initial Pb(II) concentration was 1 mg L^{-1} . After adsorption equilibrium, the adsorbent was separated by external magnetic field and the analyte quantities in the eluents were determined by FAAS.

3.2.1 Effect of media pH

The solution pH is one important parameter that can effect on metal ion adsorption. In order to figure out of pH effect on Pb(II) adsorption, variety of pH were studied in the range 3.0 to 8.0. For prevention from sedimentation, increasing pH not

continued and the results are illustrated in Fig. 7. The results show that with the increase of pH to 6.0, percent recovery continually increased and then decreased. Probably the pH effects on functional groups of IIP or the chemistry of Pb^{2+} ions. At lower pH than 6.0 and presence of higher concentration of H^+ , the active sites of the MIIP become protonated and their abilities for interaction with $\text{Pb}(\text{II})$ decreased. By increasing pH more than 6.0, Pb^{2+} ions can react by hydroxyl groups and the adsorption process would be decreased.

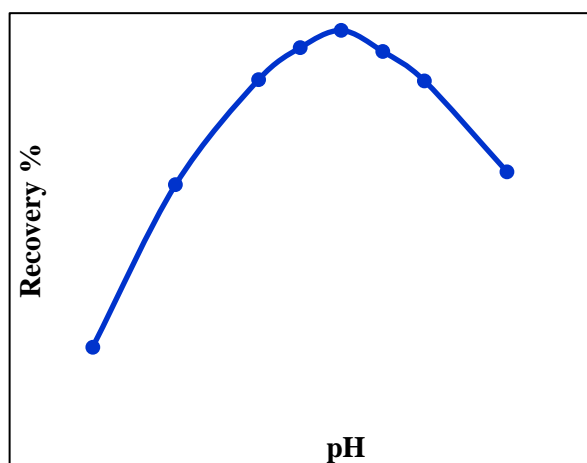


Figure 7. Effect of pH on the Pb^{2+} extraction. Condition: Pb initial concentration = 1 mg L^{-1} , adsorbent = 0.2 g, adsorption time = 7 min, desorption time = 15 min and $T = 40 \text{ }^\circ\text{C}$.

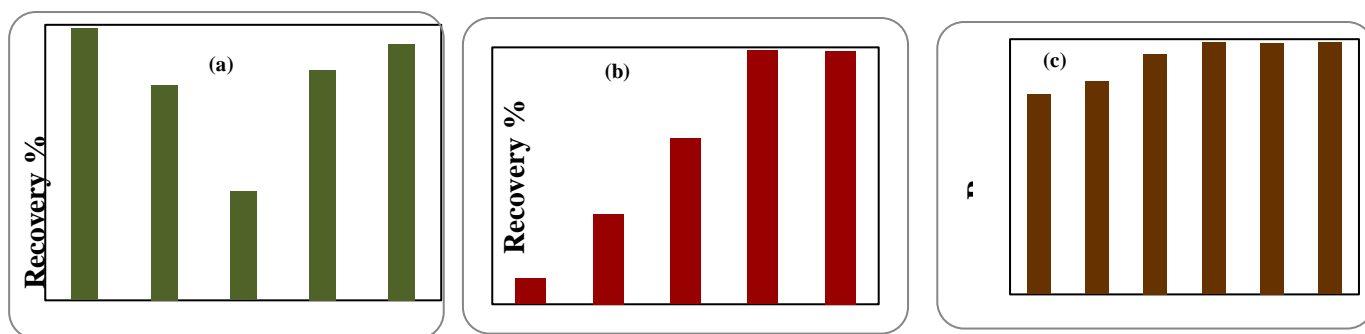


Figure 8. Effect of the eluent on the Pb^{2+} removing from MIIP, (a) Type; (b) Concentration; (c) Volume. Condition: Pb initial concentration = 1 mg L^{-1} , adsorbent = 0.2 g, pH 6.0, adsorption time = 7 min, desorption time = 15 min and $T = 40 \text{ }^\circ\text{C}$.

3.2.3 Effects of adsorption-desorption times

The adsorption and desorption times for $\text{Pb}(\text{II})$ were investigated under optimized conditions. As shown in Fig. 9a, it appears that MIIP showed good performance in adsorption during first 5 min and reached to equilibrium after 7 min and excess time does not provide any significant change in

3.2.2 Selection of eluent solvent

To achieve the eluent for complete $\text{Pb}(\text{II})$ removing from MIIP, a series of commercial solutions of HNO_3 2 mol L^{-1} , HCl 2 mol L^{-1} , acetic acid (HOAC) 2 mol L^{-1} , HOAC- HCl (2:1 mol L^{-1}), HNO_3 -HOAC (2:1 mol L^{-1}) were studied. As shown in Fig. 8a, HCl is the best eluent that can extract $\text{Pb}(\text{II})$ ions from MIIP. In the next step, diverse concentrations of HCl were investigated and as it can be seen in Fig. 8b, the best solution is HCl 2 mol L^{-1} . In the last section of eluent optimization, the volume of it optimized and as shown in Fig. 8c, 4 mL of HCl 2 mol L^{-1} was chosen as optimum condition of eluent for the experiments.

recovery. This time, probably due to plenty cavities that imprinted on the surface of thin MIIP that provide low diffusion resistance, is reliable and it can be stated that the process has fast equilibrium.

For desorption time optimization, different times (1-21 min) were studied and as it can be seen from Fig. 9b, optimum time is 15 min and this time was used in further experiments.

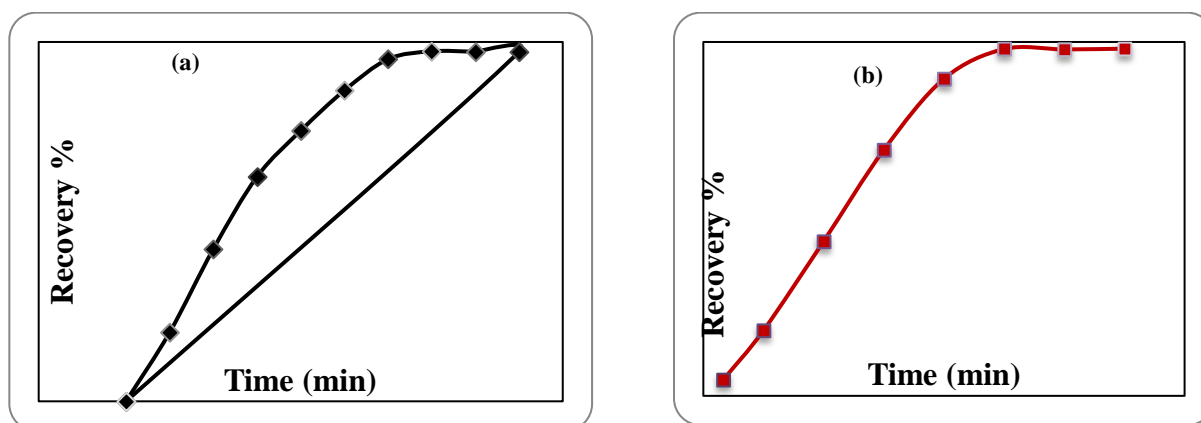


Fig. 9. Effect of the adsorption (a) and desorption time (b) on the Pb^{2+} recovery. Condition: Pb initial concentration = 1 mg L^{-1} , adsorbent = 0.2 g , pH 6.0 and $T = 40 \text{ }^\circ\text{C}$.

3.2.4 Effect of equilibrium temperature

In IIP techniques temperature has a noticeable effect on the adsorption behavior and analyte recovery. The effect of equilibrium temperature on the extraction behavior of $\text{Pb}(\text{II})$ on MIIP was shown in Fig. 10. As shown by increasing temperature from 25 to $40 \text{ }^\circ\text{C}$, the recovery yield is increased thermodynamically. It can be seen that $\text{Pb}(\text{II})$ extraction in the range of 40 to $50 \text{ }^\circ\text{C}$ drastically decreased. This manner may be related to swelling of polymer. Probably in elevated temperature the size and geometry of cavities will be changed and could not be suitable for adsorption of Pb^{2+} as target ions.

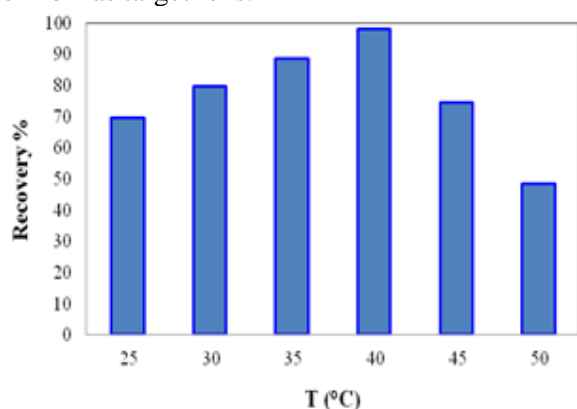


Figure 10. Effect of temperature on the Pb^{2+} recovery yield. Condition: Condition: Pb initial concentration = 1 mg L^{-1} , adsorbent = 0.2 g , $\text{pH} = 6.0$, adsorption time = 7 min , desorption time = 15 min .

3.3 Maximum adsorption capacity

For determination of maximum adsorption capacities of the ion imprinted polymer and

nonimprinted polymers, 50 mg of each sorbents separately placed in a solution of 200 mg L^{-1} $\text{Pb}(\text{II})$ in pH 6.0 and the quantity of adsorbed ions were determined in both initial and eluent solutions. From three replicates, sorption capacities of MIIP and NIIP were calculated of 92.3 and 21.3 mg g^{-1} respectively. The results showed that MIIP compare to NIIP have a higher adsorption capacity for lead ions.

3.4 Analytical characteristics

Table 1 summarizes the analytical characteristics of the MIIP under the optimal conditions. The LOD of the proposed method was determined by 7 times placing of 0.2 g MIIP in 100 mL blank solutions and it was obtained to $0.3 \text{ } \mu\text{g L}^{-1}$. The precision (RSD, %) for 7 replicate uptaking of $10 \text{ } \mu\text{g L}^{-1}$ $\text{Pb}(\text{II})$ was 2.4% . Also, the linear dynamic range of the calibration curve was obtained in $2\text{-}150 \text{ } \mu\text{g L}^{-1}$ range.

Table 1 Analytical characteristics of the proposed extraction.

Regression Equation ($n = 11$)	$A_{283.3 \text{ nm}} = 0.0041 C_{\text{Pb}} (\text{ } \mu\text{g L}^{-1}) + 0.002$
Regression coefficient (r)	0.9994
Limit of detection ^a ($\text{ } \mu\text{g L}^{-1}$)	0.3
Reproducibility ^b (RSD, %)	2.4
Linear range ($\text{ } \mu\text{g L}^{-1}$)	$2\text{-}150$
^a For 7 replicate runs of the blank ($n = 7$).	
^b For 7 replicate measurements of $10 \text{ } \mu\text{g L}^{-1}$ lead.	

Table 2 showed a comparison between the presented work and some others for preconcentration of lead (II). As seen the analytical

merits of the proposed method (e.g. adsorption time, adsorption capacity, detection limit and precision) are comparable and in general it is better than with those published reports. The main

advantages of this method are more adsorption capacity and lower LOD.

Table 2 Comparison of some lead IIP sorbents performance with this work.

Sorbent type (monomer/crosslinker)	Ligand	Adsorption time (min)	Adsorption Capacity (mg g ⁻¹)	pH	LOD (ng mL ⁻¹)	R.S.D. (%)	Ref.
MIIP (MAA/EGDMA)	Salicyl Aldoxime	250	81.83	6	Note reported	Note reported	26
IIP (AAPTS/TEOS)	-	35	19.61	7.5	Note reported	Note reported	27
MIIP (VDPC/EGDMA)	DPC	12	68.1	7	1.3	2.9	28
IIP (4-VB-18-Crown-6/EGDMA)	4-VB-18-Crown-6	60	27.95	6	Note reported	Note reported	29
IIP (Acrylamide/NNMBA)	AA	20	42	5	0.34	2.1	30
MIIP (VDPA/EGDMA)	DPA	3	76.3	6	0.7	3.3	31
IIP (4-VP/EGDMA)	4-(2-Pyridylazo) Resorcinol	5	9.8	6	0.9	3.4	12
IIP (2-VP/EGDMA)	2-Amino Pyridine	90	85.6	5	0.75	2.7	32
IIP (2-VP/EGDMA)	Diphenyl Carbazone	5	75.4	6	0.42	2.1	33
MIIP (MAA/EGDMA)	-	4	51.8	7	1.7	4.1	34
MIIP (VPyDA/EGDMA)	APDC	4	55.89	7	0.9	1.8	35
MIIP (4-VP/EGDMA)	BPHA	7	92.3	6	0.3	2.4	This work

MAA: MethAcrylic Acid, EGDMA: Ethylene Glycol Dimethacrylate, AAPTS: 3-(2-aminoethyl Amino)Propyl Trimethoxy Silane, TEOS: Tetra Ethyl Ortho Silicate, VDPC: Vinyl-Di Phenyl Carbazide, DPC: Di Phenyl Carbazide, 4-VB-18-C-6: 4-Vinyl Benzo-18-Crown-6, NNMBA: N,N'-Methylene Bisacryl Amide, AA: Alginic Acid, VDPA: Vinyl Di Pyridyl Amine, DPA: Di Pyridyl Amine, 4-VP: 4-Vinyl Pyridine, 2-VP: 2-Vinyl Pyridine, VPyDA: 4-(Vinylamino)Pyridine-2,6-Dicarboxylic Acid, APDC: 4-Amino Pyridine-2,6-Dicarboxylic, BPHA: n-Benzoyl-n-Phenyl Hydroxyl Amine.

3.5 Effect of interfering ions

In order to prove specific recognition of magnetic ion imprinted polymer towards Pb(II) in the presence of common interfering ions, the selectivity of the prepared MIIP was investigated in binary systems³⁶. The competitors examined were Na⁺, K⁺, Co²⁺, Ni²⁺, Ca²⁺ and Mg²⁺. In this approach, each interfering ion was added to 100 mL of 10 µg L⁻¹ Pb(II) solution under optimum conditions. After preconcentration by MIIP, the tolerable amount of each ion was determined separately. The tolerable amount is defined as the maximum concentration that could cause a change of less than 5% in signal compared to the initial signal of Pb²⁺ uptaking without any interference. As shown in Table 3, this Pb-MIIP have high selectivity in the existence of Co²⁺, Ni²⁺, Ca²⁺ and Mg²⁺ that probably was obtained in order to the use of BPHA as a new ligand.

Table 3 The tolerance limit of common interfering cations for Pb(II) determination.

Interfering ions	Tolerable concentration ratio (M:Pb)	Recovery %
Na ⁺	4000	99
K ⁺	4000	99
Co ²⁺	1500	98.1
Ni ²⁺	1500	97.9
Ca ²⁺	2000	96.8
Mg ²⁺	2000	95.3

3.6 Method application

The proposed procedure was applied for determination of lead content in two environmental samples and a waste water (from an ammonium perchlorate factory) solution. The amounts of Pb(II) ions were determined in the final eluents and the results are listed in Table 4. As seen, the mean recoveries for different spiking of Pb²⁺ are in the range 96.6-99.7%. Therefore, the proposed MIIP can be applied for the determination of lead in various samples.

Table 4 Recovery and precision of the determination of lead in various aqueous samples.

Samples ^a	Pb concentration (μgL^{-1})		
	Added	Found ^b	Recovery (%)
Tap water	-	Not detected	-
	5.0	4.8 ± 0.1	97 ± 3
	15.0	14.9 ± 0.8	99 ± 2
Mineral water	-	Not detected	-
	10.0	9.73 ± 0.09	97 ± 3
	30.0	29.90 ± 0.06	100 ± 2
Wastewater ^b	-	8.3	-
	5.0	13.1 ± 0.1	98 ± 3
	10.0	18.2 ± 0.7	100 ± 2
	20.0	28.2 ± 0.5	100 ± 2

^a Sample description as described in the text.

^b Average of three determinations \pm standard deviation

4. Conclusions

In this research a new magnetic ion imprinted polymer (IIP@Fe₃O₄@SiO₂-APS-MA) for Pb²⁺ target was prepared by combination of surface imprinting technique and magnetic separation. The polymer synthesis and its characterization were proved by FT-IR, SEM-ImageJ, EDX, TGA and VSM techniques. The adsorption experiments combined to FAAS system showed that this sorbent have good analytical characteristics and high selectivity with maximum adsorption capacity of 92.3 mg_(Pb) g⁻¹_(MIIP) at 40 °C and pH 6.0. Also, this adsorbent has physical and chemical stability, low cost and simple-fast operation. A comparison of the presented work with the previously reports for lead extraction (Table 2) indicates that the proposed Pb-MIIP due to the use of n-benzoyl-n-phenyl hydroxylamine, provides better analytical merits of adsorption capacity and LOD. From the results obtained, it can be concluded that this polymer can be used as an excellent substrate for the adsorption of lead ion in real aqueous solutions.

5. References

- [1] Kot, A., Namiesnik, J., The role of speciation in analytical chemistry, *Trends Anal. Chem.* 19 (2-3) (2000) 69-79. [https://doi.org/10.1016/S0165-9936\(99\)00195-8](https://doi.org/10.1016/S0165-9936(99)00195-8).
- [2] Chen, L., Xu, Z., Liu, M., Huang, Y., Fan, R., Su, Y., Hu, G., Peng, X., Lead exposure assessment from study near a lead-acid battery factory in China, *Sci. Total Environ.* 429 (2012) 191-198. <https://doi.org/10.1016/j.scitotenv.2012.04.015>.
- [3] Qin, J., Wai, M., Oo, M., Wong, F., A feasibility study on the treatment and recycling of a wastewater from metal plating, *J. Member. Sci.* 208 (1-2) (2002) 213-221. [https://doi.org/10.1016/S0376-7388\(02\)00263-6](https://doi.org/10.1016/S0376-7388(02)00263-6).
- [4] Kristensen, P., Irgens, L. M., Daltveit, A. K., Andersen, A., Perinatal outcome among children of men exposed to lead and organic solvents in the printing industry, *Am. J. Epidemiol.* 137 (2) (1993) 134-144. <https://doi.org/10.1093/oxfordjournals.aje.a116653>.
- [5] Hachem, C., Bocquillon, F., Zahraa, O., Bouchy, M., Decolourization of textile industry wastewater by the photocatalytic degradation process, *Dyes Pigm.* 49 (2) (2001) 117-125. [https://doi.org/10.1016/S0143-7208\(01\)00014-6](https://doi.org/10.1016/S0143-7208(01)00014-6).
- [6] Deng, L., Su, Y., Su, H., Wang, X., Zhu, X., Sorption and desorption of lead (II) from wastewater by green algae *Cladophora fascicularis*, *J. Hazard. Mater.* 143 (1-2) (2007) 220-225. <https://doi.org/10.1016/j.jhazmat.2006.09.009>.
- [7] Yetilmezsoy, K., Demirel, S., Vanderbei, R. J., Response surface modeling of Pb(II) removal from aqueous solution by *Pistacia vera* L.: Box-Behnken experimental design, *J. Hazard. Mater.* 171 (1-3) (2009) 551-562. <https://doi.org/10.1016/j.jhazmat.2009.06.035>.
- [8] Yetilmezsoy, K., Demirel, S., Artificial neural network (ANN) approach for modeling of Pb(II) adsorption from aqueous solution by Antep pistachio (*Pistacia Vera* L.) shells, *J. Hazard. Mater.* 153 (3) (2008) 1288-1300. <https://doi.org/10.1016/j.jhazmat.2007.09.092>.
- [9] Markovac, J., Goldstein, G. W., picomolar concentrations of lead stimulate brain protein kinase C, *Nature* 334 (1988) 71-73. <https://doi.org/10.1038/334071a0>.
- [10] Kunal, K. S., William, W., Sutherland, M. D., Role of lead in the central nervous system: effect on electroencephalography, evoked potentials, electroretinography, and nerve conduction, *Neurodiagn. J.* 55 (2) (2015) 107-121. <https://doi.org/10.1080/21646821.2015.1043222>.
- [11] Tarley, C. R. T., Corazza, M. Z., Somera, B. F., Segatelli, M. G., Preparation of new ion-selective cross-

- linked poly(vinylimidazole-coethylene glycol dimethacrylate) using a double-imprinting process for the preconcentration of Pb^{2+} ions *J. Colloid. Interface Sci.* 450 (2015) 254-263. <https://doi.org/10.1016/j.jcis.2015.02.074>.
- [12] Behbahani, M., Hassanlou, P. G., Amini, M. M., Moazami, H. R., Abandansari, H. S., Bagheri, A., Hasanzadeh, S., Selective solid-phase extraction and trace monitoring of lead ions in food and water samples using new lead-imprinted polymer nanoparticles, *Food Anal. Methods* 8 (3) (2015) 558-568. <https://doi.org/10.1007/s12161-014-9924-5>.
- [13] Clevenger, T., Novak, J., Recovery of metals from electroplating wastes using liquid-liquid extraction, *J. Water Pollut. Control Fed.* 55 (7) (1983) 984-989. <https://www.jstor.org/stable/25042006>.
- [14] Zhou, Q., Bai, H., Xie, G., Xiao, J., Temperature-controlled ionic liquid dispersive liquid phase micro-extraction, *J. Chromatogr. A* 117 (1) (2008) 43-49. <https://doi.org/10.1016/j.chroma.2007.10.103>.
- [15] Duran, C., Gundogdu, A., Bulut, V. N., Soylak, M., Elci, L., Senturk, H. B., Tufekci, M., Solid-phase extraction of Mn(II), Co(II), Ni(II), Cu(II), Cd(II) and Pb(II) ions from environmental samples by flame atomic absorption spectrometry (FAAS), *J. Hazard. Mater.* 146 (1-2) (2007) 347-355. <https://doi.org/10.1016/j.jhazmat.2006.12.029>.
- [16] Komjarova, I., Blust, R., Comparison of liquid-liquid extraction, solid-phase extraction and coprecipitation preconcentration methods for the determination of cadmium, copper, nickel, lead and zinc in seawater, *Anal. Chim. Acta* 576 (2) (2006) 221-228. <https://doi.org/10.1016/j.aca.2006.06.002>.
- [17] Chen, J., Teo, K. C., Determination of cadmium, copper, lead and zinc in water samples by flame atomic absorption spectrometry after cloud point extraction, *Anal. Chim. Acta* 450 (1-2) (2001) 215-222. [https://doi.org/10.1016/S0003-2670\(01\)01367-8](https://doi.org/10.1016/S0003-2670(01)01367-8).
- [18] Haupt, K., Molecularly imprinted polymers in analytical chemistry, *Analyst* 126 (6) (2001) 747-756. <https://doi.org/10.1039/B102799A>.
- [19] He, H., Xiao, D., He, J., Li, H., Dai, H., Peng, J., Preparation of a core-shell magnetic ion-imprinted polymer via a sol-gel process for selective extraction of Cu(II) from herbal medicines *Analyst* 139 (10) (2014) 2459-2466. <https://doi.org/10.1039/C3AN02096G>.
- [20] Liu, Y., Liu, Z. Z., Wang, Y., Dai, J. D., Gao, J., Xie, J. M., Yan, Y. S., A surface ion-imprinted mesoporous sorbent for separation and determination of Pb(II) ion by flame atomic absorption spectrometry, *Microchim. Acta* 172 (3-4) (2011) 309-317. <https://doi.org/10.1007/s00604-010-0491-1>.
- [21] Ghoohestani, S., Faghihian, H., Selective separation of Pb^{2+} from aqueous solutions by a novel imprinted adsorbent, *Desalin. Water Treat.* 57 (9) (2014) 1-10. <https://doi.org/10.1080/19443994.2014.993718>.
- [22] Fan, H. T., Sun, X. T., Li, W. X., Sol-gel derived ion-imprinted silica-supported organic-inorganic hybrid sorbent for selective removal of lead(II) from aqueous solution, *J. Sol-Gel Sci. Technol.* 72 (1) (2014) 144-155. <https://doi.org/10.1007/s10971-014-3436-z>.
- [23] Deng, H., Li, X., Peng, Q., Wang, X., Chen, J., Li, Y., Monodisperse magnetic single-crystal ferrite microspheres, *Angew. Chem.* 117 (18) (2005) 2842-2845. <https://doi.org/10.1002/ange.200462551>.
- [24] Fang, C. L., Qian, K., Zhu, J., Wang, S., Lv, X., Yu, S. H., Monodisperse $\alpha-Fe_2O_3@SiO_2@Au$ core/shell nanocomposite spheres: synthesis, characterization and properties, *Nanotechnology* 19 (2008) 125601-125607. <https://doi.org/10.1088/0957-4484/19/12/125601>.
- [25] Sarode, D. B., Ingle, S. T., Attarde, S. B., Formula establishment of colorless Pb(II) complex with N-benzoyl-N-phenyl hydroxyl amine (BPA) using atomic absorption spectroscopy, *Indo. J. Chem.* 12 (2012) 12-19. <https://journal.ugm.ac.id/ijc/article/viewFile/21366/14071>.
- [26] Zhang, H. X., Dou, Q., Jin, X. H., Sun, D. X., Wang, D. D., Yang, T. R., Magnetic Pb(II) ion-imprinted polymer prepared by surface imprinting technique and its adsorption properties, *Chem. Eng. J.* 50 (6) (2015) 901-910. <https://doi.org/10.1080/01496395.2014.978462>.
- [27] Zhang, M., Zhang, Z., Liu, Y., Yang, X., Luo, L., Chen, J., Yao, S., Preparation of core-shell magnetic ion-imprinted polymer for selective extraction of Pb(II) from environmental samples, *Chem. Eng. J.* 178 (2011) 443-450. <https://doi.org/10.1016/j.cej.2011.10.035>.
- [28] Aboufazeli, F., Lotfi Zadeh Zhad, H. R., Sadeghi, O., Karimi, M., Najafi, E. Z., Novel ion imprinted polymer magnetic mesoporous silica nano-particles for selective separation and determination of lead ions in food samples, *Food Chem.* 141 (4) (2013) 3459-3465. <https://doi.org/10.1016/j.foodchem.2013.06.062>.
- [29] Luo, X., Liu, L., Deng, F., Luo, S., Novel ion-imprinted polymer using crown ether as a functional monomer for selective removal of Pb(II) ions in real

environmental water samples, *J. Mater. Chem. A* 1 (28) (2013) 8280-8286. <https://doi.org/10.1039/C3TA11098B>.

[30] Girija, P., Beena, M., Sorption of trace amounts of Pb(II) ions on an ion imprinted interpenetrating polymer network based on alginic acid and crosslinked poly acryl amide, *Sep. Sci. Technol.* 49 (2014) 1053-1061. <https://doi.org/10.1080/01496395.2013.866682>.

[31] Sadeghi, O., Aboufazeli, H. R., Lotfi Zadeh Zhad, Karimi, M., Najafi, E., Determination of Pb(II) ions using novel ion-imprinted polymer magnetic nanoparticles: investigation of the relation between Pb(II) ions in cow's milk and their nutrition, *Food Anal. Methods* 6 (3) (2013) 753-760. <https://doi.org/10.1007/s12161-012-9481-8>.

[32] Ebrahimzadeh, H., Behbahani, M., A novel lead imprinted polymer as the selective solid phase for extraction and trace detection of lead ions by flame atomic absorption spectrophotometry: Synthesis, characterization and analytical application, *Arab. J. Chem.* 10 (2) (2017) 2499-2508. <https://doi.org/10.1016/j.arabjc.2013.09.017>.








[33] Behbahani, M., Bagheri, A., Taghizadeh, M., Salarian, M., Sadeghi, O., Adlnasab, L., Jalali, K., Synthesis and characterisation of nano structure lead (II) ion-imprinted polymer as a new sorbent for selective extraction and preconcentration of ultra trace amounts of lead ions from vegetables, rice, and fish samples, *Food Chem.* 138 (2-3) (2013) 2050-2056. <https://doi.org/10.1016/j.foodchem.2012.11.042>.

[34] Ebrahimzadeh, H., Asgharinezhad, A. A., Moazzen, E., Amini, M. M., Sadeghi, O., A magnetic ion-imprinted polymer for lead(II) determination: A study on the adsorption of lead(II) by beverages, *J. Food Compos. Anal.* 41 (2015) 74-80. <https://doi.org/10.1016/j.jfca.2015.02.001>.

[35] Sayar, O., Akbarzadeh Torbati, N., Saravani, H., Mehrani, K., Behbahani, A., Moghadam Zadeh, H.R., A novel magnetic ion imprinted polymer for selective adsorption of trace amounts of lead(II) ions in environment samples, *J. Ind. Eng. Chem.* 20 (5) (2014) 2657-2662. <https://doi.org/10.1016/j.jiec.2013.10.052>.

[36] Wei, S., Liu, Y., Shao, M., Liu, L., Wang, H., Liu, Y., Preparation of magnetic Pb(II) and Cd(II) ion-imprinted microspheres and their application in determining the Pb(II) and Cd(II) contents of environmental and food samples, *RSC Adv.* 4 (56) (2014) 29715-29723. <https://doi.org/10.1039/C4RA01948B>.

Larvicidal activity, molluscicide and toxicity of the essential oil of *Citrus limon* peels against, respectively, *Aedes aegypti*, *Biomphalaria glabrata* and *Artemia salina*

Paulo Roberto Barros Gomes¹, Marluçy Bezerra Oliveira², Dionney Andrade de Sousa², Jeremias Caetano da Silva¹, Romer Pessôa Fernandes², Hilton Costa Louzeiro³, Rayone Wesly Santos de Oliveira², Maria do Livramento de Paula⁴, Victor Elias Mouchrek Filho², Maria Alves Fontenele⁵

1 Federal Institute of Pará – Câmpus Abaetetuba, Teaching, Research and Extension Coordination, 3322 Rio de Janeiro Ave., Abaetetuba, Pará, Brazil.

2 Federal University of Maranhão, Department of Chemical Technology, 1966 dos Portugueses Ave., 1966, São Luís, Maranhão, Brazil

3 Federal University of Maranhão, Natural Sciences Degree Coordination, Pinheiro, Maranhão, Brazil

4 Federal University of Maranhão, Department of Pharmacy, 1966 dos Portugueses Ave., São Luís, Maranhão, Brazil

5 Federal University of Maranhão, Food Engineering Coordination, Imperatriz, Maranhão, Brazil

*Corresponding author: Paulo Roberto Barros Gomes, Phone: +55 98 98101 6397 email address: prbgomes@yahoo.com.br

ARTICLE INFO

Article history:

Received: February 24, 2018

Accepted: July 24, 2019

Published: October 1, 2019

Keywords:

1. limonene
2. *Aedes aegypti*
3. volatile compounds
4. hydrodistillation
5. *Biomphalaria glabrata*

ABSTRACT: In this present work, we tested the larvicidal activity, molluscicide and toxicity of the oil extracted from *Citrus limon* peels, respectively against third stage larvae of *Aedes aegypti*, snail *Biomphalaria glabrata*, and *Artemia salina*. For this, we extract the essential oil by hydrodistillation. Then, we identified and quantified the components by gas chromatography coupled to mass spectrometry (GC-MS). We tested the larvicidal and molluscicidal activity, respectively, using the method adopted by the Brazilian Ministry of Health and the World Health Organization. We calculated the lethal concentration (LC₅₀) from the Probit method for the three biological activities with 95 %. The results of the chromatographic analysis showed that the oil has 58.81% of Limonene (major constituent) and 0.11% α -Mylene (minority component). The essential oil

presented lethal concentration (LC₅₀) for larvicidal activity, molluscicide and toxicity, respectively at 15.48, 13.05 and 743.35 mg·L⁻¹. Therefore, the essential oil is active against larvae of *A. aegypti* and snail *B. glabrata* and non-toxic against larvae of *A. salina*.



1. Introduction

The essential oils extracted from citrus plants arouse in man the interest in identifying his constituents and the possible applications to society. Among the identified compounds, the main ones are limonene, β -myrene, α -pinene, p-cymene, β -pinene, terpinolene¹⁻³, and its applications are in medicine, food, cosmetics, detergents,

aromatherapy, inhibition of pathogens and control of insects.

Among the major chemical constituents found in citrus, we highlight limonene. In the nomenclature adopted by IUPAC (International Union of Pure and Applied Chemistry), it has the name of 4-isoprenyl-1-methyl-cyclohexene and constitutes more than 300 plant species. In addition, it has two enantiomers which are S - (-) - limonene R - (+) - limonene, in which R - (+) -

limonene is the major component of oils from lemon peel (*Citrus limon*) and orange peel and of the essential oil of *Carum carvi*, being responsible for the prevention of dehydration and inhibition of microbial growth⁴.

In the literature, it was observed that the limonene was found to have larvicidal and molluscicidal activity against *Dysmicoccus brevipes*⁵ and *Lymnaea acuminata*⁶. Based on this information, we asked: did the essential oil extracted from the bark of *C. limon* have larvicidal activity against the third stage larvae of *Aedes aegypti* and molluscicide against the snail *Biomphalaria glabrata*, both disease vectors, respectively, dengue and schistosomiasis? Therefore, the fight against the vectors of dengue and schistosomiasis occur through, respectively, larvicides and synthetic molluscicides. Among the larvicides and molluscicides recommended by the World Health Organization (WHO), are, respectively, the temephos and niclosamide⁷. However, the use of these larvicides and molluscicides provokes resistance of larvae and snails, low selectivity, environmental contamination and high cost⁸⁻¹⁰. Thus, it is recommended studies of extracts of plants⁷ and larvicides.

There are two essential points in the manual of the World Health Organization (WHO)¹¹ on the efficacy of a plant's molluscicidal activity, although the same does not exist for larvicidal activity. One is about the activity of the extracts. These are considered to be active when the 24 h shellfish mortality is equal to or greater than 90% at the concentration of 20 ppm for extracts and 100 ppm for the raw vegetable. Another is on toxicity and field studies. Even if the natural molluscicides are biodegradable, within the values required by the WHO, they may present risks⁷.

In this context, in our toxicity study, we chose to carry it out with *Artemia salina* for two reasons. One, low cost, easy manipulation and a good indication of non-target organisms^{12,13}. Another study, due to the good results of plants with the molluscicidal activity that used *A. salina* in the toxicities test^{14,15}. Hence, in view of the above, we chemically characterized the essential oil extracted from the bark of *C. limon* and tested the larvicidal activity against larvae in the third stage of *A. aegypti*, molluscicidal activity against the snail *B. glabrata* and toxic activity against larvae *A. salina*.

2. Materials and methods

2.1 Obtaining essential oil

We collected the fruits, branches, and leaves of *C. limon* in the district of Sá Viana (January and June 2010), in the peripheral region of São Luís/MA, directly from the lemon tree, which is free of agricultural pesticides. In the Seabra Attic Herbarium (SLS) of the Federal University of Maranhão (UFMA), we identified this species from the observation and comparison with the part already identified in the herbarium under registration number 100379 (family *Rutaceae*, genus *Citrus*). After this step, we removed the fruit peels with a stylet.

To extract the essential oil, we used a glass Clevenger extractor coupled to a 1000 mL round bottom flask and to an electric blanket as a heat source. To each essential oil extraction routine, we weigh and grind in an electric sample mill 30 g. After this step, we mixed the sample with distilled water in the proportion 1:10 and placed in a round bottom flask, coupled to the extractor system. Then we switched on the electric blanket and set the temperature to 100 °C. After 5 h the distillation was stopped, and the essential oil was collected. The oil is dried by means of percolation in anhydrous sodium sulfate. We performed these operations in triplicates and stored the samples in ampoules of amber glass under refrigeration (temperature of 15 °C) to avoid possible losses of volatile constituents. So, we determined the density of the essential oil extracted from the use of a 1.0 mL pycnometer, previously dried, tared and calibrated.

2.2 Chemical analysis

For the chemical analysis, we used the gas chromatographic technique coupled to the electron impact mass spectrometer and ion trap analyzer (GC/MS). The equipment used was of the Varian 2100 brand, using helium as drag gas with flow in the column of 1 mL min⁻¹; injector temperature 270 °C, split 1:50; (15 m × 0,25 mm) with stationary phase VF-1ms (100% methylsiloxane 0.25 µm) and oven temperature programming of 60 to 200 °C with a heating rate of 8 °C min⁻¹ and 200-290 °C with heating rate of 15 °C min⁻¹. In the mass spectrometer the manifold, ion trap, and transfer line temperatures were 50, 190 and 200 °C, respectively. 1.0 µL (automatic injector CP-8410) aliquots of the samples diluted in the proportion of

20 μL in 1.5 mL of hexane were injected. We have identified the components of the oil from the comparison of these with the data obtained from authentic substances in reference libraries¹⁶.

2.3 Collection and cultivation of *Aedes aegypti* larvae

In this way, we collected eggs at the Federal University of Maranhão, Bacanga Campus in São Luís Maranhão, through traps called ovitraps. These consist of black polyethylene pails with a capacity of 500 mL each, where we put water and insert two eucatex vanes into the mosquito. We inspect the traps weekly for replacement of the reeds and egg collection. After this step, we placed *A. aegypti* eggs to hatch at a temperature of 31 °C in a 200 mL polyethylene vessel with mineral water. We fed the larvae with cat food until they reached the third stage, when the experiments were done.

2.4 Test of larvicidal activity

We prepared a 1,000 $\text{mg}\cdot\text{L}^{-1}$ stock solution from the 50 mg weighing of the oil into a solution of 49.75 mL of distilled water and 0.25 mL of Tween-80. From this, we prepared five solutions at the concentrations 5, 10, 30, 50 and 70 $\text{mg}\cdot\text{L}^{-1}$. For each concentration, we used ten larvae and 30 mL of each solution in the cited concentrations. We performed all the tests in triplicate and as negative control we used a solution formed by 49.75 mL of water to 0.25 mL of Tween-80, and as a positive control, a solution of Temephos ([4-(4-dimethoxyphosphinothioxyloxyphenyl)sulfanylphenoxy]-dimethoxy-sulfanylidene- λ^5 -phosphane), which is equivalent to the concentration used by the National Health Foundation (Funasa) for the larvicidal control of the vector, in addition to Novaluron (N-[[3-chloro-4-[1,1,2-trifluoro-2-(trifluoromethoxy)ethoxy]phenyl]carbonyl]-2,6-difluorobenzamide) at 0.02 $\text{mg}\cdot\text{L}^{-1}$, a dose adopted by the Brazilian Ministry of Health, which indicates by the World Health Organization in the range of 0.01 to 0.05 $\text{mg}\cdot\text{L}^{-1}$.

2.5 Malacological investigation

From this, we collected the samples of snails in the natural breeding sites of the neighborhood Sá Viana, the periphery of São Luís, Maranhão. The

catch was carried out during rainy periods, with the use of PPEs (personal protective equipment), such as glove, boot seven leagues, and metal tongs. The collection technique consists of scraping the submerged areas with the shell and the collected snails were placed in a glass container with a lid, with water from the breeding site itself¹⁷. The search of the same ones was realized in several points of each breeding place, in order to obtain a good sampling. After collection, these were labeled by the breeder and taken to the laboratory for identification and analysis. From the technique of dissection of the genital apparatus¹⁸, we identified the snails as belonging to the family *Planorbidae*, genus *Biomphalaria*, species *B. glabrata*.

2.6 Snails positivity test

For instance, we placed five snails in clear glass vials (30 mL capacity) with 25 mL of dechlorinated water, that is 5 mL per snails, brought to light exposure (100 W lamps), at a distance of 30 cm, during 1 h, to stimulate the release of cercariae¹⁹. After exposure, the glasses were taken for analysis by means of a stereoscopic magnifying glass 8x. Those that were parasitized (positive) were labeled and separated for future individual analysis in order to verify which was contaminated and those that did not show signs of infection by the trematode in the period of 30 days were selected for the molluscicidal activity test. The period of analysis of the snails was every 7 days, for one month (30 days) to confirm the absence of larval stages.

So, after the positivity test, we placed the snails in polystyrene containers with dechlorinated water and fed with hydroponic lettuce for future test of molluscicidal activity.

2.7 Molluscicidal activity test

The molluscicidal activity was performed according to a manual described by the World Health Organization. To do this, we placed 10 adult snails, negative for *Schistosoma mansoni* in each beaker containing 500 mL of a solution obtained from the dilution of each oil with distilled water and 0.15 mL of Tween 80 (surfactant) at the concentrations of 100, 75, 50, 25, and 10 $\text{mg}\cdot\text{L}^{-1}$, obtaining at the end a proportion of 50 mL of solution for each snail and feeding them with hydroponic lettuce *ad libitum*²⁰. They were exposed to the solution for 24 h at room temperature. After this period, the snails were

removed from the solution and the snails were washed twice with dechlorinated water, placed in each beaker containing 500 mL of dechlorinated water, fed with hydroponic lettuce and observed every 12 h (method recommended 24 h) for four days to assess mortality. To confirm the activity, we observe the mollusks. If the cephalopods mass is retracted into the shell, release the hemolymph, or swell and extend the cephalopod out of the shell, it is considered dead²¹.

2.8 Toxicity test with *Artemia salina*

So that, the *Artemia salina* Leach cysts were transferred to an aquarium containing the synthetic saline solution (60 g of sea salt / liter of distilled water) and oxygen saturation, obtained with the aid of an air pump. The aquarium was divided into two interconnected compartments, the cysts remaining in one of the compartments, leaving the second compartment under artificial illumination of a 100 W lamp. After 24 h, the cysts hatched, the larvae migrated to the lighted compartment because they had phototropism positive. These were transferred to an aquarium containing synthetic saline and kept in incubation for another 24 h under the same lighting and oxygenation conditions. The methodology used was described by Meyer *et al.*²² but with modifications.

For the evaluation of the lethality of *A. salina* Leach, 20 mg of the oil was added to 0.02 mg of Tween 80, the volume was filled to 2 mL with artificial saline. This dilution was done to obtain a 10 mg mL⁻¹ stock solution and a concentration of 0.1% Tween 80. Samples of 5, 50, 250 and 500 µL of this stock solution were transferred to vials with 5 mL of final solution, obtaining concentrations of 10, 100, 500 and 1000 mg·L⁻¹, respectively. Ten larvae in the nauplii phase were transferred to each flask. White (saline) was made with 20 µL and the negative control (saline and 0.1% Tween 80) was made with 20 µL. After 24 h of incubation, the live larvae were counted, considering those microcrustaceans that did not move during observation and with slight agitation of the flask. Thus, we adopted the criterion established by

Amarante *et al.*²³, which consider LC₅₀ samples less than 100 mg L⁻¹, highly toxic; with LC₅₀ between 100 and 500 mg·L⁻¹, moderately toxic; and LC₅₀ greater than 500 mg·L⁻¹ nontoxic.

2.9 Statistical analysis

The statistical test used was Anova of single factor and Tukey's posterior test to identify significant differences. For the calculation of the lethal concentration (LC₅₀), we used the Probit method²⁴. For mortality results, we expressed these results with mean ± standard deviation. For all statistical tests, we considered the significance of $p \leq 0.05$.

3. Results

3.1 Evaluation of the chemical characteristics of the essential oils obtained by gas chromatography coupled to mass spectroscopy (GC/MS)

Before identifying and quantifying the components present in the oil, we performed the kinetic test for extraction in the time interval of 0.5 to 5 h to verify the best performance. From this test, we verified that from 3 to 5 h, the oil yield remained constant, obtaining a volume of 0.35 mL. We calculated the extraction yield from the mass we used, which was 30 g of the material, volume obtained after extraction, of the density measurement, which was 0.823 g·mL⁻¹ and the formula expressed by the Brazilian Pharmacopoeia⁵². From this, the result obtained was, respectively in the ratio mass / volume and mass / mass, of 1.17% and 0.96%.

From this study, we identify and quantify the components present in the oil. The result of the GC-MS analysis showed 23 peaks, which indicated the presence of 23 compounds (Fig. 1). In comparing the mass spectra of the constituents with the NIST 8 library, we identified the 15 compounds (Table 1). Based on the results, we observed that the major component is Limonene (58.81%) and the minority is the α -Mylene (0.11%) (Table 1).

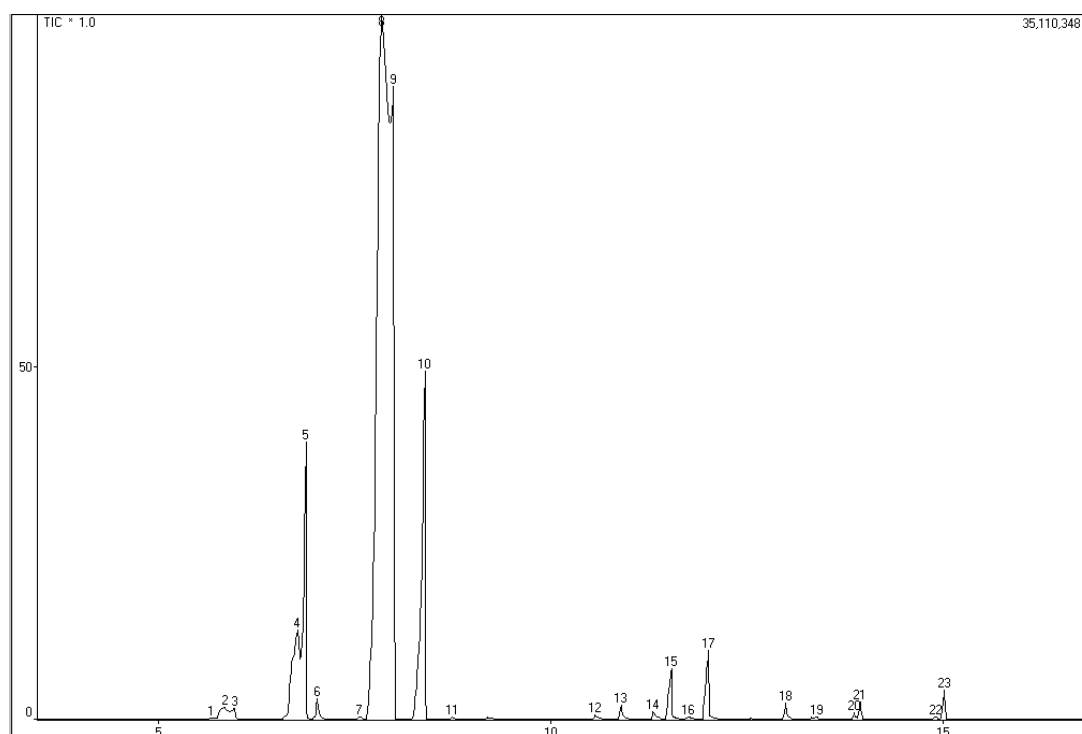


Figure 1. *Citrus limon* peel essential oil GC/MS Chromatogram.

Table 1. Compounds identified in the essential oil sample from *Citrus lemon* peel.

Peak ¹	R.T(min) ²	Components	Percentage (%)	Quality ³
1	5.858	α -Pinene	0.72	95
2	6.775	Sabinene	5.08	92
3	6.875	β -Pinene	4.91	93
4	7.033	β -Myrcene	0.45	91
5	7.845	Limonene	58.81	90
6	8.408	γ -Terpinene	9.01	93
7	10.575	Terpine-4-ol	0.13	89
8	10.892	α -Terpinenol	0.31	96
9	11.308	Trans-geraniol	0.25	92
10	11.525	β -Citral (geranial)	1.11	93
11	12.000	α -Citral (geranial)	1.61	92
12	13.000	Geranial acetate	0.32	93
13	13.400	α -Mulle	0.11	85
14	13.950	Bergamolene	0.29	92
15	15.017	β -Bisabolene (geranial)	0.50	92

Note: ¹Number of the peak in the column elution order; ²RT: Retention time of the compounds. Quality³: search index in the database that reflects the similarity of the mass spectrum obtained with the records in the libraries used.

3.2 Larvicidal activity, molluscicide and toxicity

We tested the larvicidal activity for concentrations of 5, 10, 30, 50 and 70 mg L⁻¹, molluscicide for 10, 25, 50, 75 and 100 mg L⁻¹ and

toxicity for 10, 100, 500 and 1000 mg L⁻¹. In all tests, we observed an increase in the percentage of mortality with the increase in concentration and absence of interference of the biological activity in the control test. Thus, they were higher in

concentrations of larvicidal activities, molluscicides and toxicity, respectively 70, 50 and 1000 mg L⁻¹. In addition, we observed that there were no significant differences between treatments

(Table 2). The LC₅₀ values for larvicidal activities, molluscicides and toxicity are, respectively, 15.48, 13.05 and 743.35 mg L⁻¹ (Table 3).

Table 2. Results of the larvicidal, molluscicidal and toxicity activities of the essential oil of *Citrus limon* peels.

<i>Larvicidal activity</i>	
Concentration (mg L ⁻¹)	Mortality of larvae (%)
70	100.0 ± 0.0 ^a
50	86.7 ± 0.4 ^a
30	66.7 ± 0.4 ^a
10	36.7 ± 0.4 ^a
5	13.3 ± 0.4 ^a
<i>Molluscicidal activity</i>	
Concentration (mg L ⁻¹)	Mortality of snails (%)
100	100.0 ± 0.0 ^a
75	100.0 ± 0.0 ^a
50	100.0 ± 0.0 ^a
25	86.7 ± 0.4 ^a
10	26.7 ± 0.4 ^a
<i>Toxicity activity</i>	
Concentration (mg L ⁻¹)	Mortality of larvae (%)
1000	100.0 ± 0.0 ^a
500	46.7 ± 0.4 ^a
100	13.3 ± 0.4 ^a
10	0.0 ± 0.0 ^a
The mean values and the standard deviation of the measurements in triplicate. Different letters indicate significant differences (p < 0.05).	

Table 3. LC₅₀ result of larvicidal activity, molluscicide and essential oil toxicity extracted from *Citrus limon* peel.

Biological Activity	Lethal Concentration (LC ₅₀) (mg L ⁻¹)	Lower Limit (mg L ⁻¹)	Upper Limit (mg L ⁻¹)	Standard deviation (SD)	R ² (Correlation)
Larvicidal	15.5	10.3	23.3	0.4	0.97
Molluscicidal	13.1	9.5	18.0	0.2	1
Toxicity	743.4	346.9	1593.0	0.7	1

4. Discussion

From this study, we showed that the essential oil extracted from the bark of *C. limon* has larvicidal activity, molluscicide and toxicity. This may be a viable alternative to synthetic larvicides and molluscicides, since they would act against target organisms due to their toxicity against other organisms. We found that the percentage (m/v) of the oil yield was 1.17% and that the main components are limonene (major component) and α -Mylene (minor component).

The yield that we obtained in a time of extraction of 5 h was 1.17%, in which this value remained constant in the interval of 3 to 5 h. The study of the yield allows to evaluate the time necessary to conserve the best characteristics of the oil. According to Mouchrek Filho²⁵, quoted by Gomes *et al.*²⁶, a time of rapid extraction leads to a product with the predominance of more volatile constituents, but without the best characteristics. Otherwise, slow distillation overloads the product with undesirable flavors⁵⁴. Generally, the best yields are obtained from the time of 3 h²⁶⁻³⁰.

From the chromatographic method coupled to the mass spectrometer, we identified and quantified limonene as the major component of the essential oil extracted from *C. limon* peels. Thus, we confirm what has already been described in the literature regarding this component for citrus substances. However, we observe that the quantity of this differs from other works, where they are generally above³¹⁻³³ and others below 50%. The redirection of plant metabolic pathways to lead to the biosynthesis of different compounds³⁴⁻³⁶ and abiotic factors are responsible for caused changes in the composition of *C. limon* essential oil.

In the study of larvicidal activity, the essential oil was active against the third stage larvae of *A. aegypti* in the concentration of 70 mg·L⁻¹ with 100% mortality of the larvae tested. Although this result gives us a dimension of biological activity, a statistical calculation of the lethal concentration (LC₅₀) from the method of Finney²⁴ gave us an estimate of inferring this result for a population, considering a statistical distribution of the normal type. The result of LC₅₀ was 15.48 mg·L⁻¹. From this result, we compare the criteria adopted by Cheng *et al.* (2003), since up to the moment of this research there is no criterion established the World Health Organization³⁷ to consider active larvicidal activity or inactive. According to the Cheng *et al.*³⁸

the larvicidal activity of the essential oil is active when the LC₅₀ < 100 mg·L⁻¹; inactive when LC₅₀ > 100 mg·L⁻¹ is highly active when LC₅₀ < 50 mg·L⁻¹. Thus, from this classification the essential oil we extract from the bark of *C. limon* is considered highly active.

The larvicidal activity of the essential oils are influenced by several factors. A study by Fernandez *et al.* (2014)³⁹ showed that larvicidal activity is higher in spring, summer and autumn, and lower in winter, confirming the influence of seasonality; for Leyva *et al.*⁴⁰ synergistic action among metabolites (even in small proportions), the collection period and the extraction method are responsible for this; while other studies attribute this action to terpenes, alcohols, and aldehydes⁴¹⁻⁴³.

For these reasons, the results of our study confirm the larvicidal and insecticidal activity of limonene of *C. limon* essential oil against the genus *Aedes*. The study carried out by Campolo *et al.*⁴⁴ showed the activity of this oil against *Aedes albopictus* larvae with a lethal concentration (LC₅₀) of 145.27 mg L⁻¹ after 24h exposure. However, the study of larvae, pulps and adults of *Aedes albopictus*⁴⁵ confirmed the activity of the oil with a lethal concentration (LC₅₀) of 35.99 and 34.89 mg·L⁻¹ for the enantiometric forms of limonene, respectively, R - (+) - limonene and S - (-) - limonene. Finally, the study Amer and Mehlhorn⁴⁶ confirmed that activity against third-stage larvae of *A. aegypti* was higher at 24 h exposure time when compared to shorter times. Thus, the difference that these studies have with the results of our study is in the low value of the LC₅₀ that we obtain. To explain this difference, we attribute seasonality, collection and extraction factors and synergism.

In relation to molluscicidal activity, the essential oil was active with LC₅₀ 13.48 mg·L⁻¹. In this case, to affirm this, we compare the result obtained from the LC₅₀ with the criteria used by the WHO¹¹. According to this criterion, the extract obtained from the plant is active when it causes mortality of 90% of the aquatic mollusks at the 24 h exposure time, under constant temperature and concentration up to 100 mg·L⁻¹⁴⁷. Thus, we proved that the result we obtain from the LC₅₀ of our study is within the limits established by the WHO.

Besides the molluscicidal activity which we show in this work, we observed in the literature that the limonene obtained from the *Carum cravi* seed powder showed activity against the snail *Lymnaea acuminata*⁶. Although this component caused mortality of *Lymnaea acuminata*, the inference of

the lethal concentration, LC_{50} , for a population of these snails did not meet the criteria established by WHO¹¹, whose value was $130.61 \text{ mg}\cdot\text{L}^{-1}$ in the time of 24 h. In addition, this study left craving for the percentage absence of limonene contained in the extracts, in which it left doubts about its effectiveness.

In the literature there are other plants that have molluscicidal activity against *B. glabrata*, however, the effectiveness is in the lowest value of the lethal concentration (LC_{50}). The study of thirteen *Solanum* species revealed that the extracts of the species *S. asperum*, *S. diamantinae*, *S. paludosum*, *S. sisymbriifolium* and *S. stipulaceum* present activity with lethal concentration (LC_{50}) varying from 20 to 50 mg L^{-1} ⁴⁸; *Moringa oleifera* Lam seed extracts were active in the lethal concentration, LC_{50} , 419 mg L^{-1} ⁴⁹; extracts from the stems of *Meloea quadrivalvis* and *Tabebuia aurea* and whole plants of *Adenocalymma comosum*, *Arrabidaea parviflora*, *Cuspidaria argentea*, and *Clytostoma binatum* have activity with LC_{50} concentration varying from 5.2 to 37.5 mg L^{-1} , being the most active *Cuspidaria argentea*, LC_{50} 5.2 mg L^{-1} ⁵⁰; the essential oil of *Pimenta dioica* is active with LC_{50} 18.62 mg L^{-1} , however the toxicity study showed that it is highly toxic to other organisms⁵³. Though, the *Ocotea bracteosa* essential oil has activity with concentration, LC_{50} 4.6 mg L^{-1} ⁵¹. Although *O. bracteosa* essential oil has good results in lethal concentration values, the absence of a study of toxic activity in this study raises doubts about its effectiveness in a real system.

Hence, faced with this impasse, when performing the study of toxicity, we evaluated the possibility of the action of oil against non-target organisms. In our study, we used *A. salina* because of the following characteristics: formation of dormant cysts, low cost, easy manipulation in the laboratory and indication of interference with nontarget organisms^{12,13}. Based on the toxicity parameters of Amarante *et al.*²³, the essential oil, with $LC_{50} = 743.35 \text{ mg L}^{-1}$, is non-toxic ($LC_{50} > 500 \text{ mg L}^{-1}$). In addition to our study, we found in the literature extracts from six plants of the family Bignoniaceae that have moderate to low toxicity with LC_{50} values varying from 485.5 to 815.4 mg L^{-1} ⁵⁰.

5. Conclusions

In this manner, according to the results obtained in this study, we can conclude that the essential oil extracted from the shells of *C. limon* has larvicidal activity and molluscicide, respectively, third stage larvae of *A. aegypti* and snails *B. glabrata*, and non-toxic front *A. salina*. In addition, we identified and quantified the majority and minority components, which were, respectively, limonene and α -Mulle.

References

- [1] Buettner, A., Mestres, M., Fischer, A., Guasch, J., Schieberle, P., Evaluation of the most odour-active compounds in the peel oil of clementines (*Citrus reticulata* Blanco cv. Clementine), Eur Food Res. Technol. 216 (1) (2003) 11-14. <https://doi.org/10.1007/s00217-002-0586-y>.
- [2] Caccioni, D. R., Guizzardi, M., Biondi, D. M., Agatino, R., Ruberto, G., Relationship between volatile components of citrus fruit essential oils and antimicrobial action on *Penicillium digitatum* and *Penicillium italicum*, Int J Food Microbiol 43 (1-2) (1998) 73-79. [https://doi.org/10.1016/S0168-1605\(98\)00099-3](https://doi.org/10.1016/S0168-1605(98)00099-3).
- [3] Sharma, N., Tripathi, A., Fungitoxicity of the essential oil of *Citrus sinensis* on post-harvest pathogens, World J. Microbiol. Biotechnol. 22 (6) (2006) 587-593. <https://doi.org/10.1007/s11274-005-9075-3>.
- [4] Demyttenaere, J., De Kimpe, N., Biotransformation of terpenes by fungi: Study of the pathways involved, J. Mol. Catal. B Enzym. 11 (4) (2001) 265-270. [https://doi.org/10.1016/S1381-1177\(00\)00040-0](https://doi.org/10.1016/S1381-1177(00)00040-0).
- [5] Martins, G. D. S. O., Zago, H. B., Costa, A. V., Araujo Junior, L. M. D., Carvalho, J. R. D., Chemical composition and toxicity of citrus essential oils on *Dysmicoccus brevipes* (Hemiptera: Pseudococcidae), Rev. Caatinga 30 (3) (2017) 811-817. <https://doi.org/10.1590/1983-21252017v30n330rc>.
- [6] Kumar, P., Singh, D. K., Molluscicidal activity of *Ferula asafoetida*, *Syzygium aromaticum* and *Carum carvi* and their active components against the snail *Lymnaea acuminata*, Chemosphere 63 (9) (2006) 1568-1574. <https://doi.org/10.1016/j.chemosphere.2005.08.071>.
- [7] Cantanhede, S. P. D., Marques, A. M., Silva-Souza, N., Valverde, A. L., Atividade moluscicida de plantas:

- uma alternativa profilática, *Rev. Bras. Farmacogn.* 20 (2) (2010) 282-288. <https://doi.org/10.1590/S0102-695X2010000200024>.
- [8] Colley, D.G., Bustinduy, A. L., Secor, W. E., King, C. H., Human schistosomiasis, *The Lancet* 383 (9936) (2014) 2253-2264. [https://doi.org/10.1016/S0140-6736\(13\)61949-2](https://doi.org/10.1016/S0140-6736(13)61949-2).
- [9] Gasparotto Junior., A., Brenzan, M. A., Piloto, I. C., Cortez, D. A. G., Nakamura, C. V., Dias Filho, B. P., Rodrigues Filho, E., Ferreira, A. G., Estudo fitoquímico e avaliação da atividade moluscicida do *Calophyllum brasiliense* Camb (Clusiaceae), *Quím Nova* 28 (4) (2005) 575-578. <https://doi.org/10.1590/S0100-40422005000400003>.
- [10] Diniz, M. M. C. S., Henriques, A. D. S., Leandro, R. S., Aguiar, D. L., Beserra, E. B., Resistance of *Aedes aegypti* to temephos and adaptive disadvantages, *Rev Saúde Pública* 48 (2014) 775-782. <https://doi.org/10.1590/S0034-8910.2014048004649>.
- [11] World Health Organization, Report of the Scientific working Group on Plant Molluscicide & Guidelines for evaluation of plant molluscicides, *Bull World Health Organ Geneva TDRSC* (1983). <https://apps.who.int/iris/handle/10665/60086>.
- [12] Utyama, I. K. A., Andrade, D., Watanabe, E., Pimenta, F. C., Ito, I. Y., Determinação da atividade antibacteriana e toxicidade do ácido acético e vinagres branco e tinto, *Revista Eletrônica de Farmácia* 4 (2) (2007) 202-207. <https://doi.org/10.5216/ref.v4i2.3054>.
- [13] Calow, P., Marine and estuarine invertebrate toxicity tests, *Hoffman Al Handb Cytotoxicology*, Oxford, Blackwell, Sci Publication, 1993.
- [14] Singh, A., Singh, S. K., Molluscicidal evaluation of three common plants from India, *Fitoterapia* 76 (7-8) (2005) 747-751. <https://doi.org/10.1016/j.fitote.2005.08.002>.
- [15] Luna, J. S., Santos, A., Lima, M. R. F., Omena, M. C., Mendonça, F. A. C., Bieber, L. W., Sant'Ana, A. E. G., A study of the larvicidal and molluscicidal activities of some medicinal plants from northeast Brazil, *J. Ethnopharmacol.* 97 (2) (2005) 199-206. <https://doi.org/10.1016/j.jep.2004.10.004>.
- [16] Adams, R. P., Sparkman, O., Review of identification of essential oil components by gas chromatography/mass spectrometry, *J. Am. Soc. Mass Spectrom* 18 (4) (2007) 803-806. <https://doi.org/10.1016/j.jasms.2007.01.001>.
- [17] Brasil, Ministério da Saúde. Secretaria de Vigilância em Saúde. Departamento de Vigilância Epidemiológica, Vigilância e controle de moluscos de importância epidemiológica: diretrizes técnicas: programa de vigilância e controle da esquistossomose (PCE), Brasília: Ministério da Saúde, 2008. <http://portal.arquivos.saude.gov.br/images/pdf/2015/ago/14/vigilancia-controle-moluscos-import-epidemi-2ed.pdf>.
- [18] Deslandes, N., Técnica de dissecação e exame de planorbídeos, *Rev Serv Espec Saúde Pública* 4 (1951) 371-382.
- [19] Smithers, S. R., Terry, R., The infection of laboratory hosts with cercariae of *Schistosoma mansoni* and the recovery of the adult worms, *Parasitology*, 55 (4) (1965) 695-700. <https://doi.org/10.1017/s0031182000086248>.
- [20] Malek, E. A., Snail Hosts of Schistosomiasis and Other Snail-Transmitted Diseases in Tropical America: a manual, American Society of Tropical Medicine and Hygiene, Arlington, 1985. <https://doi.org/10.4269/ajtmh.1987.36.199>.
- [21] McCullough, F. S., Gayral, P., Duncan, J., Christie, J. D., Molluscicides in schistosomiasis control, *Bull. World Health Organ.* 58 (5) (1980) 681-689. <https://www.ncbi.nlm.nih.gov/pmc/articles/PMC2395986/>.
- [22] Meyer, B. N., Ferrigni, N. R., Putnam, J. E., Jacobsen, L. B., Nichols, D. E., McLaughlin, J. L., Brine shrimp: a convenient general bioassay for active plant constituents, *Planta Med.* 45 (1) (1982) 31-34. <https://doi.org/10.1055/s-2007-971236>.
- [23] Amarante, C. B. D., Müller, A. H., Póvoa, M. M., Dolabela, M. F., Phytochemical study bioassay-guided by tests of toxicity on *Artemia salina* and antiplasmodial activity from stem of aninga (*Montrichardia linifera*), *Acta Amazonica*, 41 (3) (2011) 431-434. <https://doi.org/10.1590/S0044-59672011000300015>.
- [24] Finney, D.J., Tattersfield, F., *Probit Analysis*, Cambridge University: Cambridge, 1952.
- [25] Mouchrek Filho, V. E., Estudos Analíticos e modificações químicas por metilação e acetilação do eugenol contido no óleo essencial extraído das folhas da espécie *Pimenta dioica* Lindl, Tese de Doutorado, Universidade de São Paulo, São Paulo, Brasil, 2000.
- [26] Gomes, P. R. B., Silva, A. L. S., Pinheiro, H. A., Carvalho, L. L., Lima, H. S., Silva, E. F., Silva, R. P., Louzeiro, H.C., Oliveira, M. B., Mouchrek Filho, V. E., Avaliação da atividade larvicida do óleo essencial do

- Zingiber officinale* Roscoe (gengibre) frente ao mosquito *Aedes aegypti*, Rev. Bras. Plantas Med. 18 (2) (2016) 597-604. https://doi.org/10.1590/1983-084x/15_214.
- [27] Gomes, P. R. B., Oliveira, R. W. S., Mouchrek Filho, V. E., Nascimento, A. A., Everton, A. P., Louzeiro, H. C., Fontenele, M. A., Activity larvicide of the essential oil *Syzygium aromaticum* (carnival-of-India) in front of the mosquito *Aedes aegypti* (Linnaeus, 1762). Periodico Tche Quimica 15 (29) (2018) 184-195. <http://www.deboni.he.com.br/Periodico29.pdf>.
- [28] Gomes, P. R. B., Santos, D. P., Mouchrek Filho, V. E., Mendes, L. S. S., Fontenele, M. A., Activity larvicide of the essential oil of *Cinnamomum zeylanicum* Blume, Period Tche Quimica 16 (31) (2019) 18-26. <http://www.deboni.he.com.br/Periodico31.pdf>.
- [29] Gomes, P. R. B., Silva, A. L. S., Mouchrek Filho, V. E., Mouchrek, A. N., Everton, P. C., Avaliação físico-química do óleo essencial *Zingiber officinale* Roscoe (Gengibre), Rev. Cuba Farm. 50 (3) (2016). <http://www.revfarmacia.sld.cu/index.php/far/article/view/30/34>.
- [30] Gomes, P. R. B., Mouchrek Filho, V. E., Ferreira Rabêlo, W., Nascimento, A. A., Costa Louzeiro, H., Lyra, W. S., Fontenele, M. A., Chemical characterization and cytotoxicity of clove essential oil (*Syzygium aromaticum*), Rev. Colomb. Cienc. Quím. – Farm. 47 (1) (2018) 37-52. <https://doi.org/10.15446/rcciquifa.v47n1.70657>.
- [31] Campelo, L. M. L., Sá, C. G., Feitosa, C. M., Sousa, G. F., Freitas, R. M., Constituintes químicos e estudos toxicológicos do óleo essencial extraído das folhas de *Citrus limon* Burn (Rutaceae), Rev. Bras. Plantas Med. 15 (4 suppl 1) (2013) 708-716. <https://doi.org/10.1590/S1516-05722013000500011>.
- [32] González-Molina, E., Domínguez-Perles, R., Moreno, D. A., García-Viguera, C., Natural bioactive compounds of Citrus limon for food and health, J. Pharm. Biomed. Anal. 51 (2) (2010) 327-345. <https://doi.org/10.1016/j.jpba.2009.07.027>.
- [33] Mahalwal, V. S., Ali, M., Volatile constituents of the fruits peels of *Citrus lemon* (Linn) Burm. f. J. Essent. Oil Bear Plants 6 (1) (2003) 31-35. <https://doi.org/10.1080/0972-060X.2003.10643325>.
- [34] Blank, A. F., Costa, A. G., Arrigoni-Blank, M. F., Cavalcanti, S. C. D. H., Alves, P. B., Innecco, R., Ehlert, P. A. D., Sousa, I. F., Influence of season, harvest time and drying on Java citronella (*Cymbopogon winterianus* Jowitt) volatile oil, Rev. Bras. Farmacogn. 17 (4) (2007) 557-564. <https://doi.org/10.1590/S0102-695X2007000400014>.
- [35] Figueiredo, A. C., Barroso, J. G., Pedro, L. G., Scheffer, J. J. C., Factors affecting secondary metabolite production in plants: volatile components and essential oils, Flavour Fragr. J. 23 (4) (2008) 213-226. <https://doi.org/10.1002/ffj.1875>.
- [36] Cerqueira, M. D., Marques, E. J., Martins, D., Roque, N. F., Cruz, F. G., Guedes, M. L. S., Seasonal variation of the composition of essential oil from *Myrcia salzmannii* Berg. (Myrtaceae), Quím Nova 32 (6) (2009) 1544-1548. <https://doi.org/10.1590/S0100-40422009000600035>.
- [37] Dias, C. N., Moraes, D. F. C., Essential oils and their compounds as *Aedes aegypti* L. (Diptera: Culicidae) larvicides: review, Parasitol Res. 113 (2) (2014) 565-592. <https://doi.org/10.1007/s00436-013-3687-6>.
- [38] Cheng, S., Chang, H. T., Chang, S.T., Tsai, K. H., Chen, W. J., Bioactivity of selected plant essential oils against the yellow fever mosquito *Aedes aegypti* larvae, Bioresour Technol. 89 (1) (2003) 99-102. [https://doi.org/10.1016/S0960-8524\(03\)00008-7](https://doi.org/10.1016/S0960-8524(03)00008-7).
- [39] Fernandez, C. M. M., Barba, E. L., Fernandez, A. C. M., Cardoso, B. K., Borges, I. B., Takemura, O. S., Martins, L. A., Cortez, L. E. R., Cortez, D. A. G., Gazim, Z. C., Larvicidal activity of essential oil from *Tetradenia riparia* to control of *Aedes aegypti* larvae in function of season variation, J. Essent. Oil Bear Plants 17 (5) (2014) 813-823. <https://doi.org/10.1080/0972060X.2014.892841>.
- [40] Leyva, M., Marquetti, M. C., Tacoronte, J. E., Scull, R., Tiomno, O., Mesa, A., Montada, D., Actividad larvicide de aceites esenciales de plantas contra *Aedes aegypti* (L.) (Diptera: Culicidae), Rev. Biomed. 20 (1) (2009) 5-13. <http://revistabiomedica.mx/index.php/revbiomed/articloe/view/529>.
- [41] Lee, H. S., Mosquito larvicidal activity of aromatic medicinal plant oils against *Aedes aegypti* and *Culex pipiens pallens*, J. Am. Mosq. Control Assoc. 22 (2) (2006) 292-296. [https://doi.org/10.2987/8756-971X\(2006\)22\[292:MLAOAM\]2.0.CO;2](https://doi.org/10.2987/8756-971X(2006)22[292:MLAOAM]2.0.CO;2).
- [42] Leite, A. M., Lima, E. O., Souza, E. L., Diniz, M. D. F., Leite, S. P., Xavier, A. L., Medeiros, I. A. D., Preliminary study of the molluscicidal and larvicidal properties of some essential oils and phytochemicals from medicinal plants, Rev. Bras. Farmacogn. 19 (4) (2009) 842-846. <https://doi.org/10.1590/S0102-695X2009000600008>.

- [43] Lucia, A., Audino, P. G., Seccacini, E., Licastro, S., Zerba, E., Masuh, H., Larvicidal effect of Eucalyptus grandis essential oil and turpentine and their major components on *Aedes aegypti* larvae, *J. Am. Mosq. Control Assoc.* 23 (3) (2007) 299-304. [https://doi.org/10.2987/8756-971X\(2007\)23\[299:LEOEGE\]2.0.CO;2](https://doi.org/10.2987/8756-971X(2007)23[299:LEOEGE]2.0.CO;2).
- [44] Campolo, O., Romeo, F. V., Algeri, G. M., Laudani, F., Malacrinò, A., Timpanaro, N., Palmeri, V. Larvicidal effects of four citrus peel essential oils against the arbovirus vector *Aedes albopictus* (Diptera: Culicidae), *J. Econ. Entomol.* 109 (1) (2015) 360-365. <https://doi.org/10.1093/jee/tov270>.
- [45] Giatropoulos, A., Papachristos, D. P., Kimbaris, A., Koliopoulos, A., Polissiou, M. G., Emmanouel, N., Michaelakis, A., Evaluation of bioefficacy of three *Citrus* essential oils against the dengue vector *Aedes albopictus* (Diptera: Culicidae) in correlation to their components enantiomeric distribution, *Parasitol. Res.* 111 (6) (2012) 2253-2263. <https://doi.org/10.1007/s00436-012-3074-8>.
- [46] Amer, A., Mehlhorn, H., Larvicidal effects of various essential oils against *Aedes*, *Anopheles*, and *Culex* larvae (Diptera, Culicidae), *Parasitol. Res.* 99 (4) (2006) 466-472. <https://doi.org/10.1007/s00436-006-0182-3>.
- [47] Petersen, P. E., World Health Organization. Organisation Mondiale de la Sante, *Community Dent. Oral Epidemiol.* 31 (6) (2003) 471-471. <https://doi.org/10.1046/j.1600-0528.2003.00124.x>.
- [48] Silva, T., Batista, M., Camara, C., Agra, M., Molluscicidal activity of some *Brazilian Solanum* spp. (Solanaceae) against *Biomphalaria glabrata*, *Ann. Trop. Med. Parasitol.* 99 (4) (2005) 419-425. <https://doi.org/10.1179/136485905X36208>.
- [49] Silva, C. L. P. A. C., Vargas, T. S., Baptista, D. F., Molluscicidal activity of *Moringa oleifera* on *Biomphalaria glabrata*: integrated dynamics to the control of the snail host of *Schistosoma mansoni*, *Rev. Bras. Farm.* 23 (2013) 848-850. <https://doi.org/10.1590/S0102-695X2013000500019>.
- [50] Silva, T., Silva, T., Martins, R., Maia, G. L. A., Cabral, A. G. S., Camara, C. A., Agra, M. F., Barbosa-Filho, J. M., Molluscicidal activities of six species of Bignoniaceae from north-eastern Brazil, as measured against *Biomphalaria glabrata* under laboratory conditions, *Ann. Trop. Med. Parasitol.* 101 (4) (2007) 359-365. <https://doi.org/10.1179/136485907X176427>.
- [51] Coutinho, D. F., Dias, C. S., Barbosa-Filho, J. M., Agra, M. F., Martins, R. M., Silva, T. M., Cunha, E. V. L., Silva, M. S., Craveiro, A. A., Composition and molluscicidal activity of the essential oil from the stem bark of *Ocotea bracteosa* (Meisn.) Mez, *J. Essent. Oil Res.* 19 (5) (2007) 482-484. <https://doi.org/10.1080/10412905.2007.9699958>.
- [52] Farmacopeia Brasileira, Editora Atheneu, parte I-II, quinto fascículo, São Paulo, 4ª ed., 2004.
- [53] Gomes, P. R. B., Reis, J. B., Fernandes, R. P., Mouchrek Filho, V. E., Souza, A. G., Fontenele, M. A., Silva, J. C., Toxicidad y Actividad Moluscicidal del Aceite Esencial *Pimenta dioica* Contra El Caracol *Biomphalaria glabrata*. *Revista Peruana de Biología* 26 (1) (2019) 101-8. <https://doi.org/10.15381/rpb.v26i1.15913>.
- [54] Chaar, J. S., Estudos analíticos e modificação química por acetilação do linalol contido no óleo essencial da espécie *Aniba duckei* Kostermans, Tese de Doutorado, Universidade de São Paulo, São Paulo, Brasil, 2000. <https://doi.org/10.11606/T.75.2000.tde-28112001-085626>.